Technical Report

TR-02-14

Final report of the TRUE Block Scale project

2. Tracer tests in the block scale

Peter Andersson, Johan Byegård
Geosigma AB

Anders Winberg
Conterra AB

May 2002

Svensk Kärnbränslehantering AB
Swedish Nuclear Fuel
and Waste Management Co
Box 5864
SE-102 40 Stockholm Sweden
Tel 08-459 84 00
+46 8 459 84 00
Fax 08-661 57 19
+46 8 661 57 19

Final report of the TRUE Block Scale project

2. Tracer tests in the block scale

Peter Andersson, Johan Byegård
Geosigma AB

Anders Winberg
Conterra AB

May 2002

Keywords: Block Scale, characterisation, fracture, hydraulic, hydrochemistry, model evolution, network, structure, tracer tests, TRUE.

Foreword

This report constitutes the second in a series of four final reports of the TRUE Block Scale Project, the latter run within the framework of the Tracer Retention Understanding Experiments at the SKB Äspö Hard Rock Laboratory, Sweden.

Funding organisations of the project are;

ANDRA (France)

ENRESA (Spain)

JNC (Japan)

NIREX (United Kingdom)

POSIVA (Finland)

SKB (Sweden)

The work done could not have been accomplished without the active participation and effort of field characterisation crews and analysis teams from the organisations and countries involved. Their contributions and the contribution of the co-ordinators and staff of the Äspö Hard Rock Laboratory are hereby acknowledged.

Special thanks extended to the members of the GEOSIGMA field crew involved in the tracer experiments (Magnus Holmqvist, Mats Skålberg, Tapsa Tammela, Eva Wass, Henrik Widestrand) and to Gunnar Skarnemark, Chalmers University of Technology.

Abstract

The tracer test programme of the TRUE Block Scale Project involved 14 tracer tests campaigns, including performance of 32 tracer injections in 16 different combinations of source and sink sections (flow paths) varying in length between 10 to 130 metres, and involving one or more structures. Average travel times varied between 1.5 and >2000 hours. Tracer dilution tests performed in conjunction with cross-hole hydraulic pumping tests were found to be a very important part of the pre-tests, where the results were used to identify and screen among possible injection points, and to verify the hydrostructural model valid at a given time.

The main problem faced in the block scale tests was to select a test geometry, which gave a sufficiently high mass recovery, and at the same time enabled performance of cross-hole sorbing tracer tests within reasonable time frames. Three different injection methods were applied during the test programme; decaying pulse, finite pulse and forced pulse (unequal dipole). During the later phases of the tracer test programme it was identified that forced injection had to be employed in order to enable detection of tracer at the sink due to strong dilution, and also to avoid problems with artificially induced tailing in the injection signal.

Sorbing (reactive) tracers were selected among the radioactive isotopes of the alkali and alkaline earth metals previously used in the TRUE-1 experiments. It was decided that at least one slightly sorbing tracer and one strongly sorbing tracer should be used in each injection. Non-sorbing tracers were used for conservative reference, e.g., $^{82}Br^{-}$, $^{186}ReO_4$, HTO (tritiated water) and $^{131}I^{-}$. In two of the injections the radioactive non-sorbing tracers were rather short-lived and Uranine and Naphtionate were used as complementary conservative tracers.

Surface distribution coefficients, K_a, were evaluated from TRUE-1 and TRUE Block Scale data, making use of the retardation noted in the injection. The evaluated K_a values were found to be of a magnitude equitable to the TRUE-1 laboratory K_a values. Effects of matrix diffusion, sorption kinetics model, non-linear sorption were also explored.

The evaluation and interpretation of the block scale tracer breakthrough curves indicated response of a heterogeneous system, observed both from tests in single structures and in network of structures. Results from the deterministic Structure #20 were found to show a signature of a narrow and high-conductive single structure, whereas results from Structure #21 indicated that it is probably more complex than assumed at the onset of the investigation, probably made up of several sub-parallel structures, rather than a single fracture. The network flow paths generally have less steep tails ($t^{-4/2} - t^{-3/2}$) in log-log space than the single structure flow paths. The observed order of retention among the different species was found to be the same as in TRUE-1 and in the laboratory tests, i.e. $Na^{+}<Ca^{2+}\approx Sr^{2+}<Ba^{2+}\approx Rb^{+}<Cs^{+}$. Another similarity was that the retardation, expressed as the ratio of the time at which 50% of the sorbing tracer was recovered compared to the conservative tracer ($R_{50\%}$), was about the same for most species when comparing TRUE-1 data to the results of 17 m single structure flow paths (C1 and C4) in Structure #20. However, for the breakthroughs of sorbing tracers in the more complex flow paths C3 (Na^{+}) and C2 (Ca^{2+}) a 30–80% stronger retardation (expressed as $R_{50\%}$) was noted. The reasons for this somewhat

enhanced retardation between the two slower and more complicated flow paths (C2 and C3) and the single structure flow paths (C1 and C4) may be several; e.g. presence of gouge material (fine-grained fault gouge) in the structures, presence of gouge material in fracture intersection zones, differences in the mineralogy along the flow paths, larger portions of stagnant water to interact with along the flow path, higher porosity in the fracture rim zone.

Sammanfattning

Spårförsöksprogrammet inom ramen för TRUE Block Scale-projektet omfattade 14 spårförsökskampanjer (32 injiceringar) i 16 olika kombinationer av injicerings- och pumpsektioner. Längden på flödesvägarna varierade mellan 10 och 130 m och innefattade en eller flera av tolkade deterministiska strukturer. Medeltransporttider varierade mellan 1.5 till >2000 timmar. Utspädningsmätningar utförda i samband med olika typer av hydrauliska mellanhålsmätningar befanns vara en viktig komponent i utförda förförsök. Resultet av dessa mätningar användes till att välja mellan identifierade möjliga injiceringssektioner. Vidare användes resultaten för att verifiera den hydro-strukturella modellen vid en given tidpunkt.

Det huvudsakliga problemet med försök i blockskala var att å ena sidan åstadkomma maximal massretur, och samtidigt kunna genomföra informativa försök med sorberande spårämnen under praktiskt hanterbara tidsintervall. Tre olika typer av injiceringsförfarande utnyttjades; avklingande puls, finit puls och forcerad puls (ojämn dipol). Under de senare faserna av spårförsöksprogrammet identifierades att forcerad puls behövde utnyttjas för att möjliggöra detektion i samband med rådande högt utspädning, och vidare för att undvika problemet med artificiellt inducerade svanseffekter i genombrottet.

Sorberande (reaktiva) spårämnen valdes ut bland ämnen i grupperna alkalimetaller och alkaliska jordartsmetaller, som tidigare utnyttjats framgångsrikt inom ramen för TRUE-1 och tillhörande laboratorieförsök. Det bestämdes att åtminstone ett svagt sorberande och ett starkt sorberande ämne skulle ingå i varje injicering. Icke-sorberande spårämnen användes som konservativ referens; ex. $^{82}Br^{-}$, $^{186}Re^{-}$, HTO (tritierat vatten) samt $^{131}I^{-}$. Dessutom ingick även ett fluorescerande färgspårämne i två av injiceringslösningarna.

Ytsorptionskoefficienter (K_a) utvärderades från TRUE-1 och TRUE Block Scale data genom att utnyttja den retention som observerats i injiceringsdata. De utvärderade värden på K_a befanns vara i samma storleksordning som noterats i laboratoriedata från TRUE-1. Effekter av matrissdiffusion, sorptionskinetik samt icke-linjär sorption analyserades också.

Utvärderingen och tolkningen erhållna genombrottskurvor indikerar respons av ett heterogent geologiskt system, observerat både i data från försök i enskilda strukturer samt i nätverk av strukturer. Resultat från försök i den deterministiska Struktur #20 visar en signatur från en smal men högtransmissiv enskild struktur. Resultat från Struktur #21 indikerar en mer komplex struktur än vad som inledningsvis antagits. Genombrottskurvorna för flödesvägar i nätverk av strukturer visar genomgående en mindre lutning i log-log ($t^{-4/2} - t^{-3/2}$). Den noterade inbördes fördröjningen av de sorberande ämnena var densamma som tidigare noterats i laboratorium samt i TRUE-1, dvs. $Na^{+}<Ca^{2+}\approx Sr^{2+}<Ba^{2+}\approx Rb^{+}<Cs^{+}$. En annan likhet var att retentionen, uttryckt som förhållandet mellan tiden då 50% av det sorberande ämnet anlänt och motsvarande tid för det konservativa spårämnet, var ungefär detsamma för de flesta av spårämnena vid jämförelse mellan den 17 m långa flödesvägen i Struktur #20 (C1/C4). Genombrotten för de sorberande spårämnena i C3 (Na^{+}) och C2 (Ca^{2+}) indikerade för samma mått en 30–80% högre retention. Orsaken till denna något förhöjda retention i de två mer

långsamma och mer komplicerade flödesvägarna kan vara flera (och samverkande) och innefattar t.ex. tillgång på (mer) sprickfyllnadsmaterial (gouge), tillgång på sprickfyllandsmaterial i skärningar mellan sprickor (FIZ), skillnader i mineralogi mellan de två typerna av flödesvägar, större tillgång på stagnanta zoner längs flödesvägen, och högre porositet i den omvandlade zonen närmast sprickan/-orna.

Executive summary

Overview

The TRUE Block Scale project aims at improving understanding of radionuclide transport and retention in a network of structures in crystalline rock. Within the context of the project a series of tracer experiments have been conducted at different times and with variable objectives. The report focuses of the experimental results of the experiments performed as part of the Tracer Test Stage, including tests performed as part of Phases A through C, the latter including tests with radioactive sorbing tracers.

The tracer tests performed in the TRUE Block Scale borehole array covered a very large span of distances (11–130 m) and travel times (1.5 – >2000 hours), providing an unique data set for transport in fractured crystalline rock. The tracer tests with non-sorbing (conservative) tracers have mainly been focused on identifying flow paths with sufficiently high mass recovery (>80%), but have also provided the possibility to obtain transport parameters for 13 different (single structure and multi-structure) flow paths within a rock volume of about 50×50×50 m.

The present report presents the results of tracer tests performed within the scope of the TRUE Block Scale Project with special emphasis on the concluding tests with radioactive sorbing tracers. The report also presents results of preliminary basic evaluation. A more comprehensive modelling-based evaluation is presented in a subsequent report.

Tests performed

During the project different types of tests with tracers have been conducted at various times and with different objectives and levels of ambition. Early tests had i.a. the objective of showing feasibility of running cross-hole tracer experiments in the block scale (L=10–100m) These have been carried out in conjunction with cross-hole interference tests. Tracer dilution tests were also performed in conjunction with cross-hole tests. These tests were perhaps the most important of the pre-tests, performed to identify and screen among possible injection points, and to verify the hydrostructural model valid at a given time. The latter tests have been conducted both at ambient flow conditions and during pumping at a specified location. A large drawdown response combined with a “flow response” was in general considered to single out a potential injection section.

In addition to the single-hole tracer tests (tracer dilution tests), a large number of cross-hole tracer tests were subsequently performed with the ultimate objective to select the tracer test geometry (source-sink combinations) suitable for tests with radioactive sorbing tracers. The main factor for selection was the tracer mass recovery. Even though the main purposes of cross-hole tests were to verify connectivity and mass recovery and help to select flow paths for retention experiments, a secondary objective was to actually characterise the flow paths, i.e. to determine advective transport properties. A specific objective coupled to transport was also to study possible effects of fracture intersection zones (FIZ).

One of the key problems with tracer tests run on larger length scales was to select a test geometry, which gave a sufficiently high mass recovery, and at the same time enabled performance of informative cross-hole sorbing tracer tests within reasonable time frames. Experience from the TRUE-1 experiments /Winberg et al, 2000/ showed that the use of tracer dilution tests in combination with cross-hole interference tests was a good set of tools for optimising the selection of potential injection and sampling points for tracer tests.

The TRUE Block Scale tracer test programme involved 14 tracer tests campaigns, performance of 32 tracer injections in 16 different combinations of source and sink pairs (flow paths). This set of in situ data is one of the largest ever collected concerning transport of solutes in fracture networks over distances ranging from 10 to 130 metres.

Tracer test methodology

The injection equipment was designed to create an internal circulation in the injection borehole. The circulation enabled a homogeneous tracer concentration inside the borehole and the possibility to sample the tracer concentration outside the borehole in order to monitor the dilution of the tracer with time.

Three different injection methods were applied during the test programme; decaying pulse, finite pulse and forced pulse (unequal dipole). In later stages of the project, after having decided which sink to use for the tracer retention tests (Phases B and C) it was identified that forced injection had to be employed in order to enable detection of tracer at the sink due to dilution, and also to avoid problems with the tailing of the injection curve which could potentially mask retention processes manifesting themselves at late times. Also, for the injection of Helium it was necessary to minimise the tracer residence time in the injection section to avoid diffusion of Helium through the equipment. The obvious advantage in this context is that tracer quickly leaves the injection borehole when forced injection is employed. The main disadvantage is that the convergent flow field is disturbed and that the tracer mass is spread out in a basically uncontrolled way over a larger area around the injection section.

Tracers used

In order to facilitate a sufficient number of conservative tracers, a literature review and an in situ pilot test were conducted. The field tests were performed in a relatively short flow path (3.2 m) with a relatively short mean residence time (about one hour). Even though the travel distance and residence time were short, clear indications of delay (or degradation) of the tested tracers could be noted. The results of the tests in combination with cost aspects and the dynamic range of the tracers (relation between maximum solubility and minimum detectability), identified three groups of possible new tracers:

- Fluorescent dyes (Naphtionate, Pyranine, Dimethylfluorescein).
- Metal complexes (In-, Yb-, Lu-, Tm-, Tb-EDTA, Gd-, Ho-, Dy-, Eu-DTPA) and Re as ReO_4^-.
- Dissolved Helium gas.

Among the fluorescent dye tracers used, Uranine, Eosin Y, Dimethylfluorescein, Naphtionate, Pyranine and "UV-1" behaved satisfactorily in the in situ pilot tracer test and were therefore considered as possible candidates. Furthermore, a HPLC detection procedure was developed in which simultaneous detection could be performed for Uranine, Eosin Y, Dimethylfluorescein, Naphtionate and Sulforhodamine G.

Three fluorescent dye tracers performed unsatisfactorily in the in situ pilot tracer experiment. A significant precipitation/sorption occurred for Rose Bengal and Phloxine B already in the injection borehole. The recovery of Sulforhodamine G was significantly lower than the simultaneously injected Uranine.

A study concerning the application of solvent extraction for volumetric enrichment of Fluorescein (Uranine) and Fluorescein derivatives showed promising results in that volumetric enrichment could be performed of all Fluorescein derivatives used. A combination of solvent extraction for volumetric enrichment and HPLC-detection could significantly increase dynamic range and the potential for use of fluorescent dye tracers in future tracer tests.

The pilot study in total identified a large number (>15) of possible non-sorbing tracers that could be used in future tracer tests at the TRUE Block Scale site, and elsewhere.

Sorbing (reactive) tracers were selected among the elements of the alkali and alkaline earth metals previously used in the TRUE-1 experiments /Winberg et al, 2000/. These are featured by ion exchange as the main sorption mechanism. General observations from the TRUE-1 in situ experiments were; Na^+, Ca^{2+} and Sr^{2+} were transported only very slightly retarded compared with the non-sorbing tracers, Rb^+ and Ba^{2+} moderately retarded and Cs^+ strongly retarded. Using the concept of a retardation coefficient for each tracer, it was identified as necessary to use tracers like Rb^+, Ba^{2+} and Cs^+ to be able to observe a significant retardation. However, it was also considered likely that transport over longer distances (like in TRUE Block Scale) would result in increased retardation, and that breakthrough would only be obtained from slightly/weakly sorbing tracers (like Na^+, Ca^{2+} and Sr^{2+}). It was therefore decided that at least one slightly sorbing tracer and one strongly sorbing tracer should be used in each injection.

Apart from the radioactive sorbing tracers, radioactive non-sorbing tracers were used as a complimentary conservative reference, e.g., $^{82}Br^-$ in injection C1, $^{186}ReO_4^-$ in injection C2, HTO (tritiated water) in injection C3 and a combination of $^{82}Br^-$ and $^{131}I^-$ injection C4. In the injections C1 and C2 the radioactive non-sorbing tracers were rather short-lived and it was therefore decided to also use Uranine (C1) and Naphtionate (C2) as tracers.

Interpretation of retention from tracer injection data

Previously in the TRUE Programme, values of the surface distribution coefficient K_a have been evaluated from performed laboratory experiments /Byegård et al, 1998/. As part of the TRUE Block Scale Project attempts were made to evaluate surface distribution coefficients from the retardation noted in the injection curves from TRUE-1 /Winberg et al, 2000/ and TRUE Block Scale. The K_a values evaluated were found to be of a magnitude equitable to the laboratory K_a values from TRUE-1. In addition, effects of matrix diffusion, sorption kinetics model, non-linear sorption were analysed using both TRUE-1 and TRUE Block Scale data.

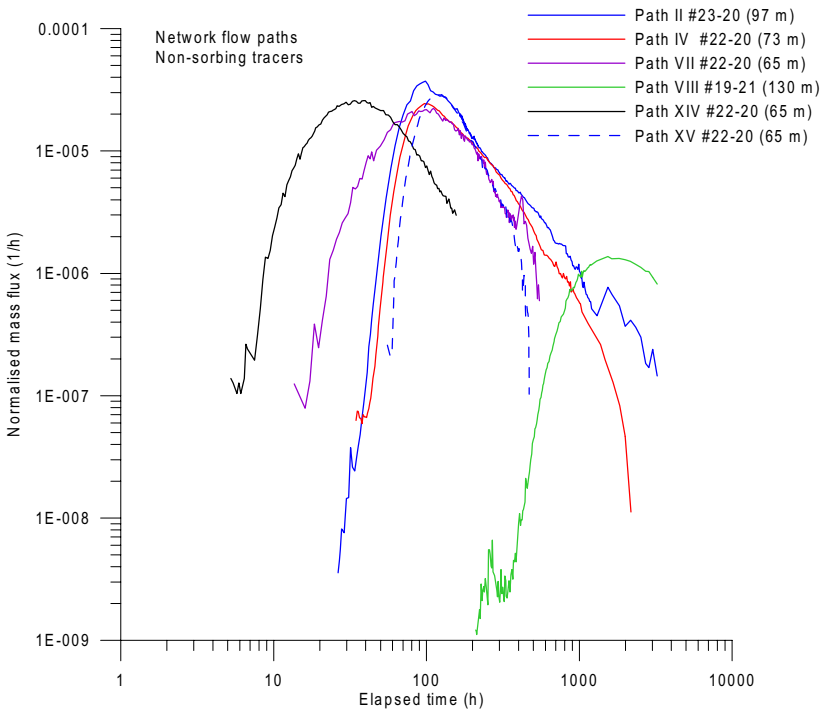

Figure EX-1. *Comparison of tracer breakthrough in six "network" flow paths.*

Conservative transport

The evaluation and interpretation of the tracer breakthrough curves indicated response of a heterogeneous system, observed both within single structures and in network of structures. The two single structures investigated with tracer tests, #20 and #21, both showed an internal variation of about one order of magnitude in evaluated hydraulic fracture conductivity, equivalent fracture aperture and flow porosity. However, the two structures were found to be different in character where Structure #20 is more of a narrow and high-conductive single structure whereas Structure #21 probably is more complex than assumed at the onset of the investigations. The latter has a lower hydraulic fracture conductivity but a higher flow porosity and a characteristic of the breakthrough curves more resembling that of the network flow paths. Thus, Structure #21 more likely consists of several sub-parallel structures than a single fracture.

The six network flow paths investigated over distances between 12–55 m in space and 57–130 m along the structures, according to the developed hydro-structural model, show a large variation in mean travel times (42–2200 hours), cf Figure EX-1, but at the same time exhibit a relatively narrow range of evaluated hydraulic fracture conductivity and equivalent fracture aperture (within a factor 3). Notable is also that the transport parameters obtained are within the same span as for Structure #21. This again may indicate that Structure #21 is made up of a network of structures.

Retention

Three flow paths (I–III) were investigated with a set of radioactive sorbing tracers, mainly monovalent and divalent cations from the alkali metal and alkaline earth metal groups. When compared with the results from the TRUE-1 tracer tests, both similarities

and differences are observed. Firstly, the order of retention between the different species was found to be the same as in TRUE-1 and in the laboratory tests, i.e. $Na^{+}<Ca^{2+}\approx Sr^{2+}<Ba^{2+}\approx Rb^{+}<Cs^{+}$. Another similarity is that the retardation, expressed as the ratio of the time at which 50% of the sorbing tracer was recovered divided by the time of 50% recovery of the conservative tracer ($R_{50\%}$) is about the same for most species when comparing TRUE-1 to the results of injection C1 and C4 in Structure #20, cf Figure EX-2. No breakthrough of $^{137}Cs^{+}$ (C2) and $^{83}Rb^{+}$ (C3) is noted after some 3300 hours of pumping. However, for the breakthrough of sorbing tracers in C3 (Na^{+}) and C2 (Ca^{2+}) a 30–80% stronger retardation (expressed as the ratio between time at which 50% of the mass of sorbing tracer has arrived and the corresponding time for the conservative tracer, $R_{50\%}$) was noted. The reasons for this somewhat enhanced retardation between the single flow paths (C1 and C4) and the two slower and more complicated flow paths (C2 and C3) may be several:

- Presence of gouge material (fine-grained fault gouge) in fractures/structures.
- Presence of gouge material in fracture intersection zones.
- Differences in the mineralogy along the flow paths.
- Larger portions of stagnant water to interact with along the flow path.
- Higher porosity in the fracture rim zone.

A detailed evaluation of the observed retardation is performed through an analysis using a number of different modelling concepts which is described by /Poteri et al, 2002/.

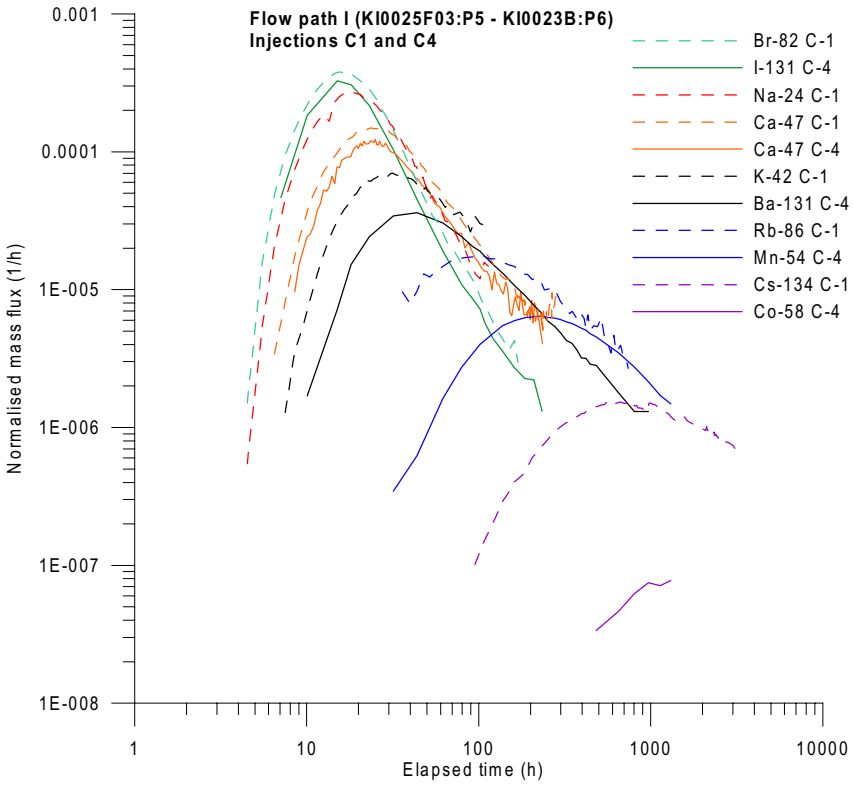

Figure EX-2. *Normalised tracer breakthrough for all tracers injected in tests C1 and C4.*

Contents

1 Introduction

1.1 Background

Concepts for deep geological disposal of spent nuclear fuel include multi-barrier systems for isolation of nuclear waste from the biosphere. Waste forms, and concepts for encapsulation of the waste and engineered barriers may vary between countries, but most concepts rely on a natural geological barrier which should provide a stable mechanical and chemical environment for the engineered barriers, and should also reduce and retard transport of radionuclides released from the engineered barriers. In case of an early canister damage, the retention capacity of the host rock in relation to short-lived radionuclides such as Cs and Sr become important.

In planning the experiments to be performed during the Operating Phase of the Äspö Hard Rock Laboratory, the Swedish Nuclear Fuel and Waste Management Company (SKB) identified the need for a better understanding of radionuclide transport and retention processes in fractured crystalline rock. The needs of performance assessment included improved confidence in models to be used for quantifying transport of sorbing radionuclides. It was also considered important, from the performance assessment perspective, to be able to show that adequate transport data and parameters (distribution coefficients, diffusivity, parameters similar to the "flow wetted surface area", etc) could be obtained from site characterisation, or field experiments, and that laboratory results could be related to retention parameters obtained in situ. To answer these needs, SKB in 1994 initiated a tracer test programme named the Tracer Retention Understanding Experiments (TRUE). The objectives of TRUE are given in Section 1.2.

The First Stage of TRUE /Winberg et al, 2000/ was performed in the detailed scale (0–10 m) and was focused on characterisation, experimentation and modelling of an interpreted single feature. Work performed included staged drilling of five boreholes, site characterisation, and installation of multi-packer systems to isolate interpreted hydraulic structures. Subsequent cross-hole hydraulic tests and a comprehensive series of tracer tests were used to plan a series of three tracer tests with radioactive sorbing tracers. The in situ tests were supported by a comprehensive laboratory programme performed on generic as well as on site-specific material from the studied feature. In addition techniques for characterisation of the pore space of the investigated flow paths using epoxy resin have been developed and successfully tested in situ.

The various phases of tracer testing performed as part of TRUE-1 were subject to blind model predictions and subsequent evaluation /Elert, 1999; Elert and Svensson, 2001/. The results of the TRUE-1 experiments showed clear evidence of diffusion, attributed by some researchers as diffusion into the rock matrix with associated sorption on inner pore surfaces. Other researchers claim that the observed retention can be attributed to diffusion/sorption in fine-grained fault gouge material. A clearer distinction between the two alternative interpretations can only be achieved with a full implementation of the developed resin technology to the investigated feature.

When the TRUE Programme was set up it was identified that the understanding of radionuclide transport and retention in the Block Scale (10–100 m) also required attention in terms of a separate experiment.

This report presents the results of tracer tests performed with non-sorbing (conservative) and sorbing (reactive) tracers performed in the identified fracture network in the investigated TRUE Block Scale rock volume.

1.2 Rationale

1.2.1 Performance assessment

The block scale is important since it corresponds to the distance, "security distance" as defined by various national programs, between the geological repository and the nearest major fracture zone. In such geological environments it is also assumed that the bulk of the retention provided by the natural bedrock barrier is provided in this region.

As a consequence, the block scale is also an important modelling issue, cf Section 1.2.3. Prioritised aspects are to improve understanding of the nature of transport paths in block scale crystalline rock and the geological control on retention, and to assess the flow wetted surface, or equitable entities, on the scale in question.

1.2.2 Site characterisation

The block scale is also important from a characterisation perspective. Firstly, to provide the necessary data from which the geometrical, conceptual and numerical models are built, which are used to assess a given site. Secondly, the data collected in the block scale, whether obtained from the surface or from underground openings, are important for the detailed layout and design of a repository. This applies both to the positioning of storage tunnels and possible canister boreholes.

An experiment on the block scale hence provides a training ground for developing tools and methodologies to be employed in future site characterisation for a geological repository, and as support for moels and concepts utilised in performance assessments.

1.2.3 Modelling

The block scale (10–100 m) is an important scale in that it may be the smallest scale at which the stochastic continuum approach to groundwater flow and transport in fractured rock can be used with good results for prediction of flow and transport phenomena. At smaller scales, with the need to include a higher degree of complexity/heterogeneity, discrete approaches may be more appropriate.

At the same time, the block scale constitutes a challenge for the more performance assessment related approaches such as the LaSAR and POSIVA approaches. Despite the simplification of the natural system employed in the TRUE Block Scale modelling the question remains; do the employed models provide adequate descriptions of flow and transport and are the model results adequate?

One of the basic ideas embedded in the TRUE Programme is that experimentation at various scales, laboratory (< 0.5 m), detailed scale (< 10 m) and block scale (10–100 m) will provide a basis for improved understanding on how to model flow and transport, and how link transport models and transport parameters at different scales. It is expected that through this platform the uncertainties associated with extrapolation and prediction on a site scale (0.1–1 km) will be reduced. The TRUE Block Scale experiment here constitutes the higher end member of the studied experimental scales.

1.2.4 Transport and retention

The principal difference between the TRUE-1 and TRUE Block Scale experiments is obviously the difference in spatial scale in the experimentation. Of principal interest is whether the longer transport distances in themselves, through a higher degree of heterogeneity will provide exposure to larger surface area, and thus more retention.

In addition, the performance of tracer tests in a network of structures implies that flow paths/transport routes will, to a variable degree, be affected by fracture intersection zones (FIZ) which are formed by intersecting structures. Although TRUE Block Scale does not provide an experimental array with the specific aim to investigate FIZs, the results from the performed experiments may still provide indirect evidence of the possible effects of FIZs. In TRUE Block Scale, both multi-structure flow paths and interpreted single structures have been identified and tested using transport experiments, the division being about 50:50 amongst performed tests with conservative tracers.

The results from the TRUE-1 experiments /Winberg et al, 2000/ showed a consistent relative order amongst the utilised radioactive sorbing tracers (in order from lowest sorptivity); $Na^{+} < Ca^{2+} \approx Sr^{2+} << Rb^{+} \approx Ba^{2+} < Cs^{+}$. This relative order was observed both in the laboratory and in situ. An observation of this relative order in larger scale would prove a conceptual verification of the retention properties.

Explicit evidence for the existence of gouge material (fault breccia/fine-grained fault gouge) have not been found in the investigated Feature A at the TRUE-1 site /Winberg et al, 2000/. Modelling performed within the Äspö Task Force has shown that assumptions of a geologic material with increased porosity/sorptivity in direct contact with the flowing groundwater, e.g., gouge material, can explain the observed increased retention in TRUE-1. Fault gouge can be very weak and difficult to recover, even using sophisticated triple-tube coring. In the network of structures investigated as part of TRUE Block Scale, however, there is a firm evidence of fault breccia from the core logging, cf /Andersson et al, 2002/. Laboratory analyses, with all due respect to uncertainties about the distribution of fault gouge material along a flow path, are expected to provide means for assessing the relative contribution to retention from the rock matrix and fault gouge material, respectively.

1.3 Previous experience of tracer tests in the block scale

A compilation of in situ tracer tests at various test scales and conditions, relevant to the Swedish nuclear waste research programme has been presented by /Andersson, 1995/. The account below is partly based on tests that are part of that compilation.

1.3.1 Finnsjön

Transport scale: 150–200 m

At the Finnsjön test site, central eastern Sweden, a subhorizontal major fracture zone was investigated during 1984 through 1990. The objective of the study was to characterise the flow and transport properties of the zone and to localise potential pathways for groundwater flow and transport of solutes essential for the safety of a nuclear repository. At the site there are a number of gently dipping (0–30 degrees) fracture zones common in the foliated granodiorite at the site. Identification and characterisation of these fracture zones were accomplished through a broad range of geological, geophysical, geomechanical, geochemical and hydrological investigations.

Through these investigations, a gently dipping fracture zone, denoted Zone 2, was defined over an area of about 1500x500 m with a depth range of 100–300 m below ground surface The zone, which is about 100 m thick, was developed 1.7–1.6 Ga as a ductile shear zone at a depth of approximately 10–15 km, and repeated reactivation has occurred during Precambrian time and later /Ahlbom and Smellie, 1991/. The identified zone was selected for detailed studies aimed at understanding flow and transport in the zone, and its interactions with the surrounding bedrock. Hydraulic measurements of the zone included piezometry, single-hole hydraulic tests at different scales (section lengths), cross-hole interference tests, groundwater flow measurements, and tracer tests (converging and dipole flow fields).

It was found that the upper part of the zone is highly permeable with a transmissivity in excess of 10^{-3} m^2/s. The highly permeable sections have widths of about 0.5 m. This enhanced permeability as seen over a vast area was attributed to recent opening of the zone during the most recent glaciation period. The performed cross-hole interference tests have shown that the identified highly conductive section is interconnected over distances of several hundred meters.

The objective of the performed radially converging tracer test was to determine flow and transport characteristics in a major fracture zone. Secondary objectives included testing and improvement of equipment, experimental design and methods of interpretation. A converging flow field was established in the subhorizontal fracture zone (Zone 2) by extracting water at 120 l/min from a packed off interval enclosing the whole thickness of the zone. The pumping lasted 6 months after beginning of the tracer injections. Conservative tracers (rare earth metal DTPA and EDTA complexes, ions and fluorescent dyes, 11 different tracers in all), were injected from 9 borehole sections. Straight-line flow path distances ranged from 155 to 200 m. The hydraulic gradient during the test was low (0.005 m/m). Interpretation of the tests was facilitated by independently calculated data (tracer mass release per unit time into the fracture)

enabled by the developed injection techniques. Analysis of possible interconnected sub-zones was checked by sampling major hydraulic conductors in the pumping borehole. Flow rates, hydraulic head, delay and dispersion in the pumping well were also measured. Evaluation was done using both one- and two-dimensional models. Tracer breakthrough was observed from all nine injection points, with first arrivals ranging between 24 to 3200 hours. Evaluated flow and transport parameters included flow porosity, dispersivity, fracture aperture and hydraulic conductivity in the flow paths. Directional variations in the determined flow and transport parameters were found, attributed to heterogeneity and/or anisotropy, and found to be more pronounced at depth in Zone 2. The upper part of Zone 2 was found to highly conductive and continuous over hundreds of meters. Dispersion expressed as Peclet numbers ranged from 16–40, flow porosity in the upper part was 0.001–0.05 and 0.01–0.1.

Subsequently a dipole tracer test was conducted in the upper highly conductive part of Zone 2. The objective of this test was to determine the transport parameters for Zone 2 and to test the applicability of the method for characterising major fracture zones at larger scales. The geometry employed allowed direct comparison with the preceding radially converging tracer experiment. The dipole experiment involved a total of 15 injections. Tracers used included 15 short-lived radionuclides and 5 inactive tracers. Cocktails including both sorbing and non-sorbing tracers were injected, and some of them on several occasions. The dipole length was of 168 m with intermediate observation (sampling) holes inside the flow field at distances of 157 and 223 m, respectively. Evaluation of the dipole tracer tests, using 2D SUTRA numerical model analysis and 1D analysis of breakthrough curves, included inverse modelling of breakthrough curves with the aim to quantify certain parameters which could be related to the flow and transport properties of the zone and the tracers used.

In the dipole test, it was found that the variation in residence times, dispersivities and recoveries of the anionic non-sorbing tracers ($^{82}Br^-$, $^{131}I^-$ and $^{186}ReO_4^-$) was small. The EDTA metal-complexes used, i.e., $^{51}CrEDTA^-$, $^{58}CoEDTA^-$, $^{111}InEDTA^-$, $^{160}TbEDTA^-$ and $^{169}YbEDTA^-$ were recovered with similar residence times as the non-sorbing tracers. However, the recovery decreased in the order Yb>In>Cr>Co>Tb, indicating varying amount of irreversible losses occurring due to de-complexation of the EDTA from the metal ions. The DOTA complexes used, $^{140}LaDOTA^-$ and $^{177}LuDOTA^-$ together with the fluorescent dye Rhodamine WT, were all found to be somewhat delayed compared to the non-sorbing tracers, indicating a weak reversible sorption to the geologic material in the fracture. $^{24}Na^+$ was not delayed but showed lower peak values and less mass recovery, while no recovery at all was obtained for the other cationic tracers used, i.e., $^{58}Co^{2+}$, $^{86}Rb^+$ and $^{201}Tl^+$. Three injections were performed of the anionic form of Tc, i.e., $^{99m}TcO_4^-$ without any recovery being observed. The main transport mechanism during the experiments is advection and the only other mechanism needed to explain the test results is dispersion. Matrix diffusion was found to be negligible.

The Finnsjön experiments were the focus of model analysis within the International INTRAVAL project /Andersson and Winberg, 1994/. Results and interpretation of the dipole experiment results has been given by /Byegård et al, 1991, 1992, 1999, 2000; Andersson et al, 1993/.

1.3.2 El Berrocal

Transport scale: 15–25 m

The international El Berrocal project, performed at an uranium deposit some 90 km SW of Madrid, constituted an integrated exercise in geological, geochemical and hydrogeological characterisation with the ultimate aim to model and understand the past and present-day migration processes that control the behaviour and distribution of naturally occurring radionuclides in a granitic environment /Rivas et al, 1998/. The objectives were broadly focused on those particular processes, which have relevance to safety assessments for geological repositories for radioactive waste /Guimerà et al, 1997/.

Performed studies included geological, structural, mineralogical, geochemical and hydrogeochemical studies at various scales. Tracer tests were performed at two sites involving a total of 5 boreholes /Guimerà et al, 1996/. Hydrogeological investigations were conducted as part of the planning and design of tracer tests at the two sites.

The field tracer programme included tracer test runs in the most conductive zones between boreholes over distances ranging from 14 to 25 metres. Forced and non-forced injections in steady convergent flow fields using non-sorbing tracers were employed. The programme also included tracer dilution tests, supporting laboratory tests and development of new down-hole and injection/sampling equipment.

1.3.3 Grimsel

Transport scale: 5–70 m

At the Grimsel Test Site, a fracture system flow test (BK) has been performed. The objectives of this test /Liedke and Zuidema, 1988/ were to; 1) provide more information on transport of dissolved materials in fracture systems, 2) develop a technique for investigating fracture systems, and 3) develop and test equipment. The ultimate aim, 4) was to integrate the findings and developments into a comprehensive strategy for site assessment. In total, some 10 boreholes were drilled in a fan-type array in which different types of hydraulic tests were conducted. The major conducting fractures and fracture zones were packed-off with packer systems. In assessing solute transport, injections of brines were used. The background salinity of the Grimsel waters facilitates the use of brine and also enables use of borehole radar to map the evolving plume of migrating salt. The brine tracer tests performed in the BK site cover distances between 5 to 70 m /Liedke et al, 1994/.

During Phase II and III of the Grimsel experiments, renewed attention was given to the BK site with comprehensive investigation programmes including fluid logging, hydraulic cross-hole testing, combined salt/heat tracer tests and a project for integrating, visualising and modelling the site /Marschall and Vomvoris, 1995/. It was identified that the most valuable information about the internal structure of the BK site stems from the fracture mapping of the drill cores and tunnel walls. The large number of boreholes drilled (N~20) provided a detailed description of boundaries, main fracture sets and their relevance for the flow system. However, the large number of boreholes was found

to disturb considerably the flow conditions by short-circuiting hydraulic features. Not only did the overall connectivity increase, but also the hydraulic pressure distribution changed completely. As a result the NAGRA researchers strongly recommended to keep the number of boreholes down in future site characterisation, and to avoid preferential orientation of the boreholes, in order to avoid bias in inferred fracture orientations. Because of the strong element of short-circuiting, the long-term monitoring of pressure at the site did not fully meet expectations, and also affected performed hydraulic tests and tracers tests.

Despite the identified drawbacks and problem areas, the greatest benefit of the BK programme is found to be the development of equipment and methodologies for site characterisation. One interesting component in the Phase III research being the use of combined salt and heat tracer experiments. The use of combined flow fields and combined tracers were identified as means to obtain a better understanding of basic processes, which govern flow and transport in fractured formations.

1.3.4 Kamaishi

Transport scale: <10 m

The Kamaishi mine located on the north-eastern coast of the Honshu island has been the setting for a comprehensive study on fluid flow and mass transport properties of fractured granite /Shimo et al, 1999/. The investigations consisted of three major stages; 1) characterisation of the geometry and geology of the fracture system, 2) hydraulic characterisation of the fracture system and 3) tracer tests. The experimental area is located at a depth of about 350 m below surface. The geology is featured by metamorphic iron-bearing formations and intrusions of granodiorite. The test area is located in the latter rock type.

Initial characterisation, test design and definition of the testing program was largely driven by the discovery of a flow barrier in one of the boreholes drilled to investigate the boundary conditions. Minute measurements of pressure revealed a sudden increase in pressure from 200 kPa (20 m) to 2 MPa (200 m), indicating a barrier between the part of the fracture network being drained towards the mining works, and parts of the network with high pressure having poor connection to the underground openings. A strategy was developed which targeted the region characterised by high groundwater pressure for tracer tests. The area could be reached by relatively short boreholes (<80 m) and minor effects of the mine could be noted.

The experimental area was developed in an iterative fashion where the groundwater pressures in packed-off borehole sections were monitored during the drilling of each new borehole. A total of seven boreholes were drilled. After drilling the new boreholes, they were flow-logged with a 1-m resolution and surveyed using borehole TV and core examination to identify the geological attributes associated with noted flow anomalies. More than 3000 fractures were mapped in the seven boreholes. The flow logging in 1-m sections governed the positioning of the packers of the multi-packer system to be emplaced in each new borehole. Up to ten packers were used /Sawada et al, 2000/. The flow logging also provided estimates of transmissivity. A synthesis of performed pressure registrations indicated that the initial model with two regions with different

hydraulic pressure was too simplistic. At least six hydraulically isolated zones (compartments) were identified, featured by similar static hydraulic head, and common response pattern to a given outer disturbance. The latter also included analysis of the transient response, which also showed distinct differences between the compartments.

After completion, a series of cross-hole pressure interference tests were run by withdrawing water from selected test sections. The test results confirmed the interpreted compartment geometry and provided additional information on hydraulic properties. Three fractures/zones, identified in 2–5 boreholes with a separation of approximately 2–8 m, were subsequently used for tracer tests in dipole configuration /Sawada et al, 2000/. A total of fifteen tests using NaCl as a tracer were performed in the three structures with dipole ratios varying between 1 to 8 to study the heterogeneity, anisotropy and effects of reversed flow fields and dipole relative strength (plume spread) within the studied structures.

1.3.5 Stripa Mine (3D tracer migration and SCV tracer migration)

Transport scales: 10–60 m

The Stripa mine has over a long period time, 1978 –1992, been a testing ground for development of techniques and methodologies for site characterisation for a geological repository.

In Phase 2 of the Stripa work an investigation was undertaken to study the migration of tracers in a large mass of fractured granitic rock in the Stripa mine /Abelin and Birgersson, 1987; Abelin et al, 1987a,b,c/. This investigation known as the 3-D tracer migration experiment, had multiple objectives, including in particular the development of techniques for performing large scale tracer tests in low-permeability fractured rock. The other objectives involved obtaining information of longitudinal and transverse dispersion and channelling in the studied rock mass, along with a determination of flow porosity and assessment of applicability of transport models. The experiment involved construction of a 100 m long drift and injection of 9 conservative tracers in borehole sections at various distances (up to 56 m) from the drift, with the aim to assess variations in transport properties of the rock. Injection was made at constant pressure over a period of 20 months at injection flow rates varying between 1–20 ml/h in selected borehole sections. Breakthrough of the injected tracers to the drift was monitored in about 350 sampling areas on the 700 m^2 walls/roof of the drift (2 m^2) for a period of 6 months after termination of injection. Groundwater inflow to the plastic sheets showed a large degree of variability with 50% of the inflow emanating from 3% of the covered area. One sheet.alone accounted for 10% of the total inflow, the latter which was 700 ml/h. Travel times of the seven tracers showing breakthrough varied between 2000 and 7000 hours with mass recoveries ranging between 3 and 65%. Injection points were selected on the basis of borehole radar, core logging and water inflow measurements. This information was however not found adequate to provide the basis for explaining the tracer migration results in their entirety /Gnirk, 1993/. The experiment clearly demonstrated the need for a greater amount of detail concerning the structure of the rock mass and the distribution of circulating groundwater. It was also evident that attention had to be paid not only to effectively collecting water from the tunnel walls and roof, but also from the floor of the tunnel.

The Site Characterisation and Validation (SCV) Project was performed as a part of Phase 3 of the OECD/NEA Stripa Project from 1986 to 1992. The objectives of the project were to test the predictive capabilities of newly developed radar and seismic characterisation methods and numerical groundwater models /NRS, 1996/. A basic experiment was designed to predict the distribution of water flow and tracer transport through a volume of granitic rock before and after excavation of a subhorizontal drift (the validation drift) and to compare these predictions with actual field measurements. A multidisciplinary characterisation programme was implemented from drifts and boreholes drilled from the drifts. The dimensions of the investigated volume were approximately 150x150x150 m. A large scale tracer test, known as the tracer migration experiment, was conducted at the SCV site as part of the site characterisation and validation programme /Birgersson and Ågren, 1992; Birgersson et al, 1992,a,b,c/. The objectives of this experiment were to study tracer migration in a fracture zone, as well as in an averagely fractured rock outside the fracture zone. Further, in order to obtain data to be used in evaluation of the validity of the groundwater flow and transport models applied at the SCV site. The site had a rather well defined steeply dipping fracture zone, 6 m wide, intersected by the so-called Validation Drift, and verified by radar, seismics and hydraulic tests in boreholes. Detailed characterisation of the interior structure of the zone was made by mapping injected saline solutions using borehole radar. Injection points for tracer were located principally within the zone, with one point in the competent rock. These points were located between 10 to 25 m from the drift. A combination of 12 different tracers was injected over periods of months to seven months. Tracer breakthrough in the drift was monitored by a combination of plastic sheets on side walls and roof, and drift and sump holes in the lower walls and floor. Some 150 breakthrough curves were obtained, indicating breakthrough for all tracers, but in varying amounts (mass recoveries between 10 and 60%). Mean residence time varying between 1500 to 400 hours was noted. Apart from hydrodynamic dispersion, transport in channels with different transport properties was hypothesised /Gnirk, 1993/.

1.3.6 Whiteshell (URL)

Transport scale: 10–50 m

The Moderately Fractured Rock (MFR) Experiment /Frost et al, 1998; Jensen, 2001/ was initiated in 1993 at the Underground Research Laboratory (URL), with the intent of increasing the knowledge of mass transport through fractured crystalline rock. The experiment is a multi-disciplinary undertaking involving the characterisation and numerical simulation of groundwater flow and mass transport in an approximately 100,000 m^3 volume of MFR located on the 240 Level of the URL. The primary objective of the experiment is to explore the validity of the Equivalent Porous Medium (EPM) approximation for simulation of mass transport through an interconnected fracture network. Experimental activities also intend to examine issues of relevance to geosphere Performance Assessment (PA) in the context of the characterisation and description of flow domain spatial variability, parameter scale dependence, and derivation of abstracted effective mass transport properties for PA model simulations.

The initial phase of the MFR experiment, which involved the characterisation and development of a conceptual flow model for the MFR domain, was completed in 1998. Characterisation activities included litho-structural mapping, fracture infilling

mineralogy identification, hydrogeochemical sampling, cross-hole geophysical surveys, single and cross-bore hydraulic testing and hydraulic head monitoring within a array of ten sub-horizontal boreholes. An internally consistent conceptual flow model derived from these data provided a basis for a deterministic numerical realisation of groundwater flow using the 3-dimensional finite element code MOTIF. Calibration of this MFR mathematical model was achieved through comparison with cross-hole hydraulic interference test results.

Phase II of the MFR experiment included a sequence of tracer experiments at scales of 10 to 50 metres in a divergent field, one source interval and 1–3 sink intervals. Section intervals were 30–40 m with a separation distance of 13–50 m. The tracer experiments were performed as forced gradient non-circulating dipole tests with halide (LiBr and RbI), fluorescent dye (Lissamine) tracers and fluorescent latex colloids (0.19, 0.22 and 0.56 μm). Tracer breakthrough was observed for Br, I, Li and Lissamine FF. Mass recoveries of the conservative species were less than 30%, attributed to divergent flow fields. Interestingly, supporting batch sorption laboratory experiments had indicated that Li was selectively sorbed on montmorillonite clays. However, the observed similarity between the Br and the Li breakthrough suggested transport of Li without significant retardation. The moderately sorbing Rb was not observed at any of the withdrawal sections. More surprisingly, the fluorescent latex colloids were not detected at any of the withdrawal sections, suggesting effective filtration within the fracture network.

The tracer tests with non-reactive, reactive and colloidal tracers have served to explore the applicability of continuum models for prediction of flow and mass transport. Performed modelling has incorporated the use of geostatistical techniques to explore the influence of permeability field variability on mass transport.

1.3.7 Äspö HRL

Transport scale: 100–380 m

The so-called LPT-2 experiment was conducted as the final part of the pre-investigation phase of Äspö HRL project. The experiment was a combined large scale pumping and tracer test designed to evaluate site scale responses, and included a large number of boreholes/borehole intervals. The specific objectives were to 1) verify major conductive structures, especially connectivity between structures (confirmation of structural model and geohydrological interpretation), 2) act as a calibration case for the site scale groundwater flow model, and 3) attempt to provide data on transport of solutes on the site scale /Rhen et al, 1992/.

Identification of suitable injection sections around the proposed pumping borehole (KAS06) was identified through a comprehensive tracer dilution measurement campaign (68 measurements) in neighbouring boreholes. Tracer injections were made in five neighbouring boreholes in six different sections. Four different non-sorbing tracers were used (^{114}InEDTA$^-$, $^{131}I^-$, $^{186}ReO_4^-$ and Uranine. The use of short-lived radioactive tracers facilitated detection in low concentrations and the possibility of in situ detection in boreholes (location of inflow of traced water). Injections were made as decaying pulse injections. Gamma spectrometry measurements using a down-hole NaI(Tl) scintillation detector probe were made at 8 different levels in the pumped

borehole, corresponding to conductive structures, five of them labelled fracture zones. Breakthrough was observed from four of the injections and with a distributed breakthrough along the pumped borehole, indicating that a number of multi-structure flow paths had been activated in the test. The evaluated trajectories along the interconnected structures vary between 220 and 380 m. It was found that the tracer test results were consistent with the framework of the fracture zones contained at the structural model of Äspö at the time. Evaluated residence times varied between 220–1135 hours. Evaluated flow porosities ranged between $2 \cdot 10^{-4}$ and $5 \cdot 10^{-2}$.

The LPT-2 experiment was used a modelling task in the analysis within the Äspö Task Force on Modelling of Groundwater Flow and Solute Transport /Gustafson and Ström, 1995/.

1.4 Main findings from the First TRUE stage

The first stage of the Tracer Retention Understanding Experiments (TRUE-1) /Winberg et al, 2000/ was performed as a SKB funded project. The overall objectives of TRUE are to develop the understanding of radionuclide migration and retention in fractured rock, to evaluate the realism in applied model concepts, and to assess whether the necessary input data to the models can be collected from site characterisation, cf Section 1.5. Further, to evaluate the usefulness and feasibility of different model approaches, and finally to provide in situ data on radionuclide migration and retention. The strive to address with multiple model approaches was facilitated through a close collaboration with the Äspö Task Force on Modelling of Groundwater Flow and Transport of Solutes. The TRUE programme is a staged programme which addresses various scales; from laboratory (< 0.5 m), detailed scale (< 10 m) and block scale (10–100 m). The First TRUE Stage was performed in the detailed scale with the specific objectives of providing data and conceptualising the investigated feature using conservative and sorbing tracers. Further, to improve methodologies for performing tracer tests, and to develop and test a methodology for obtaining pore volume/aperture data from epoxy resin injection, excavation and subsequent analyses.

The experimental site is located at approximately 400 m depth in the north-eastern part of the Äspö Hard Rock Laboratory. The identification of conductive fractures and the target feature has benefited from the use of BIPS borehole TV imaging combined with detailed flow logging. The assessment of the conductive geometry has been further sustained by cross-hole pressure interference data. The investigated target feature (Feature A) is a reactivated mylonite, which has later undergone brittle deformation. The feature is oriented northwest, along the principal horizontal stress orientation, and is a typical conductor for Äspö conditions. Hydraulic characterisation shows that the feature is relatively well isolated from its surroundings. The near proximity of the experimental array to the tunnel (10–15 m) implies a strong hydraulic gradient (approximately 10%) in the structure, which has to be overcome and controlled during the experiments.

A methodology for characterising fracture pore space using resin injection, excavation using large diameter coring and subsequent analysis with photo-microscopic and image analysis techniques was developed and tested at a separate site. The results show that epoxy resin can be injected over several hours, and that the estimated areal spread is in the order of square metres. The mean apertures of the two investigated samples were 239 and 266 microns, respectively. Assessment of spatial correlation shows practical ranges in the order of 3–5 millimetres.

Performed tracer tests with conservative tracers in Feature A show that the feature is connected between its interpreted intercepts in the array. The parameters evaluated from the conservative tests; flow porosity, dispersivity and fracture conductivity are similar, indicating a relative homogeneity.

Previous work has identified cationic tracers, featured by sorption through ion exchange, as the most suitable tracers for sorbing tracer experiments at ambient Äspö conditions. Laboratory experiments on generic Äspö material and site-specific material included batch sorption experiments on various size fractions of the geological material, and through diffusion experiments on core samples of variable length on a centimetre length scale. The sorbtivity was found to be strongly affected by the biotite content and the sorption was also found to increase with contact time. The sorbtivity was found to follow the relative order; $Na^+ < Ca^{2+} \approx Sr^{2+} << Rb^+ \approx Ba^{2+} < Cs^+$.

The field tracer tests, using essentially the same cocktail of sorbing tracers as in the laboratory, were found to show the same relative sorbtivity as seen in the laboratory. A test using $^{137}Cs^+$ showed that after termination of the test, some 60% of the injected activity remained sorbed in the rock.

The interpretation of the in situ tests with sorbing tracers performed by the project team was conducted using the LaSAR approach /Cvetkovic et al, 2000/, developed as a part of the TRUE project. In this approach the studied flow path is viewed as a part of an open fracture. Key processes are spatially variable advection and mass transfer. The evaluation showed that laboratory diffusion data are not representative for in situ conditions, and that a close fit between field and modelled breakthrough is obtained only when a parameter group which includes diffusion/sorption is enhanced with a factor varying between 32–50 for all tracers and experiments (except for Cs) and 140 for Cs^+. The interpretation is that the enhancement is mainly due to higher diffusivity/porosity and higher sorption in the part of the altered rim zone of the feature which is accessible over the time scales of the in situ experiments, compared to data obtained from core samples in the laboratory. Estimates of in situ values of the important transport parameters are provided under an assumption of a valid range of porosity in the accessible part of the rim zone in the order of 2–2.4%.

Unlimited diffusion/sorption in the matrix rock was interpreted as the dominant retention mechanism on the time scales of the TRUE-1 in situ experiments. The effects on tracer retention by equilibrium surface sorption and sorption in gouge material were found to be observable, but of secondary importance. Similarly, the effect of sorption into stagnant water zones was found to be limited.

Alternative conceptualisations and interpretations of the performed experiments were performed i.a. as part of the work in the Äspö Task Force. An overview of the alternative interpretations of the TRUE-1 experiments is provided by /Elert, 1999; Elert and Svensson, 2001/ and in /SKB, 2001/. Interpretations attributing the bulk of the retention to matrix diffusion effects associated with multiple flow paths and fault gouge /Mazurek et al, 2002; Jacob et al, 2002/ and 3D effects /Neretnieks, 2002/ have been proposed, respectively.

1.5 Objectives

The overall objectives of the Tracer Retention Understanding Experiments (TRUE) are to:

- develop an understanding of radionuclide migration and retention in fractured crystalline rock,
- evaluate to what extent concepts used in models are based on realistic descriptions of a rock volume and if adequate data can be collected in site characterisation,
- evaluate the usefulness and feasibility of different approaches to model radionuclide migration and retention,
- provide in situ data on radionuclide migration and retention.

The specific objectives of the TRUE Block Scale Project given in the developed test plan /Winberg, 1997/ are:

1. increase understanding of tracer transport in a fracture network and improve predictive capabilities,
2. assess the importance of tracer retention mechanisms (diffusion and sorption) in a fracture network,
3. assess the link between flow and transport data as a means for predicting transport phenomena.

1.6 Overview of project

The TRUE Block Scale project is an international partnership funded by ANDRA, ENRESA, Nirex, POSIVA, JNC and SKB /Winberg, 1997/. The Block Scale project is one part of the Tracer Retention Understanding Experiments (TRUE) conducted at the Äspö Hard Rock Laboratory. The project, which was initiated mid 1996, is divided into a series of defined stages; Scoping Stage

- Preliminary Characterisation Stage /Winberg (ed), 1999/.
- Detailed Characterisation Stage /Winberg (ed), 2000/.
- Tracer Test Stage.
- Evaluation and Reporting Stage.

The staged approach also has an embedded iterative approach to characterisation and hydro-structural modelling, cf Section 1.9, whereby the results of the characterisation of each drilled borehole has been used to plan the subsequent borehole. As part of the initial four stages of TRUE Block Scale, a total of 5 boreholes have been drilled and characterised. An additional four boreholes have been completed as part of adjacent projects and have been utilised as verification and monitoring boreholes. The principal characterisation tools to establish the conductive geometry have been BIPS borehole imaging supported by POSIVA flow logging and connectivity established from responses to drilling and performed cross-hole interference tests. During the course of the project, 5 versions of the descriptive hydro-structural model have been developed, cf /Andersson et al, 2002/.

At the conclusion of the Detailed Characterisation Stage in mid 1999, the feasibility of performing tracer tests in the identified network of structures in the block scale (10–100 m) had been firmly demonstrated /Winberg (ed), 1999/. As a consequence a series of tests i.a. with radioactive sorbing tracers were performed as part of the Tracer Test Stage which ran from mid 1999 through 2000.

The respective updates of the hydro-structural model have been used to simulate, and in some cases perform blind predictions, of performed hydraulic and tracer tests /Winberg (ed), 2000; Poteri et al, 2002/. The analysis has been performed with various modelling approaches /Poteri et al, 2002/ including Stochastic Continuum, Discrete Feature Network, Channel Network, the LaSAR approach /Cvetkovic et al, 2000/ and the so-called POSIVA approach /Hautojärvi and Taivassalo, 1994/.

In support of the in situ experimentation, a series of laboratory investigations have been performed on geological material from the interpreted structures which make up the studied fracture network. The analyses performed include mineralogical and geochemical analyses, porosity determinations using water absorption and PMMA techniques, cf /Andersson et al, 2002/. In addition, water samples collected during drilling and from packed off sections have been analysed for chemical composition and isotope content and used in support of the hydro-structural models. Cation exchange capacity for fault breccia material from different intercepts, deduced from mineralogical

composition, have been used in combination with ambient groundwater chemistry from the different test sections to estimate volumetric distribution coefficients (K_d), cf /Andersson et al, 2002/.

1.7 Tested hypotheses

Three basic questions have been posed in relation to the performed tracer tests /Winberg, 2000/, their planning and evaluation. These are:

Q1) "What is the conductive geometry of the defined target volume for tracer tests within the TRUE Block Scale rock volume? Does the most recent structural model reflect this geometry with sufficient accuracy to allow design and interpretation of the planned tracer tests?"

Q2) "What are the properties of fractures and fracture zones that control transport in fracture networks?"

Q3) "Is there a discriminating difference between breakthrough of sorbing tracers in a detailed scale single fracture, as opposed to that observed in a fracture network in the block scale?"

On the basis of these questions corresponding hypotheses have been formulated /Winberg (ed), 2000/, to be addressed by the tracer tests and the subsequent evaluation;

H1) "The major conducting structures of the target volume for tracer tests in the TRUE Block Scale rock volume trend northwest and are subvertical. Being subvertical, and subparallel, they do not form a conductive network in the designated target volume. For the purpose of testing fracture network flow and transport effects in the current borehole array, second-order NNW features are required to provide the necessary connectivity between the major conducting NW structures!"

H2a) "Fracture intersections have distinctive properties and have a measurable influence on transport in fracture/feature networks. These distinctive properties may make the intersection a preferential conductor, a barrier, or a combination of both!"

H2b) "In-plane heterogeneity and anisotropy have a measurable influence on transport of solutes in a block scale fracture network!"

H3) "It is not possible to discriminate between breakthrough curves of sorbing tracers in a single fracture from those obtained in a network of fractures"!

1.8 Location and configuration of experiment

1.8.1 Location of experiment

A restriction in selecting a block for TRUE Block Scale was the overall usage of the experimental level of the Äspö HRL, cf Figure 1-1. The north-eastern part of the laboratory was allocated for the REX and TRUE-1 experiments. At the time of locating the TRUE Block Scale Experiment the inner part of the tunnel spiral, south of the TBM assembly hall was used by the ZEDEX experiment, the Demonstration Repository facility and by the Long-term tests on buffer materials. The area inside the tunnel spiral and north of the TBM was not used by any experiment. However, previous analysis had shown that the inner part of the laboratory exhibits a high degree of hydraulic connectivity /Winberg et al, 1996/. In the western part of the laboratory the Chemlab experiments was in progress in borehole KA2512A. This experiment is sensitive to changes in the chemical composition of the groundwater, but does not create any hydraulic disturbances. The final part of the TBM tunnel was allocated for the development of the Prototype Repository project.

A set of desired experimental conditions were defined to be used in positioning the TRUE Block Scale experiment /Winberg, 1997/. Of particular relevance for performance of block scale tracer tests are;

- Location of experimental site outside the tunnel spiral.
- Location away from major fracture zones (i.e. EW-1 and NE-1).
- Access from multiple locations (vertically) in the laboratory.
- No adverse hydraulic interference from other activities in the laboratory.
- Transmissivity range of fractures making up the studied fracture network in the range ; $T = 5 \cdot 10^{-8} – 5 \cdot 10^{-7}$ m^2/s.
- Small hydraulic gradient ($I < 0.05$).
- Flow velocities such that diffusion can be made a measurable process.

The rationale for selecting the particular site used for TRUE Block Scale is discussed by /Hermanson et al, 2002/ and /Winberg and Hermanson, 2002/ and the final location of the experimental volume is indicated in Figure 1-1. All the above criteria were met by the experimental site selected /Andersson et al, 2002/.

1.8.2 Definitions

The TRUE Block Scale site is located in the south-western part of the experimental level at the Äspö HRL, cf Figure 1-1. The area covered by the developed borehole array is denoted “TRUE Block Scale Rock volume” and has a lateral extent of 250x200 m, cf Figure 1-1, and extends between –500 masl to –350 masl in the vertical direction. The area containing the fracture network used in the tracer tests is about 100x100x50 m and is denoted the “TRUE Block Scale Tracer Test volume (TTV)”, cf Figure 1-1.

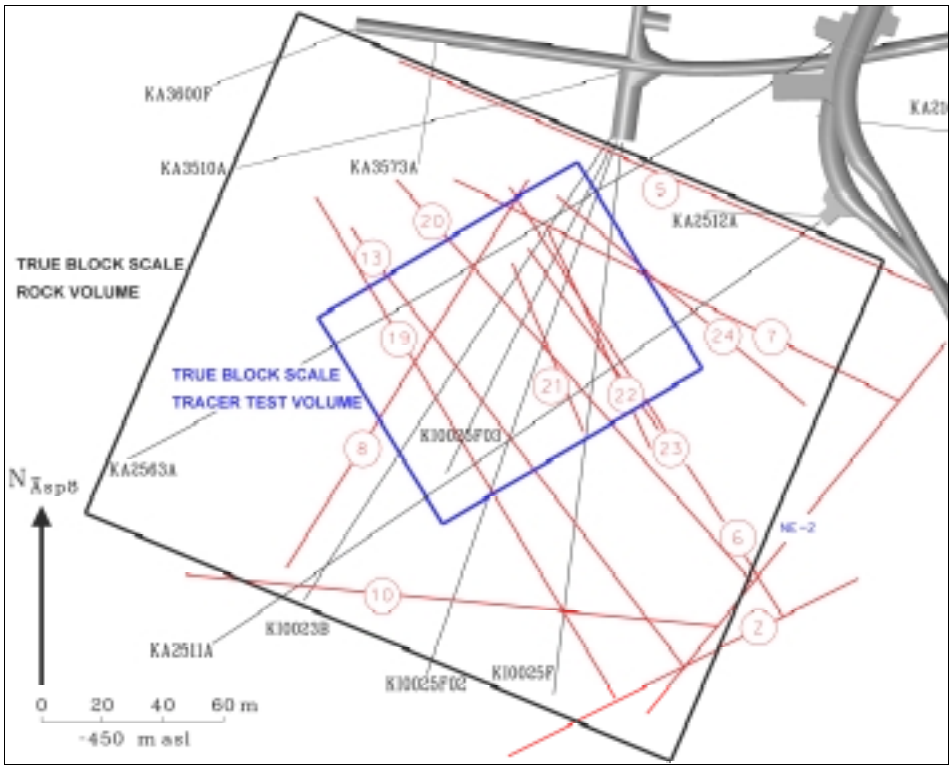

Figure 1-1. *Location of the TRUE Block Scale Experiment and definition of experimental volumes. Boreholes are indicated as black traces. Structures are indicated as red tracers, cf Figure 1-2.*

1.9 Experimental strategy and staging

The TRUE Block Scale Project adopts a staged approach. The key element desired in the experimental strategy was expressed as “Iterative characterisation with strong interaction between modelling and experimental work to ensure flexibility”. This implied that site characterisation data from each new borehole was used to update the hydro-structural model of the investigated block, whereby a successive refinement is obtained which is implemented in design, predictive modelling, performance and evaluation of block scale experiments. The performed work has been divided into five basic stages;

The “Scoping Stage” was intended to determine whether the identified experimental site fulfils the basic requirements /Andersson et al, 2002/. Field work included drilling and characterisation of boreholes KA2563A and KA3510A. The Scoping Stage was followed by a technical review in October 1997 and a decision to proceed in accordance with the developed test plan.

The field work of the Preliminary Characterisation Stage included drilling and characterisation of boreholes KI0025F and KI0023B. A series of cross-hole hydraulic interference and tracer dilution tests were carried out /Andersson et al, 2001a/. One of the tracer dilution tests was prolonged and the breakthrough of the injected tracer was observed. The basic results of this stage is presented by /Winberg (ed), 1999/.

The field work of the Detailed Characterisation Stage included drilling and characterisation of borehole KI0025F02. In addition a comprehensive series of cross-hole hydraulic interference and tracer dilution and tracer tests were carried out /Andersson et al, 2001b/.

The Tracer Test Stage included drilling and characterisation of the final borehole, KI0025F03, which was drilled to verify the March'99 hydro-structural model /Doe, 2001/ with an additional objective also to furnish additional injection points for tracer. The resulting hydro-structural model /Hermanson and Doe, 2000/ with predominantly steeply dipping interpreted structures is presented in Figure 1-2. The work scope of this stage included, apart from drilling and characterisation of a new borehole, optimisation of existing multi-packer installations. However, the main activity was a series of three tracer test phases; Phase A which was focused on identifying the best pumping (sink) section /Andersson et al, 2000a/, Phase B which was devoted to demonstrating sufficiently high mass recovery of non-sorbing species to allow usage of radioactive sorbing tracers /Andersson et al, 2000b/, and finally Phase C /Andersson et al, 2001c/, which included performance of four injections with radioactive sorbing tracers in three sections.

The last of the five stages, the Evaluation and Reporting Stage, included evaluation of experimental data and modelling results and reporting. The defined deliverables are defined in Section 1.11.

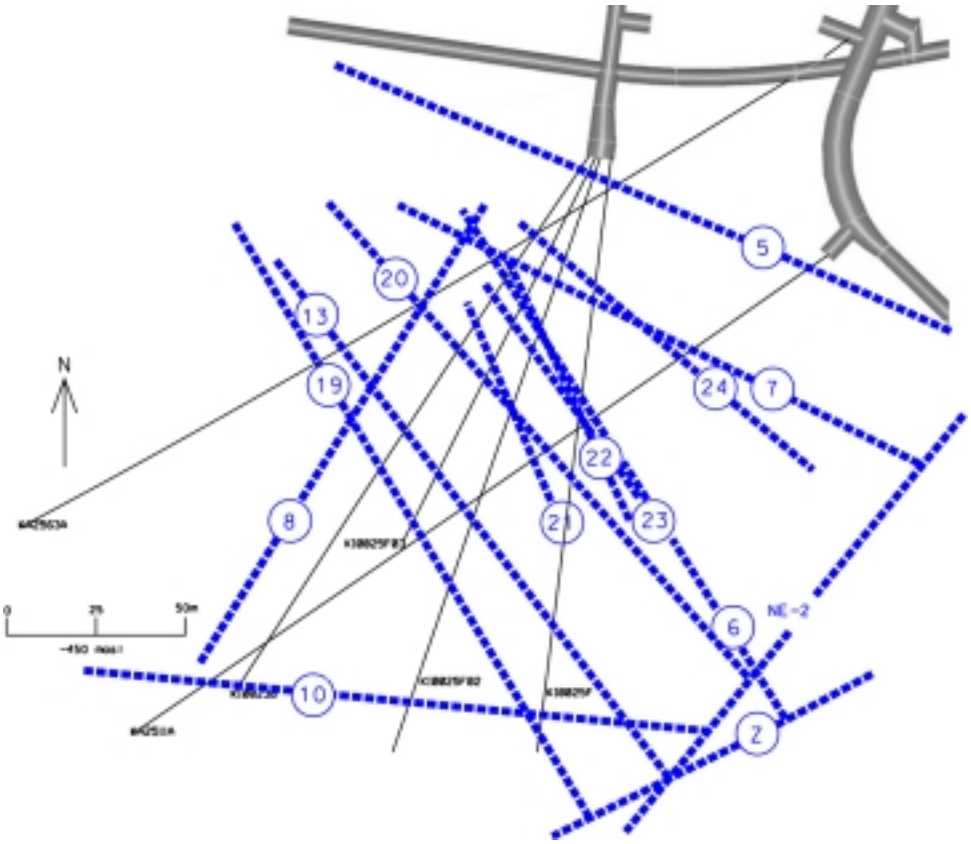

Figure 1-2. *Hydro-structural model based on characterisation data from KI0025F03 /Hermanson and Doe, 2000/.*

1.10 Boreholes and installations

1.10.1 Boreholes

The TRUE Block Scale borehole array is made up of 10 cored boreholes. Five of those have been drilled specifically within the TRUE Block Scale Project. The remainders have been drilled as part of the development of the spiral access tunnel, or as part of the characterisation for other projects, i.a. the Prototype Repository project.

The boreholes are with two exceptions of 76 mm drilled using the triple-tube technique, cf Section 3.1. The boreholes penetrating the investigated rock volume are presented in Table 1-1 and Figure 1-3.

Table 1-1. Compilation of data on boreholes penetrating the TRUE Block Scale Rock volume. TT= Triple tube core barrel, Solexp.= ANDRA/Sol-experts multi-packer system.

Borehole Id	Diameter (mm)	Length (m)	Completed	Project
KA2511A	56	293.0	1993-09-05	Turn 2
KA2563A	56	263.4	1996-08-24	TRUE BS
KA3510A	76 TT	150.1	1996-09-09	Various
KI0025F	76 TT	193.8	1997-04-25	TRUE BS
KI0023B	76 TT, Solexp.	200.7	1997-11-20	TRUE BS
KI0025F02	76 TT, Solexp.	204.2	1998-08-25	TRUE BS
KI0025F03	76 TT	141.7	1999-08-13	TRUE BS
KA3548A	76 TT	30.0	1998-06-26	Prototype
KA3573A	76 TT	40.1	1997-09-11	Prototype
KA3600F	76 TT	50.1	1997-09-24	Prototype

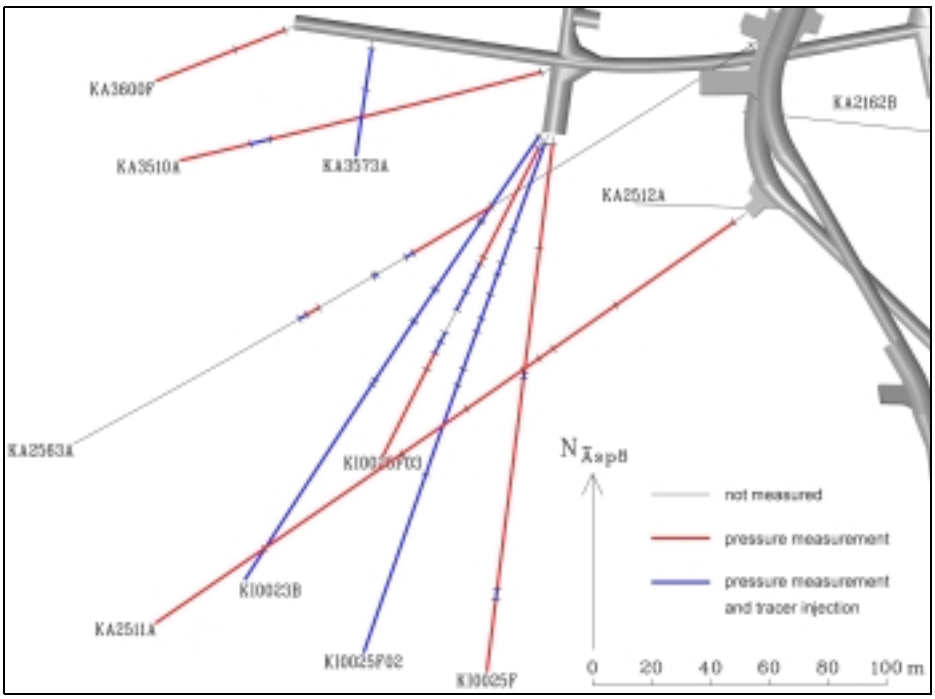

Figure 1-3. *TRUE Block Scale borehole. Tics indicate packer location defining packed off intervals in the boreholes (per June 2000) used for various purposes. Test sections numbered from bottom of hole.*

1.10.2 Installations

Of the boreholes listed in Table 1-1, seven have been instrumented as part of the project. An additional three boreholes have been drilled and instrumented as part of the Prototype Repository experiment. In the boreholes instrumented by the TRUE Block Scale Project two types of packer equipment have been utilised; The so-called "SKB/GEOSIGMA system" and the ANDRA/Solexperts system". A brief description of the two systems is provided in /Andersson et al, 2002/.

1.11 Outline of report series

The series of final reports from the TRUE Block Scale Project include the following four parts;

1. Characterisation and model development /Andersson et al, 2002/,

2. Tracer tests (this report),

3. Modelling of flow and transport /Poteri et al, 2002/,

4. Synthesis of flow, transport and retention in the block scale /Winberg et al, 2002/.

2 Overview of tracer test programme

2.1 Purpose of tracer tests

Tracer tests have been used in the TRUE Block Scale Project with many different purposes. The main objective has been to characterise the TRUE Block Scale rock volume and to determine retention properties for some selected flow paths, but tracer tests have been used throughout the project also for other purposes.

During the characterisation phases, tracer tests were mainly used to verify the hydro-structural model. This was done in combination with cross-hole interference tests by adding a slug of tracer to different borehole (observation) sections and measuring the dilution of tracer with time in the observation section, so called tracer dilution tests, cf Andersson et al, 2002. This was done both before and after the start of the pumping in the withdrawal section. These measurements gave indications of the ambient flow and gradients at the site as well as relative strengths of the connectivity in combination with pressure responses.

In addition to these single-hole tracer tests (tracer dilution tests), a large number of cross-hole tracer tests were performed with the ultimate objective to select tracer test geometry (source-sink combinations) suitable for tests with radioactive sorbing tracers. The main factor for selection was in this case the tracer mass recovery. A few simpler cross-hole tracer tests were also performed to check how well two sections were connected within borehole KI0023B. The first, between sections P3 and P4, to check the leakage in the borehole installation caused by a collapsing inner tube, cf Figure 1-3. The second, between sections P6 and P7, was performed to check that the short-circuit between two structures in section P7 could be controlled by using section P6 as a sink.

Even though the main purposes of cross-hole tests have been to verify connectivity and mass recovery and help to select flow paths for retention experiments, a secondary objective has been to characterise the flow paths, i.e. to determine advective transport properties. A specific objective coupled to the transport properties has been to study possible effects of fracture intersection zones (FIZ).

2.2 Strategy for selection of suitable test geometry

One of the key problems with tracer tests run on larger length scales is to select a test geometry, which gives a sufficiently high mass recovery, and at the same time enable performance of cross-hole tracer tests within reasonable time frames. Experience from the TRUE-1 experiments /Winberg et al, 2000/ showed that the use of tracer dilution tests in combination with cross-hole interference tests was a good set of tools for selecting potential injection and sampling points for tracer tests. Thus, this strategy was also employed for the TRUE Block Scale Project.

Another important factor to consider, at least in the early parts of the project, was to select points with high flow rates for tracer injection. The reason for this being that the tracer injection system was designed for passively injecting tracer with the ambient flow. Thus, a low ambient flow would result in a very long injection period with a resulting long tail in the breakthrough curve which potentially could mask active transport processes such as diffusion, that otherwise would be indicated by the shape of the tail, cf Chapter 6.2.

Based on these considerations and experiences from TRUE-1 the following strategy for selecting suitable tracer test geometries was employed.

- Select a withdrawal section (sink) that is located in one of the identified/interpreted deterministic hydraulic structures, preferably in the centre of the borehole array to allow tracer injections in various directions and at various distances from the sink.
- Perform a combined interference test and tracer dilution test, at ambient flow conditions (without pumping) and during pumping at the selected sink. An example of a good "flow response" is shown in Figure 2-1.
- Choose injection sections indicating a "good flow response" and a high ambient flow rate.
- Use high recovery (>80%) flow paths for tests with sorbing tracers.

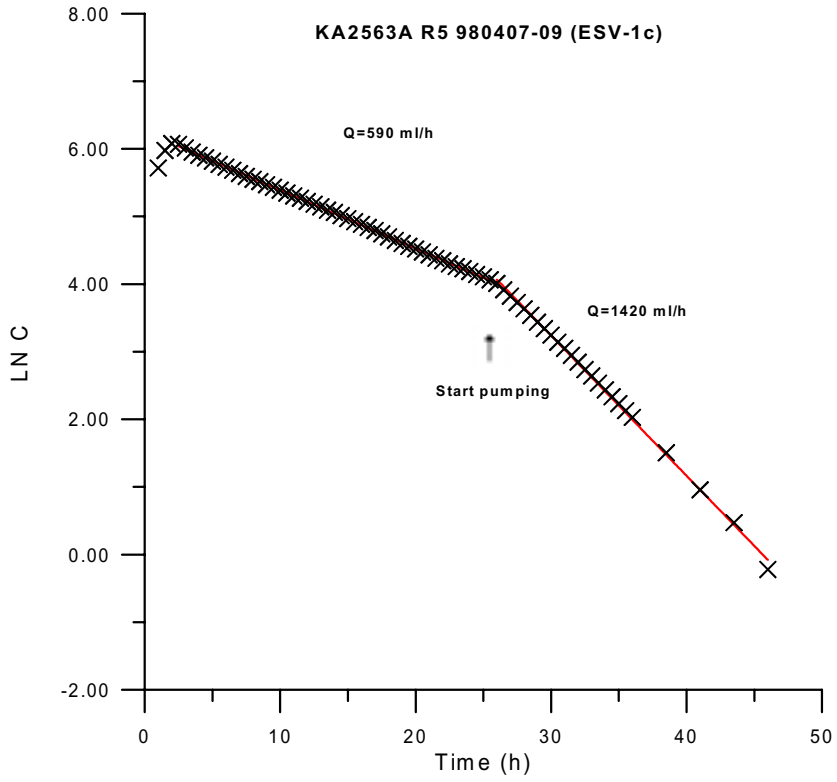

Figure 2-1. *Tracer dilution curve (Logarithm of the tracer concentration versus time) in borehole section KA2563A:R5 before and after pump start for interference test ESV-1c (pumping in KI0023B:P6).*

It should also be noted that a “good flow response” may not necessary imply that the pressure response is good also. One example is section KI0025F02:P3 (Structure #21) which does not respond so well hydraulically, but has an excellent “flow response” and in fact was one of the sections finally chosen for retention studies. It is not likely that this section would have been considered at all for tracer injection without having information regarding “flow response”. On the other hand, the use of “flow response” is somewhat ambiguous due to the fact that the measured flow is a vector entity. Hence, a situation where the actually measured ambient and “pumped” flow rates are identical but in reality have been doubled may occur, see Figure 2-2. However, in the measurements performed most sections respond with an increase of a factor 2–50 implying that the ambient flow direction is of less importance for most of the measurements.

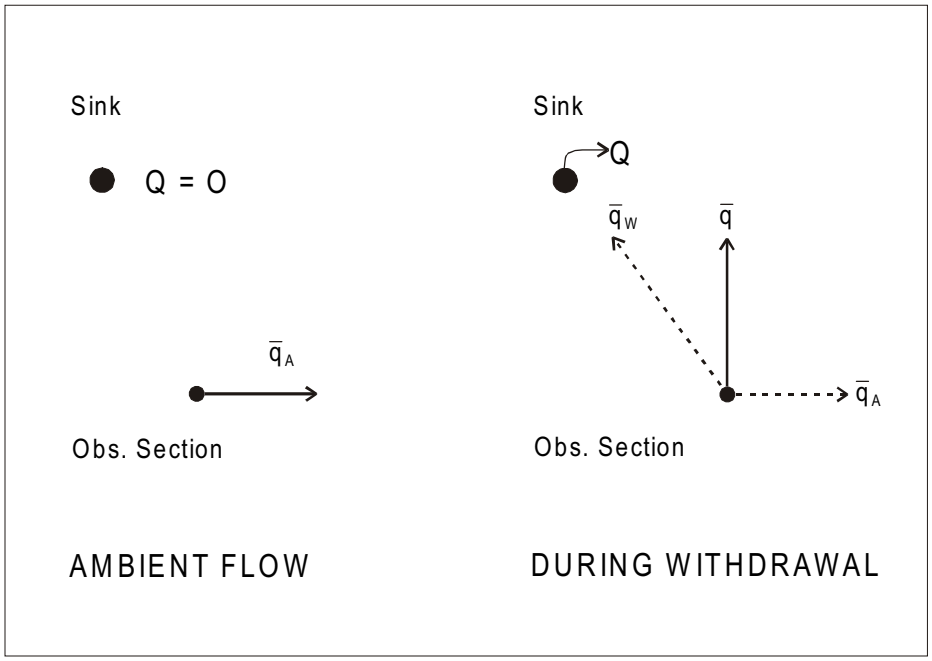

Figure 2-2. *Illustration of the relation between ambient flow and what is measured during a tracer dilution test.*

2.3 Tests performed

The TRUE Block Scale tracer test programme has involved 14 tracer test campaigns, involving 32 tracer injections in 16 different combinations of source and sink pairs (flow paths). This data set is certainly one of the largest ever collected concerning transport of solutes in fracture networks over distances ranging from 10 to 130 metres, cf Chapter 1.3. Table 2-1 summarises all tests performed within the project, their main purposes, evaluated mass recovery and references to reports where a more detailed description may be found.

Table 2-1. Summary of tracer tests performed within the TRUE Block Scale Project.

Test	Main Purpose	Injection section(s)	Pumping section	Mass recovery	Reference
ESV-1c	Possibility to perform tracer tests in the block scale	KA2563A:R5 KI0025F:R4 KI0023B:P4	KI0023B:P6	44% 0% 0%	/Andersson et al, 2001a/
KI0023B	Leakage between sections in KI0023B	KI0023B:P3	KI0023B:P4	<1%	Internal report
KI0025F02	Connectivity during drilling of KI0025F02	KI0023B:P4	KI0025F02	0%	Internal report
Pre-PT-4	Check of direction of gradient in KI0023B	KI0023B:P7	KI0023B:P6	100%	/Andersson et al, 2001b/
PT-4	Transport connectivity and properties	KA2563A:S4 KA2563A:S1 KI0025F02:P3 KI0025F02:P6	KI0023B:P6	51% <1% >75% >80%	/Andersson et al, 2001b/
A-4	Transport connectivity and properties	KI0025F03:P5 KI0025F03:P6 KI0025F03:P7	KI0023B:P6	>31% >34% 0%	/Andersson et al, 2000a/
A-5	Transport connectivity and properties	KI0025F02:P3 KI0025F02:P5 KI0025F02:P6 KI0025F03:P6 KA2563A:S4	KI0025F03:P5	0% 97% >27% 57% 47%	/Andersson et al, 2000a/
B-1	Helium diffusion, FIZ*, heterogeneity, new flow path	KI0025F03:P5 KI0025F03:P6 KI0025F02:P5	KI0023B:P6	100% >46% >37%	/Andersson et al, 2000b/
B-2	Helium diffusion, FIZ*, heterogeneity, network transport properties, selection of injection sections for Phase C	KI0025F03:P6 KI0025F02:P3 KA2563A:S1 KI0025F03:P7 KI0025F03:P3 KI0025F03:P5 KI0025F02:P6	KI0023B:P6	60% 98% >35% 88% 49% 100% 49%	/Andersson et al, 2000b/
C1	Retention	KI0025F03:P5	KI0023B:P6		/Andersson et al, 2001c/
C2	Retention	KI0025F03:P7	KI0023B:P6		/Andersson et al, 2001c/
C3	Retention	KI0025F02:P3	KI0023B:P6		/Andersson et al, 2001c/
C4	Retention	KI0025F03:P5	KI0023B:P6		/Andersson et al, 2001c/

* FIZ = Fracture Intersection Zones

3 Tracer test methodology

3.1 Experimental requirements

The concept used for the tracer tests very much relies upon the experiences and method developments made within the TRUE-1 tracer tests /Winberg et al, 2000/ and earlier experiments (e.g. Finnsjön, Grimsel). The main idea was to maintain a well-controlled flow field with a minimum of disturbance to the flow field from existing installations and injection/sampling procedures employed. In addition a number of additional requirements were put upon the tracer test methodology:

- It should be possible to detect tracer breakthrough despite large dilution caused by ambient background groundwater flow.
- All materials included in the system should be chemically inert to avoid sorption or chemical interaction with the added tracers.
- It should be possible to use the test equipment for a variety of different test configurations (radially convergent tests, dipole tests, and dilution tests) and a variety of tracers (including radioactive sorbing and helium tracers).
- It should be possible to monitor tracer injection and breakthrough on-line from a remote location.

The TRUE Block Scale tracer tests were performed over distances between 15–130 metres mostly in radially convergent flow geometry. This implies that the dilution of the injected tracer solution is one order of magnitude larger than in the TRUE-1 tests due to the radial geometry. The dilution based on pure geometry, assuming that the release of tracer solution occurs over the entire borehole diameter would be in the order of 10^3. Added to this is the initial dilution in the injection borehole, 10^2, and the effects of transport processes (dispersion, diffusion, etc). Summing up these figures and the urge to follow the breakthrough at least over three orders of magnitude in concentration equates to a dilution of about 10^8. Therefore a study was initiated within the project to try to find a set of suitable tracers /Holmqvist et al, in prep/, cf Chapter 4.

The injection equipment (Figure 3-1) is designed to create an internal circulation in the injection borehole. The circulation makes it possible to obtain a homogeneous tracer concentration inside the borehole and to sample the tracer concentration outside the borehole in order to monitor the dilution of the tracer with time. The down-hole system is designed such that a minimisation of the volumes in the packed-off borehole intervals is achieved by minimising the length of the intervals and by installation of volume reducers (dummies) to reduce the water volume.

Circulation is controlled by a pump with variable speed (A) and measured by a flow meter (B). Tracer injections are made either directly into the circulating loop with a HPLC plunger pump (C), which also could be used to create a forced injection (cf Section 3.2), or by switching a three-way valve such that the circulating water passes through a stainless steel vessel (E2) filled with tracer solution. The tracer solution in the circulation loop can also be replaced with unlabelled water by switching the three-way

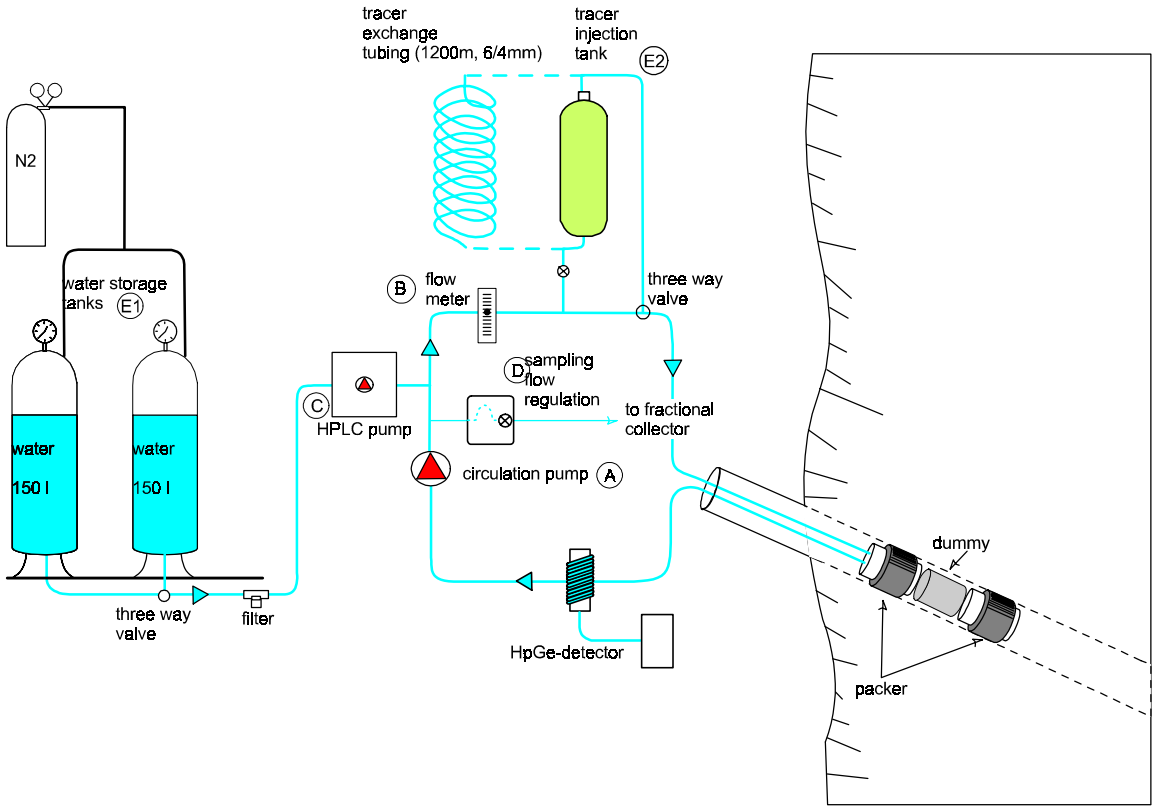

Figure 3-1. *Schematic drawing of the injection system for the TRUE Block Scale tests with sorbing tracers.*

valve so that the circulating water passes through a long (1200 m) tube filled with unlabelled water. Tracer solution then enters from one side of the tube and unlabelled water enters the circulation loop from the other side of the tube, thus completing the exchange (cf Chapter 3.2). The tracer concentration in the injection loop is measured both in situ (radioactive tracers) and by sampling and subsequent analysis. The sampling is made by continuously extracting a small volume of water from the system through a flow controller (constant leak) to a fractional sampler (D). The in situ monitoring of the radioactive tracer content (activity) in the injection system is achieved by use of a HPGe-detector measuring in line on the tubing.

3.2 Injection methodology

The quality of tracer test data is often dependent on how well the injection of tracer can be performed and monitored. There are many different views on how to best inject tracer, but the success of all methods rely on two main components/circumstances; that 1) the tracer is well mixed and 2) that the input signal can be monitored well. The circulating system applied has the advantage that the input concentration can be monitored in a relatively simple way outside the borehole. In principle, it would be better with down-hole monitoring but this is in reality very difficult due to the high

ambient pressure and the problem of monitoring more than one tracer. Another advantage with the circulating system is that a fast homogenisation of the tracer solution can be achieved.

Three different injection methods were applied during the test programme; decaying pulse, finite pulse and forced pulse (unequal dipole). An example from test A-4 where all three methods were used /Andersson et al, 2000a/ is given in Figure 3-2. The figure illustrates some of the advantages and disadvantages with the different methods. The most commonly used method in the project, the decaying pulse, is by far the simplest to perform, but has the disadvantage that the long tailing may mask influence of transport processes (e.g. diffusion). However, during the earlier stages of the project, when the main focus was on characterisation, this method worked well.

To avoid this long tailing, one can exchange the tracer solution with ambient, unlabelled water, i.e. creating a finite pulse. One potential advantage would be that the long tailing is avoided. However, due to the relatively long tubing and large volumes of the system, it was difficult to achieve a good exchange and a large portion of the tracer mass still remained in the injection section. This method was therefore only used in a few tests.

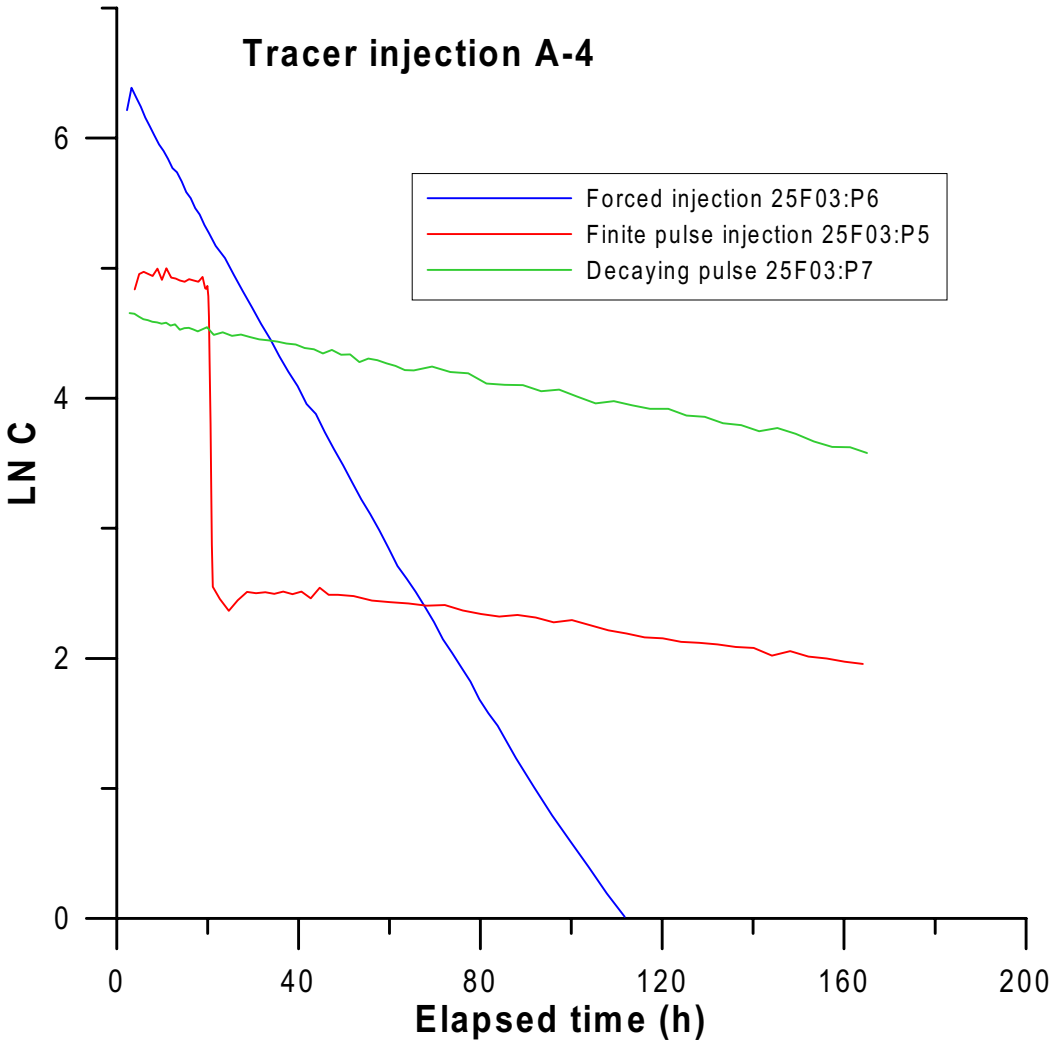

Figure 3-2. *Tracer concentration [C] in the injection section as a function of time. Examples of different injection techniques from TRUE Block Scale Phase A tracer tests (Test A-4).*

In later stages of the project, after deciding which sink to use for the tracer retention tests (Phase B and C), a somewhat changed strategy was applied. Some of the sections showing a good "flow response" had such low ambient flow rates that it would be difficult to detect the tracer at the sink due to dilution, and also that the tailing of the injection curve would be a disturbing element as described above. Also, for the injection of Helium it was necessary to minimise the tracer residence time in the injection section to avoid diffusion of Helium through the equipment. Thus, the obvious advantage with the forced injection is that the tracer quickly leaves the injection borehole. The disadvantage is that the convergent flow field is disturbed and that the tracer mass is spread out in an uncontrolled way over a larger area around the injection section. The implications of this condition for transport is discussed in Chapter 6 where some tests performed in the same geometry, but with different injection methods, are compared.

The forced injection also requires water from an external source, which may be a potential problem. In the Phase B and C tests a volume of about 500 litres/week was required. Given that the tests should run for months it was obvious that such a large volume could not be collected and stored in advance. It is also not possible to use a borehole within the TRUE Block Scale array for water supply as this would disturb the ongoing tests. Therefore, a borehole with very similar groundwater chemistry was used (KA3385A). This borehole was directly connected to the large nitrogen filled, pressurised (600–1000 kPa) stainless steel storage vessels and could be filled without releasing the pressure to atmospheric pressure. A pressure release from about 4000 to 1000 kPa could not be avoided due to economic and practical reasons.

The equipment for tracer injection generally worked very well. The problems encountered during the project have been relatively few, but there are some that need to be solved for future experiments. These are:

- The circulation capacity of the tracer injection system need to be improved during forced injections. In tests with injection rates higher than 10ml/min, the mixing was not good enough and parts of the injected water entered the fracture without mixing completely with the tracer solution. This effect was noted as a difference between actually measured pump capacity and flow rate measured based on tracer dilution.

- The use of HPLC plunger pumps for long-term injection of water or tracer solution should be avoided. Membrane plunger pumps of industrial type that withstand the harsh ambient environment at the Äspö HRL should be used instead.

- Methods and equipment for creating finite pulse injections need to be improved, possibly by further reducing of the free water volumes in the system.

- Circulation of water through fine-meshed filters, used for distributing tracer evenly around the perimeter of the borehole, over long time may create clogging of the filters. This problem may be solved simply by increasing the mesh size.

- The data acquisition system consists of many different sub-systems (Äspö Hydro Monitoring System, field data loggers, internal equipment specific loggers, etc). It would be preferable to have a common system where all parameters could be monitored on-line and accessed from a remote location.

3.3 Sampling methodology

The sampling system is based on the same principle as the injection system, namely a circulating system with a circulation pump and a flow meter, cf Figure 3-3. In this case however, water is withdrawn from the borehole with a constant flow rate by means of a flow regulation unit or, as in the case of the Phase C tests, simply by opening the flow lines completely. The flow regulation unit consists of a mass flow meter coupled to a motorised valve enabling a fast and accurate flow regulation.

The sampling and monitoring is made with three independent systems; a "constant leak" system producing samples (same as in the injection loop) integrated over a given time interval (typically 5–240 minutes) and a 24-valve sampling unit producing discrete samples (sampling intervals between 5 minutes up to 100 hours). The water is also led through an in-line electrical conductivity probe and a redox probe. For the radioactive tracers an in-line HpGe-detector was used. To increase the water volume around the detector and thereby also decrease the lower measurement level, a larger diameter tube was coiled around the detector.

A similar system was used for the TRUE-1 tests where problems were found with FeOOH precipitates on the wall of the tubing, probably as a result of the pressure release directly before the measurement cell. This led to a high concentration of the ^{214}Pb and ^{214}Bi (radionuclides originating from the decay of the naturally occurring radioisotope ^{222}Rn) in the measurement cell, probably because of sorption of these radionuclides onto the precipitates. As a result of this the γ-background activity became high and the measuring capability of the on-line measurement cell was not as good as expected. To avoid this problem in the TRUE Block Scale experiment, a continuous injection of concentrated acid (HNO_3) was introduced in the flow line immediately before passing the detector.

The sampling methodology with three separate systems, discrete samples, time-averaged samples and in line detection has been found to work well. All three systems have their advantages and weaknesses, listed in Table 3-1, but if possible, it is recommended that all three are used simultaneously.

Table 3-1. Comparison between different sampling methods used in the TRUE Block Scale tracer tests /Holmqvist et al, in prep/.

System	Advantages	Weaknesses
Discrete sampling	Correct time, any volume of sample possible	Leakage in sampling valve may destroy samples. Sensitive to bacterial growth and precipitates.
Time averaged sampling (Constant leak)	Very reliable	Delay in tubing, smoothing of concentration peaks.
In line detection	Direct control in situ or at remote location through data modem.	Long term drift, discrete samples still needed for check and calibration.

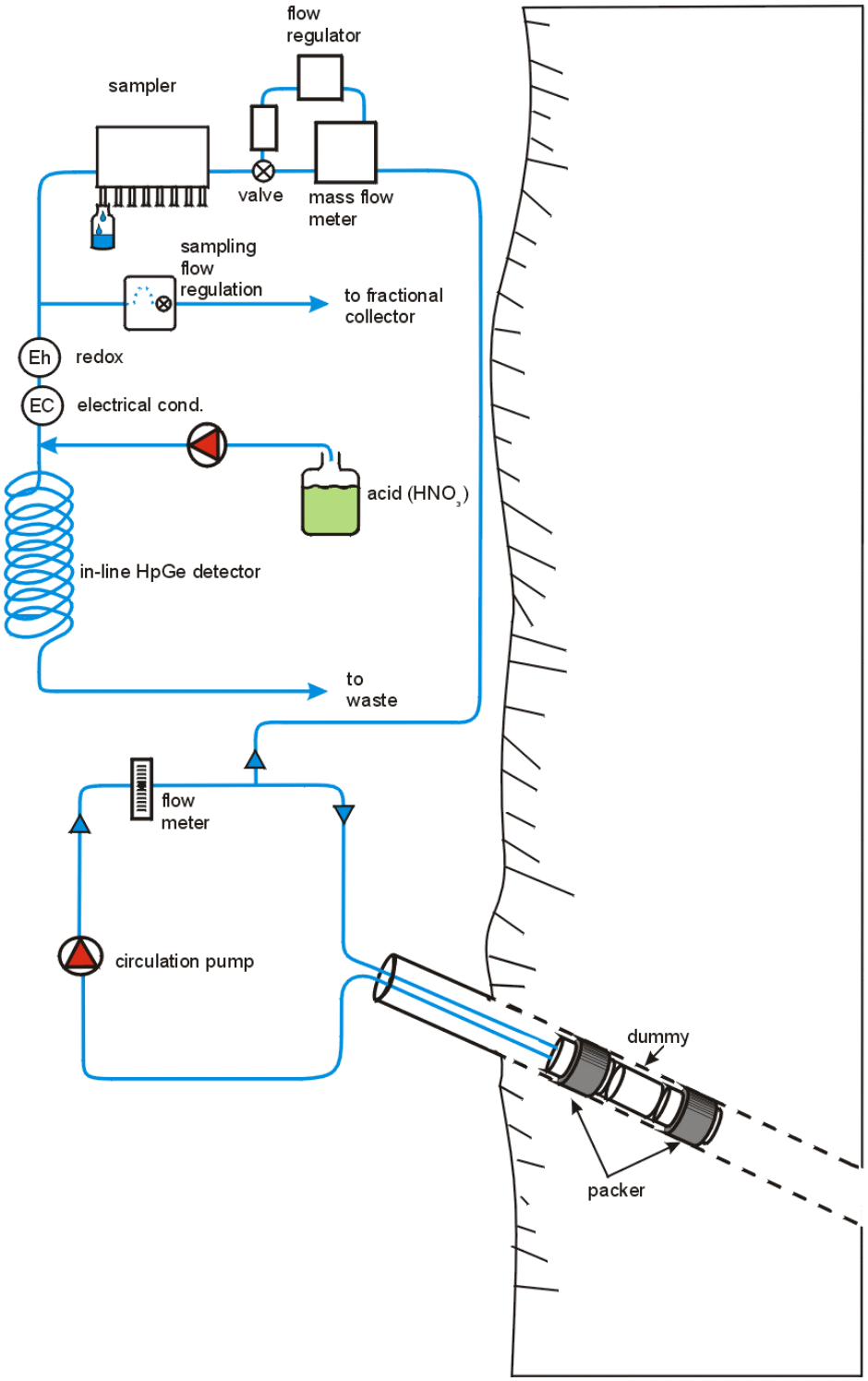

Figure 3-3. *Sampling equipment for the TRUE Block Scale tracer tests.*

4 Tracers and analysis methods

4.1 Non-sorbing tracers

All of the 32 tracer injections performed within the project have included at least one non-sorbing tracer. Thus, a number of different non-sorbing tracers were required to avoid interference from earlier tests. Due to the limited number of "truly" non-sorbing tracers available, or possible to use at Äspö HRL, a study was initiated to identify new tracers possible to use at Äspö /Holmqvist et al, in prep/. The work started with a literature study including the tracers listed in Table 4-1, followed by an in situ feasibility test performed at the TRUE-1 test.

The literature study identified about 20 candidate non-sorbing tracers to be tested in a field test at the TRUE-1 site at Äspö HRL. The tests with dissolved Helium gas were of special interest for the project since Helium potentially could be used to indicate matrix diffusion processes. The Helium runs are therefore discussed separately in Section 4.2.

The field tests were performed in a relatively short flow path (3.2 m) with a relatively short mean residence time of about one hour. Even though the travel distance and residence time were short, clear indications of delay or degradation of the tested tracers could be noted, e.g. for the dye tracers Rose Bengal and Phloxine. The results of the

Table 4-1. Non-reactive tracers studied in the literature study /Holmqvist et al, in prep/.

Tracer	Name	Analysis	Dynamic Range	Comment
Dissolved gases	He-3	Mass spectrometry	Large	Used by NAGRA
	Ar, Ne, Xe		?	Research needed
Stable isotopes	Deuterium	Mass spectrometry	?	Expensive analysis
	N-15, C-13, 0-18		?	
Dyes	Eosin B, Y	Fluorometry	Large	Used in TRUE-1
	Phloxine			Used in Stripa
	Rose Bengal			Used in Stripa
Metal-Complexes	m-EDTA	ICP-MS	Large	Used in Finnsjön, Stripa, TRUE-1
	m-DTPA			
	m-DOTA			
Halogenated hydrocarbons	Many different	Gas chromatography	Large	Used in USA, Hydroisotop has experience. Possible environmental constraints
Benzoates	TFMBA and others	HPLC	Large?	Used by SANDIA in USA
Particles		Particle counter	?	Study at CTH Nuclear Chemistry
Others	ReO_4^-	ICP-MS	Large	Used in Finnsjön
	CS_2	?	?	

tests in combination with cost aspects and the dynamic range of the tracers (relation between maximum solubility and minimum detectability), identified three groups of possible new tracers:

- Fluorescent dyes (Naphtionate, Pyranine, Dimethylfluorescein).
- Metal complexes (In-, Yb-, Lu-, Tm-EDTA, Gd-, Ho-DTPA) and Re as ReO_4^-.
- Dissolved Helium gas.

It should be noted that most of these tracers have been used previously in tests at other sites in crystalline rock, but they are all new in the Äspö HRL context.

The main advantage of the fluorescent dyes is that they are cheap to buy and analyse as no sophisticated equipment or procedure is required. That is also the reason why these tracers were used as much as possible during the characterisation of the TRUE Block Scale site. The main drawback is that they are sensitive to light, and during the project it was also found that the most commonly used tracer, Uranine, was completely lost in some test tubes and the colour of the tracer turned to pink. A loss of fluorescence intensity is known to occur when pH is lower than 7 /Smart and Laidlaw, 1977/ although they claimed that the process could be reversed by buffering to a higher pH when analysing the sample. This process did not work on the waters at the TRUE Block Scale site, possibly due to a combination of some other, yet unknown process. However, the problem was solved by pre-treatment of the sampling tubes with buffer solution (Borax buffer, pH ≅9) prior to the sampling.

The metal complexes were successfully used during Phase B of the project. The advantages of these compounds are that they could be detected in extremely low concentrations and the background values are very low. A third advantage is that all metals are detected in the same analysis through ICP-MS analysis. The drawback is that the price for analysis is rather high.

In summary, the project has identified a large number (>15) of possible non-sorbing tracers that can be used in future tracer tests at the site and at other similar sites.

4.2 Helium

Helium has previously been successfully used in tracer tests at the Grimsel Laboratory in Switzerland /Eikenberg et al, 1992/. The main reason for using Helium is that the diffusivity is significantly higher (about 5 times) than e.g. the water molecule, which increases the possibility to detect and evaluate diffusion effects. High background values of ^4He made it necessary to use the isotope ^3He.

The Äspö waters are very different from the ones at Grimsel (more than 100 times more saline and high content of dissolved gas at Äspö) and pressures are significantly higher. The transfer of the He tracer equipment to the Äspö HRL therefore required a few equipment modifications. The two most critical items for feasibility of the He tracer tests at the Äspö test site are the high static heads and the loss of He in polyamide flow

lines. Both these problems were addressed in laboratory tests and could also be solved. A new silicone membrane was developed for the Helium gas detector and the loss through flow lines could be minimised through short residence times and/or exchange to stainless steel lines /cf Holmqvist et al, in prep/. A schematic picture of the Helium detection method is shown in Figure 4-1.

The pilot tracer tests at the TRUE-1 site showed that Helium could be used and also gave a first indication that diffusion occurred although the residence times were very short (hours). The diffusive nature of Helium also made it necessary to introduce the tracer solution more rapidly into the fracture and avoid long residence times in the injection borehole. Thus, injection of Helium was made with an excess pressure creating an uneven dipole configuration between injection and sampling boreholes (a 1:50 ratio between injection and sampling flow rate).

Dissolved ^{3}He in combination with other non-sorbing tracers was successfully used in two flow paths during Phase B of the TRUE Block Scale Tracer Test Stage /Andersson et al, 2000b/. The results are presented in Chapter 6.2.

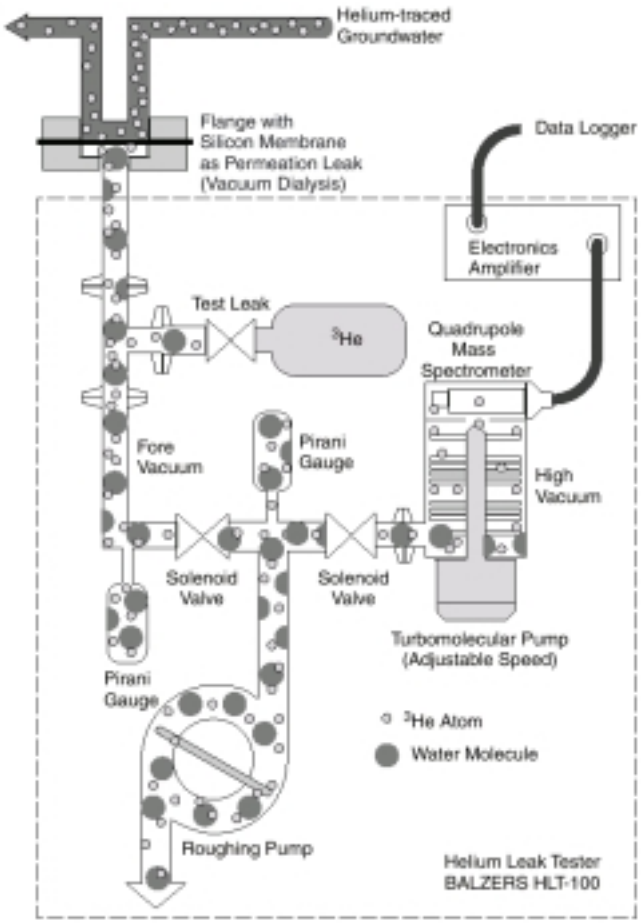

Figure 4-1. *Schematic illustration of the Helium detection methodology /Frick et al, 1992/.*

4.3 Sorbing tracers

With regards to selection of sorbing (reactive) tracers, the main set are elements of the alkali and alkaline earth metals previously used in the TRUE-1 experiments /Winberg et al, 2000/, which are all characterised by ion exchange as the main sorption mechanism. A general trend could be observed in the in situ experiment in the TRUE-1 programme; Na^+, Ca^{2+} and Sr^{2+} were transported only very slightly retarded compared with the non-sorbing tracers, Rb^+ and Ba^{2+} moderately retarded and Cs^+ strongly retarded. Using the assumption of a retardation coefficient for each tracer, it was necessary to use tracers like Rb^+, Ba^{2+} and Cs^+ to be able to observe a significant retardation. However, it was possible that transport over longer distances (like in TRUE Block Scale) would result in increased retardation and that breakthrough would only be obtained from slightly sorbing tracers (like Na^+, Ca^{2+} and Sr^{2+}). It was therefore decided that at least one slightly sorbing tracer and one strongly sorbing tracer were to be used in each injection.

Besides the sorbing tracers, it was decided to use radioactive non-sorbing (presumed) tracers, e.g., $^{82}Br^-$ in injection C1, $^{186}ReO_4^-$ in injection C2, HTO (tritiated water) in injection C3 and a combination of $^{82}Br^-$ and $^{131}I^-$ injection C4, cf Table 2-1. In the injections C1 and C2 the radioactive non-sorbing tracers were rather short-lived and it was therefore decided to also use Uranine (C1) and Naphtionate (C2) as tracers.

An attempt to address the impact of hydrolysis on sorption in an in situ tracer experiment was made by using three different di-valent transition metal cations as tracers; cations with a variation in their hydrolysis constants. Injection C4 was performed using the tracers $^{54}Mn^{2+}$, $^{57}Co^{2+}$ and $^{65}Zn^{2+}$ for which the first hydrolysis constant, log β_1^*, has been reported to be –10.6, –9.7 and –9.0, respectively /Smith and Martell, 1989/. Based on the generally concluded dependence of the sorption strength on the hydrolysis constant /e.g., James and Healy, 1972/, it was hypothesised that this concept could be applied for the prediction of the relative breakthrough of these tracers; i.e. an in situ retardation in the order $Mn^{2+} < {}^{57}Co^{2+} < {}^{65}Zn^{2+}$ should be observed.

The strategy for the choice of the sorbing tracers was similar to the strategy used earlier within the TRUE programme, i.e.;

1. In order to avoid increase of the concentrations, which may cause over-saturation and/or non-linear sorption effects, radioactive isotopes of each sorbing tracer were used. This makes it possible to obtain large dynamic ranges without significant increase in the natural chemical concentrations of the cations.

2. Isotopes with γ-radiation decay were preferred since they can be measured with γ-spectrometry; a technique which makes it possible to measure a large number of tracers simultaneously with only very small interference between the individual tracers.

3. The only tracer used without measurable γ-radiation was tritiated water (HTO). This tracer was measured using liquid scintillation; a technique that has only limited possibilities to discriminate the β-decay from different radioisotopes. However, a combination of the injection of comparably high activity of HTO with the fact of the low β-energy in the decay of tritium, makes it possible in most cases to measure HTO without having to make any separation procedures.

Table 4-2. TRUE Block Scale Phase C. Specification of the tracers used in tracer injections C1 – C4.

Injection C1

Tracer	Half-life	Measuring method	Injected activity (MBq)	Chemical concentration[A] in stock solution
Uranine	n.a.	Spectrofluorometry	–	4000 mg/l
$^{82}Br^-$	1.47 d	γ-spectrometry	138±1	29 mg/l
$^{24}Na^+$	15 h	γ –spectrometry	15.6±0.6	1930 mg/l
$^{42}K^+$	12.4 h	γ –spectrometry	229±10	7.5 mg/l
$^{47}Ca^{2+}$	4.54 d	γ –spectrometry	10.7±0.3	1289 mg/l
$^{86}Rb^+$	18.7 d	γ –spectrometry	13.3±0.7	130 µg/l (55 µg/l)
$^{134}Cs^+$	2.06 y	γ –spectrometry	7.79±0.08	5 µg/l

Injection C2

Tracer	Half-life	Measuring method	Injected activity (MBq)	Chemical concentration[A] in stock solution
Naphtionate	n.a.	Spectrofluorometry	–	16000 mg/l
$^{186}ReO_4^-$	3.78 d	γ –spectrometry	171±2	64 µg/l (B)
$^{47}Ca^{2+}$	4.54 d	γ –spectrometry	56.4±0.5	1289 mg/l
$^{131}Ba^{2+}$	11.5 d	γ –spectrometry	25.7±0.3	150 µg/l (<80 µg/l)
$^{137}Cs^+$	30 y	γ –spectrometry	23.5±0.1	24 µg/l (5 µg/l)

Injection C3

Tracer	Half-life	Measuring method	Injected activity (MBq)	Chemical concentration[A] in stock solution
HTO	12.3 y	Liquid scintillation	244±7	~100%
$^{22}Na^+$	3.78 d	γ –spectrometry	21.6±0.2	1930 mg/l
$^{85}Sr^{2+}$	64.9 d	γ –spectrometry	22.1±0.2	17 mg/l
$^{83}Rb^+$	86.2 d	γ –spectrometry	45.9±0.3	55 µg/l
$^{133}Ba^{2+}$	10.5 y	γ –spectrometry	0.55±0.03	2400 µg/l (80 µg/l)

Injection C4

Tracer	Half-life	Measuring method	Injected activity (MBq)	Chemical concentration[A] in stock solution
$^{82}Br^-$	1.47 d	γ –spectrometry	11.4±0.3	29 mg/l
$^{131}I^-$	8.0 d	γ –spectrometry	9.8±0.3	0 (B)
$^{47}Ca^{2+}$	64.9 d	γ –spectrometry	1.9±0.2	1289 mg/l
$^{131}Ba^{2+}$	86.2 d	γ –spectrometry	65.1±0.8	300 µg/l (<80 µg/l)
$^{54}Mn^{2+}$	312 d	γ –spectrometry	71.1±0.5	0 (0.5 mg/l)
$^{57}Co^{2+}$	271 d	γ –spectrometry	28.9±0.2	0 (0.1 µg/l)
$^{65}Zn^{2+}$	244 d	γ –spectrometry	20.0±0.5	0 (10 µg/l)

A Element concentrations in the stock solutions of the different injections. Within parenthesis, the natural background concentrations in the TRUE Block Scale groundwater are given /Säfvestad and Nilsson, 1999/. When no parenthesis value is given, the injected concentration corresponded to the background concentration.

B No concentration values available.

4. Optimisation of the radioactive tracers with respect to their half-lives had to be done; i.e., the most short-lived tracers could only be used for injection in the KI0025F03:P5 section (injections C1 and C4).

5. The amount of injected activity for the tracers used was optimised using the following constraints:

   a. The total injected amount of each tracer should not exceed 10 ALI (1 ALI = Annual Limit of Intake, corresponds to the amount of a particular radioisotope that with an oral intake causes of dose equivalent of 12mSv, the maximum allowed dose per year).

   b. The total amount of radioisotopes in one injection should not exceed 100 ALI..

   c. The total amount of activity in the pumped outgoing water should not exceed 1MBq/h. (using a flow-rate of 2 litres per minute, this corresponds to maximum concentration of ~10 kBq/l).

   d. The external dose-rate at the fence enclosing the experimental site should not at any time exceed 2 μSv/h.

4.4 Discussion and conclusions regarding tracers

4.4.1 Conservative tracers

The in situ pilot pre-test at the TRUE-1 site was initiated for the selection of non-sorbing tracers for the Phase B tracer test /Holmqvist et al, in prep/ gave valuable comparative information about the non-sorbing tracers used. The discussion and conclusions in the following sections pertain to all different groups of tracers studied in the pre-tests and used in the in situ tracer tests performed in the TRUE Block Scale target area.

Fluorescent dye tracers

Among the fluorescent dye tracers used, Uranine, Eosin Y, Dimethylfluorescein, Naphtionate, Pyranine and "UV-1" behaved satisfactorily in the in situ tracer test and were therefore considered as possible candidates. Furthermore, a HPLC detection procedure was developed in which simultaneous detection could be performed for Uranine, Eosin Y, Dimethylfluorescein, Naphtionate and Sulforhodamine G. This method was found to be very promising since spectral interferences between different fluorescent dye tracers can be avoided and thereby increase the possibility of using several tracers simultaneously. The disadvantage with the HPLC method is that the detection limit is higher than when normal fluorescence spectrophotometry is used.

Three fluorescent dye tracers behaved unsatisfactorily in the in situ tracer experiment. A severe precipitation/sorption occurred for Rose Bengal and Phloxine B already in the injection borehole. The recovery of Sulforhodamine G was significantly lower than for the simultaneously injected Uranine.

Solubility tests done in laboratory experiments indicated that a possible explanation to the behaviour of Rose Bengal and Phloxine B could be that the relative high concentration of Ca^{2+} in Äspö groundwater causes precipitation of the tracers. Precipitation in high concentrations of Ca^{2+} could also be observed for Eosin Y and Eosin B. For the other Fluorescein derivatives (Dibromo-fluorescein, Diiodo-fluorescein, Dinitro-fluorescein, Carboxy-fluorescein, Tetrachloro-fluorescein) included in the laboratory experiment, no precipitation could be observed.

The study concerning the application of solvent extraction for volumetric enrichment of Fluorescein (Uranine) and Fluorescein derivatives showed promising results. The results indicated that volumetric enrichment can be performed for all Fluorescein derivatives used which when applied in in situ experiment could increase the dynamic range of the experiment. A combination of solvent extraction for volumetric enrichment and HPLC-detection could significantly increase the potential for fluorescent dye tracer in tracer tests in the future.

In the in situ tracer experiment, the fluorescent dye tracers generally behaved as expected. However, some problems with potential degradation of Uranine was found during the phase B experiments which was overcome by buffering the samples directly at the sampling stage. Furthermore, a significant delay of Uranine compared to $^{82}Br^-$ was found in the phase C experiment; an observation which is associated with a temporary contact of the Uranine to strong (0.15 M) hydrochloric acid during the preparation of the tracer cocktail in that experiment.

Anions

Radioactive isotopes of Br^- and I^- were used as tracers in two of the phase C injections with satisfactory results. The perrhenate anion (ReO_4^-) was used as a non-radioactive tracer (measured using ICP-MS) in the pilot tracer tests and in the Phase B tracer test; all with satisfactory results. In the Phase C tracer experiment, the radioactive tracer ($^{186}ReO_4^-$) was injected, yielding a very low chemical concentration (start concentration <50 ppb). The results showed a non-sorbing behaviour and a high mass recovery.

Metal complexes

In the pilot tracer tests and in the Phase B tracer tests, EDTA complexes of In^{3+}, Yb^{3+} and Lu^{3+} together with DTPA complexes of Gd^{3+} and Ho^{3+} were used as tracers. The selection was based on earlier experiences concerning the behaviour of metal complexes in in situ experiments and on considerations on the stability of the complexes from laboratory experiments /Byegård et al, 1999/.

In the pilot tracer tests, satisfactory results were obtained from all the tracers mentioned above. An additional metal complex tracer tested, Ni-EDTA^{2-} showed initial loss and very low recovery; indicating limited stability of this particular complex.

In the Phase B tracer tests, Yb-EDTA^{-}, In-EDTA^{-}, Gd-DTPA^{2-} and Ho-DTPA^{2-} were selected as tracers. The results were satisfactory. Regarding the use of metal complexes in future experiments, it is likely that the other metal ions in the middle of the lanthanide series (e.g., Eu^{3+}, $Tb^{3+}$and Dy^{3+}) are possible candidates to be used as DTPA complex tracers. Another way of obtaining a larger number of metal complex tracers is to use radioactive isotopes of the metals. However, this requires that the experiment is performed with the restrictions that are applied when radioactive isotopes are used; i.e., the complexity of the experiment is increased.

Water tracers

Water tracer refers to the water molecule in which an enrichment of a less abundant isotope has been performed. In the pilot tracer tests of the TRUE Block Scale experiments, deuterated water (D_2O or $H^2{}_2O$, stable isotope) was tested as tracer. As expected, the shape of the breakthrough curve and the recovery rate show a satisfactory behaviour of the tracer. A general problem using deuterated water as tracer is the high background concentration (~150 ppm) that limits the dynamic range of the tracer. In the pilot tracer tests, the lowest measured concentration is reported as a C/M_{tot}-value of ~$1 \cdot 10^{-6}$ ml^{-1}.

Tritiated water (HTO or HH^3O, radioactive isotope) was used in the Phase C experiments and gave satisfactory results. However, using the tracer together with other radioactive tracers may give problems due to the non-specific measuring method (liquid scintillation, cf /Andersson et al, 2001c/) used for tritium.

Fluorinated benzoic acids

A test of five different fluorinated benzoic acids as groundwater tracers was performed within the pilot tracer tests of the TRUE Block Scale experiment. Measurements of the tracers were performed on preserved samples more than two years after the experiment. In order to measure the sub-ppm concentrations obtained in the effluent water, an improved detection method /cf Holmqvist et al, in prep/ was developed within the project. To our knowledge, this experiment is the first time that fluorinated benzoic acids have been used as tracers with this low concentrations (7–40 µg/l) in the effluent water.

The results of the pilot tracer tests indicate that the shapes of the breakthrough curves of the different fluorinated benzoic acids are similar to the simultaneously injected Uranine. However, the mass recoveries of the fluorinated benzoic acids are significantly lower. One can only speculate about the reasons for the noted discrepancies. Laboratory and in situ experiments described in literature /Stetzenbach and Farnham, 1994/ have not identified any problem with sorption and/or degradation of the fluorinated benzoic acids. However, both the long preservation time and the significant lower

concentrations in the present experiments are potential reasons for a different behaviour of the tracers compared to the experiments described in the literature.

The fluorinated benzoic acids have great potential as groundwater tracers in future experiments. The HPLC make it possible to measure several tracers simultaneously and with the newly developed detection method, concentrations >0.1 ppb can be measured. However, the reason for the lower recoveries has to be investigated further before further use of the tracers.

Helium

In all of the TRUE Block Scale experiments where helium was used as a tracer, the breakthrough curves of He show a pronounced retardation, indicative of matrix diffusion. The use of He is therefore a very promising technique.

One consideration for future experiments is that the use of He as tracer requires use of equipment made of non-diffusive material, e.g., stainless steel. For the use of sorbing tracers, e.g., different cations, stainless steel is suspected to cause sorption and should therefore be avoided. It is therefore likely that careful planning and optimisation of the equipment material has to be performed if a new multi-tracer programme was to be performed.

4.4.2 Sorbing tracers

The sorbing tracers were mainly used for obtaining information of the retention characteristics of the flow paths studied and these items are thoroughly discussed in Chapters 6 through 7, including conclusions which can be drawn with any resort to modelling, cf Section 6.3.1. In this section, only one general conclusion concerning the detection technique of the radioactive sorbing tracers is given.

The construction of a large volume on-line flow cell which was used for the γ-spectrometry measurement at the withdrawal made it possible to obtain better breakthrough data for the short-lived tracers used in the various injections (e.g., $^{42}K^{+}$ $t_{½}$=12.4 h, $^{24}Na^{+}$ $t_{½}$=12.4 h, $^{47}Ca^{2+}$ $t_{½}$=4.7 d and $^{131}Ba^{2+}$ $t_{½}$=11.5 d). The possibility of using short-lived tracers increases the flexibility of studying several flow paths at the same time.

5 Interpretation of tracer test data

5.1 Evaluation of tracer dilution tests

Flow rates are calculated from the lowering of tracer concentration versus time through dilution with natural unlabelled groundwater, cf /Winberg (*ed*), 1996/. The so-called "dilution curves" are plotted as the natural logarithm of concentration versus time (Figure 2-1). Based on the equation of continuity, a straight-line relationship exists between the natural logarithm of the relative tracer concentration (C/C_0) and time (t). The straight-line fit to experimental data produced within the TRUE-1 and TRUE Block Scale Projects has generally been very good. The equation may be written:

$$Q_{bh} = -V \cdot \Delta \ln (C/C_0) / \Delta t \qquad (5\text{-}1)$$

where Q_{bh} (m^3/s) is the groundwater flow rate through the borehole section and V (m^3) is the volume of the borehole section. The flow, Q_{bh}, may be translated into a Darcy velocity by taking into account the distortion of the flow caused by the borehole and the angle between the borehole and flow direction. In practise, a 90° angle between the borehole axis and the flow direction is assumed and the relation between the flow in the rock, the Darcy velocity, q_w (m/s), and the measured flow through the borehole with a dilution test, Q_{bh}, can be expressed as:

$$Q_{bh} = q_w \cdot L_{bh} \cdot 2r_w \cdot \alpha \qquad (5\text{-}2)$$

where L_{bh} is the length of the borehole section (m), r_w is the borehole radius (m) and α is the factor accounting for the distortion of flow caused by the borehole. The factor α is commonly given the value 2 in the calculations, which is the theoretical value for a homogeneous porous media.

5.2 Evaluation of tracer tests

5.2.1 Interpretation of retention parameters from the injection curves

Surface distribution coefficient concepts

For the case of an isolated borehole section with a fracture of flowing water transecting the section, the mass balance of a non-sorbing aqueous tracer introduced to the section gives:

$$Q_{\text{in}} \cdot C_{\text{in}} \cdot dt - Q_{\text{out}} \cdot C_{\text{out}} \cdot dt = d\left(C_{\text{aq}} V\right) \qquad (5\text{-}3)$$

where Q_{in} and Q_{out} (m^3/s) are the flow rate in and out of the borehole section, respectively, V (m^3) is the system volume, C_{in} and C_{in} are the aqueous tracer concentrations in the water going in and out of the borehole section, C_{aq} (mole/m^3) is the aqueous tracer concentration in the borehole section, and t (s) is the time.

If the tracer can sorb on the exposed borehole wall and a linear sorption approach can be used, i.e.,

$$C_{\text{ads}} = K_a \cdot C_{\text{aq}} \tag{5-4}$$

where C_{ads} (mole/m^2) is the concentration of tracer on the borehole wall, K_a (m) is the surface sorption coefficient, the mass balance is instead written:

$$Q_{\text{in}} \cdot C_{\text{in}} \cdot dt - Q_{\text{out}} \cdot C_{\text{out}} \cdot dt = d\left(C_{\text{aq}} V\right) + d\left(C_{\text{ads}} A_s\right) \tag{5-5}$$

where A_s (m^2) is the geometric surface area of the exposed borehole wall.

Rearrangement and insertion of (5-4) in (5-5) yields

$$Q_{\text{in}} \cdot C_{\text{in}} \cdot dt - Q_{\text{out}} \cdot C_{\text{out}} \cdot dt = d\left(C_{\text{aq}} V\right) + d\left(C_{\text{aq}} K_a A_s\right) \tag{5-6}$$

Normally, the following conditions are applicable:

$$\begin{aligned} &Q_{\text{in}} = Q_{\text{out}} = Q_{bh} \\ &C_{\text{in}} = 0 \\ &dV = 0, dK_a = 0, dA_s = 0 \\ &C_{\text{out}} = C_{\text{aq}} \end{aligned} \tag{5-7}$$

and (5-6) can therefore be written as:

$$-Q_{bh} \cdot C_{\text{aq}} \cdot dt = dC_{\text{aq}} \left(V + K_a A_s\right) \tag{5-8}$$

With the boundary condition C_{aq}=$C_{\text{aq,0}}$ at t=0, Equation (5-8) has the analytical solution:

$$K_a = \frac{Q_{bh} t}{A_s \cdot \ln\left(\frac{C_{aq,0}}{C_{aq}}\right)} - \frac{V}{A_s} \tag{5-9}$$

In this model, it is assumed that the injection section can be approximated with an ideally mixed tank. For the validity of the model, it is therefore important that the dilution flow rate across the borehole section is low compared to the circulation flow rate. The model also implies that no diffusion and sorption into the rock matrix occurs, i.e., the only mass transfer process is the surface sorption.

From the straight-line decrease in concentration in semi-logarithmic scales of the non-sorbing tracers (i.e., K_a=0), the dilution flow rate can be calculated. A deviation in the slope for a sorbing tracer makes it possible to calculate K_a-values. These sorption coefficients could be of interest to compare with sorption coefficients obtained in laboratory experiments and with retention data obtained from the modelling of the in situ breakthrough results in the pumping borehole. Attempts were therefore made to fit Equation (5-9) to some of the experimental results from TRUE-1 /Winberg et al, 2000/ and TRUE Block Scale. It should in this context be noted that dedicated tests on

sorption of relevant tracers on tubings and materials showed negligible sorption on equipment /Ittner and Byegård, 1997/.

It should be noted that during this evaluation of the injection curves from the TRUE-1 and TRUE Block Scale experiments, the C_{aq} refers solely to the concentration of the injected radioactive tracer of the element used. The impact of any changes in the total chemical concentrations of the different element used as tracers is discussed below.

Data from TRUE-1

Fitting of Equation (5-9) to the experimental data for STT-1 and STT-2 (experiments within the TRUE-1 programme) are shown in Figure 5-1 and 5-2, respectively. The derived surface distribution coefficients for Rb^+, Cs^+ and Ba^{2+} are given in Table 5-1. The sorption for the Na^+, Ca^{2+} and Sr^{2+} is very weak and was not evaluated since the slope of the dilution curves of those tracers did not deviate significantly from the dilution curve of the non-sorbing tracers. A slightly increased sorption is observed in STT-2 compared to STT-1, which may be explained by the observed decreased salinity in the STT-2 experiment compared to the STT-1 experiment. It should be noted that K_a values were estimated by this method although the tracers, due to probable reasons discussed in the following sections, do not show an ideal straight line for the whole time interval studied. The K_a values evaluated from the injection data agree reasonably to the to the values obtained in the TRUE-1 laboratory experiments /Byegård et al, 1998/. The laboratory values used for comparison are determined using non-altered Äspö diorite (cf /Byegård et al, 1998/ for mineralogical composition) and the conditions in the laboratory experiment are thus very similar to the in situ conditions.

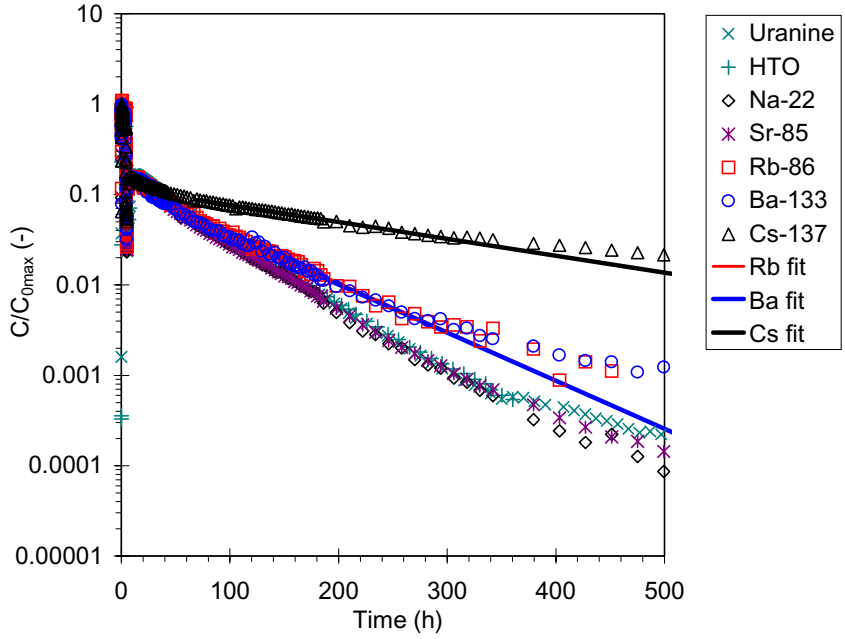

Figure 5-1. *Results of fitting Equation (5-9) to the injection data of the STT-1 experiment. The data for the time interval 70–200 h were used for the calculations.*

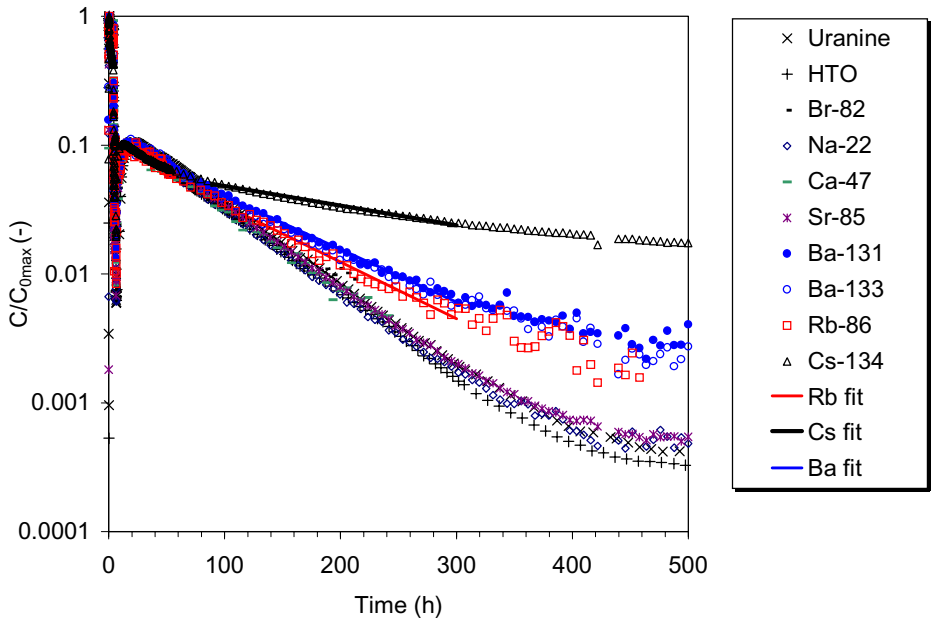

Figure 5-2. *Results of fitting Equation (5-9) to the injection data of the STT-2 experiment. The data for the time interval 70–300 h were used for the calculations.*

Table 5-1. Surface distribution coefficients, K_a, obtained from the fitting of injection data from the STT-1 and STT-2 experiments (TRUE-1) and the C3 injection (TRUE Block Scale). For comparison, the K_a values obtained in the TRUE-1 laboratory experiments are also presented.

Tracer	TRUE-1 K_a STT-1 (Eq. 5-9)	K_a STT-2 (Eq. 5-9)	TRUE Block Scale K_a C3 (Eq. 5-9)	Laboratory K_a Lab /Byegård et al, 1998/
$^{83,86}Rb^{+}$	$1.4 \cdot 10^{-3}$	$2.0 \cdot 10^{-3}$	$2.3 \cdot 10^{-3}$	$5 \cdot 10^{-4} – 4 \cdot 10^{-3}$
$^{133}Ba^{2+}$	$1.5 \cdot 10^{-3}$	$2.6 \cdot 10^{-3}$	–	$2 \cdot 10^{-4} – 6 \cdot 10^{-4}$
$^{134,137}Cs^{+}$	$1.6 \cdot 10^{-2}$	$1.7 \cdot 10^{-2}$	–	$8 \cdot 10^{-3} – 1 \cdot 10^{-2}$

Data from TRUE Block Scale

A forced injection was used in two of the injections in Phase C of the TRUE Block Scale Experiment. As a result, a significant increase in the injection flow rate was obtained in the TRUE Block Scale Experiment compared to the TRUE-1 experiment. In the injections C1/C4 and C2 the flow rate was 2600 ml/h and 600 ml/h, respectively, which can be compared to the injection flow rate of the TRUE-1 experiment (~30 ml/h). The implication of this is that the sorption process has less time for equilibration and that the injection flows no longer are negligible compared to the circulation flow (12 000 ml/h). The duration time in the injection section becomes shorter and doubts

can be raised about the validity of the assumption of the borehole section as an "ideal tank". It is a risk therefore that during the initial phase of the injection, non-homogeneously mixed tracer solution might have been directly injected into the fracture system. The calculation of the mass balance within the borehole section therefore becomes uncertain.

The concept of fitting Equation (5-9) to the injection experimental data was therefore only applied for injection C3 (cf Figure 5-3) in the case of TRUE Block Scale. This injection was performed without applying any extra injection flow, i.e., the observed dilution was only a result of the pumping performed in the pump borehole. As for the TRUE-1 injections, the deviations in the behaviour of the weakly sorbing tracers used in C3 (Na^+ and Sr^{2+}) from that of the non-sorbing tracer (HTO) were not large enough to allow a calculation of the K_a. Furthermore, the general uncertainty of the behaviour of the $^{133}Ba^{2+}$ tracer used (mainly because of the low activity used for that tracer) also excluded any meaningful analysis of that tracer. The fitting calculation was therefore only done for Rb^+ where data for the 70–300 h interval was used for a K_a-calculation according to Equation (5-9). The result is given in Table 5-1 and is in good agreement with both the TRUE-1 results and the laboratory data. It should be noted, however, that the declining Rb^+ concentration is not linear over a longer time period, which somewhat contradicts the assumption of a sorption model constituted by a fast reversible sorption only on the borehole walls.

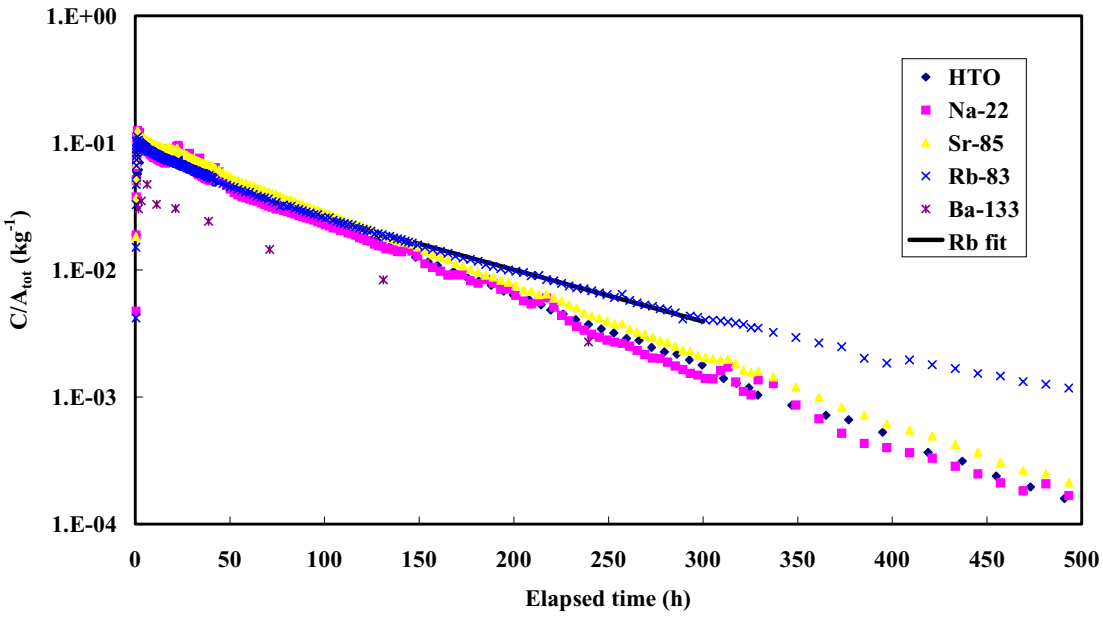

Figure 5-3. *Dilution curves for injection C3 including the fit Equation (5.9) to the Rb^+ data in the time interval 70–300 h.*

Matrix diffusion approach

As shown in the previous section, deviations are observed in the experimental data from the model including only dilution and surface sorption. A possible explanation for this may be that the tracers diffuse into the pores of the rock matrix where sorption may take place. Observing the dilution curves for STT-2 in log-log scale (cf Figure 5-4) a tendency of a slope of –3/2 is indicated after 500 h, which could be indicative of diffusion out of the rock matrix being the rate limiting process (described by e.g., /Heer and Hadermann, 1996/).

An interesting observation in the TRUE Block Scale injections C1 and C2, cf Figure 5-4, is that the slopes for the injection curves for Cs^+ in log-log scale after 200h approach –3/2. This time-dependence in the concentration may indicate that diffusion is the rate limiting process for the de-sorption of Cs^+. Furthermore, the same tendency of a late time slope of –3/2 in the log-log scale can be observed in injection C3 for Rb^+ and in injection C4 for Ba^{2+} and Mn^{2+}.

For the non- or very weakly sorbing tracers used (e.g., HTO, Na^+, Sr^{2+}) a change in the slope in the log-log scale can be observed after 500 h, both for STT2 (TRUE-1) and for injection C3 (TRUE Block Scale) all data in Figure 5-4.

However, one should be aware of the fact that the impact of sorption/de-sorption kinetics may give deviations in the injection curves similar to the proposed matrix diffusion processes. Laboratory experiments /e.g., Byegård et al, 1998/ have indicated limited sorption reversibility, especially for Cs^+ but to some extent also for Rb^+ and Ba^{2+}. The impact of sorption kinetics is investigated below.

Non-linear sorption approach

Sorption on surfaces in crystalline rocks has in many studies been interpreted using a Freundlich isotherm, i.e.;

$$C_{\text{ads}} = K_{\text{F}} \cdot C_{\text{aq}}^{\ n_F} \qquad (5\text{-}10)$$

where K_{F} (mole$^{n\text{F}-1}$ m$^{(3n\text{F}-2)}$)and n_{F} (–) are empirical constants used in the Freundlich isotherm and C_{ads} and C_{aq} are referring to the chemical concentration of the element studied. With n_{F}=1 the sorption is linear and equivalent to Equation (5-4). Using n_F<1 implies that the relative sorption (C_{ads} / C_{aq}) will increase as the total concentration of the element decreases, i.e., an example of non-linear sorption. The latter has often been observed for e.g., Cs in laboratory experiments /e.g., Skagius et al, 1982; Andersson, 1983/ and n_{F}≈0.5 is a typical interpretation.

However, in the TRUE experiments chemical concentration gradients are avoided by the use of radioactive tracers which are thus always injected in concentrations found naturally in the groundwater. For the total chemical concentration of the elements used as tracers, it therefore seems reasonable to assume that C_{in}=C_{out} in Equation (5-5). This will imply that dC_{ads}=0 and dC_{aq}=0, i.e., no total concentration changes will occur with time in the system and a linear sorption approach should be applicable.

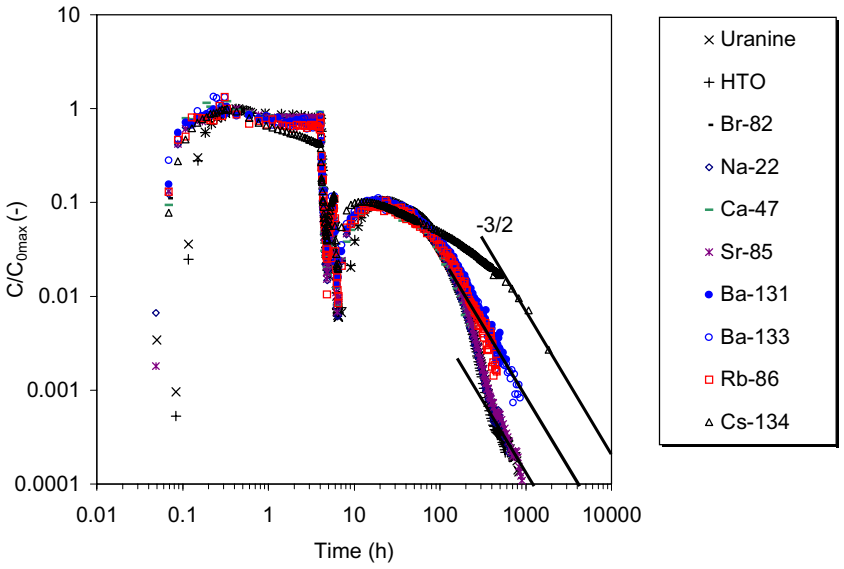

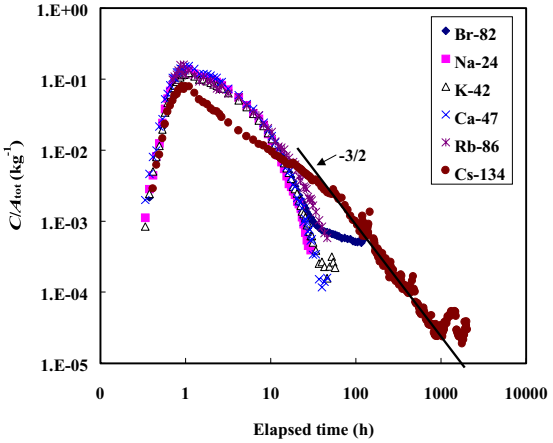

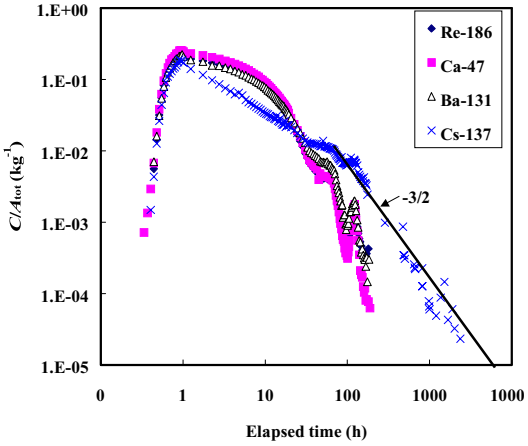

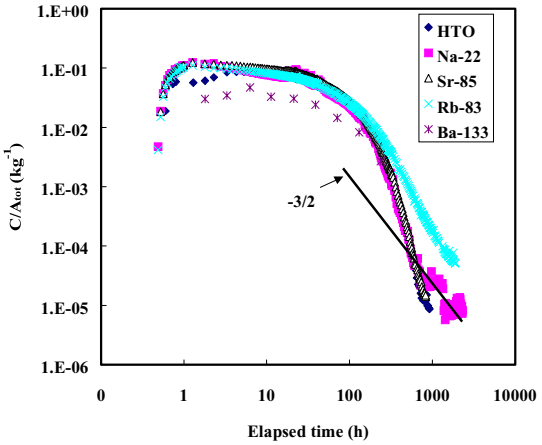

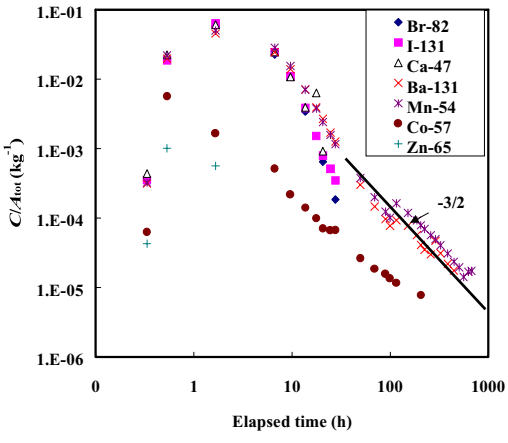

Figure 5-4. *Injection curves for STT2 experiment in TRUE-1 (top), TRUE Block Scale injection C1 (middle, left), injection C2 (middle, right), injection C3 (bottom, left) and injection C4 (bottom, right).*

Nevertheless, a non-linear approach has been tested in order to investigate what effects non-linear sorption possibly could have on the interpretation of the injection curves of the TRUE Block Scale experiments. In this approach, it is assumed that the non-linearity is caused by the changes in concentration of the radioactive tracers, i.e. any influence from the background concentration of the stable isotopes of the element is neglected. Equation (5-10) is therefore inserted in (5-5) under the assumption that C_{ads} and C_{aq} are the concentration of radioactive tracer in the adsorbed phase and in the aqueous phase, respectively. By also applying the conditions in (5-7), the following expression for the dilution of a non-linearly sorbing tracer is obtained:

$$-Q \cdot C_{aq} \cdot dt = d\left(C_{aq} V\right) + d\left(C_{aq}^{n_F} K_F A_s\right) = V \cdot dC_{aq} + K_F A_s \cdot d\left(C_{aq}^{n_F}\right) \qquad (5\text{-}11)$$

Equation (5-11) can be solved by the Euler integration technique and by using the boundary condition $C_{aq}=C_{aq,0}$ at $t=0$.

The dilution curves for $^{134}Cs^+$ in injection C1 and for $^{83}Rb^+$ in injection C3, together with the STT2 injection of $^{134}Cs^+$ in TRUE-1, have been used to exemplify the impact of this non-linear sorption approach. K_F and n_F have been used as fitting parameters. The results (Figure 5-5 and Table 5-2) indicate that the non-linear approach gives rather good fits to the experimental results. For Cs^+ the initial loss is not satisfactorily explained by the non-linear approach; however, the straight line in log-log scale at late time is reproduced by the non-linear approach. For Rb^+ the whole dilution curve can be reproduced satisfactorily, except for the behaviour after 500 h where the slope in the experimental results deviates from the tested model. For both tracers, it is noted that the experimental results give slopes that are smaller than what the fit of the non-linear sorption behaviour gives.

It is an interesting observation that the non-linear approach with a Freundlich isotherm can reproduce the form of the injection curves of Cs^+ and Rb^+ quite well. However, it is difficult to find any mechanistic explanation for a non-linear sorption behaviour. The concentrations of the injected radioactive tracers are ~$1\cdot10^{-10}$ M (Rb^+) and ~$1\cdot10^{-8}$ M (Cs^+) can be compared to the natural background concentration of $6\cdot10^{-7}$ M and $4\cdot10^{-8}$ M for Rb^+ and Cs^+, respectively. It is therefore difficult to explain a change in the total concentration, leading to a variation of the relative sorption, as stated by Equation (5-10).

One can speculate that the background concentration of these elements being present in another chemical form (e.g., colloidal microscopic rock fragments) compared to the ionic form in which the radioactive tracers are injected. The loss observed for the radioactive tracer would then be equivalent to the concentration decrease of the ionic species of the elements, and the Freundlich isotherm (5-10) would be valid. However, explaining the behaviour of Rb^+ and Cs^+ in the injection curves for TRUE Block Scale with non-linear effects would imply that some type of saturation effect would occur below $1\cdot10^{-10}$ M. It is generally agreed that sorption should be more or less linear when the concentrations are decreased. However, /Andersson, 1983/ reports that a Freundlich isotherm with an exponent $n_F=0.5$ could explain the sorption of Cs^+ on Stripa granite down to a total concentration of $1\cdot10^{-8}$ M, the lowest concentration studied in that experiment.

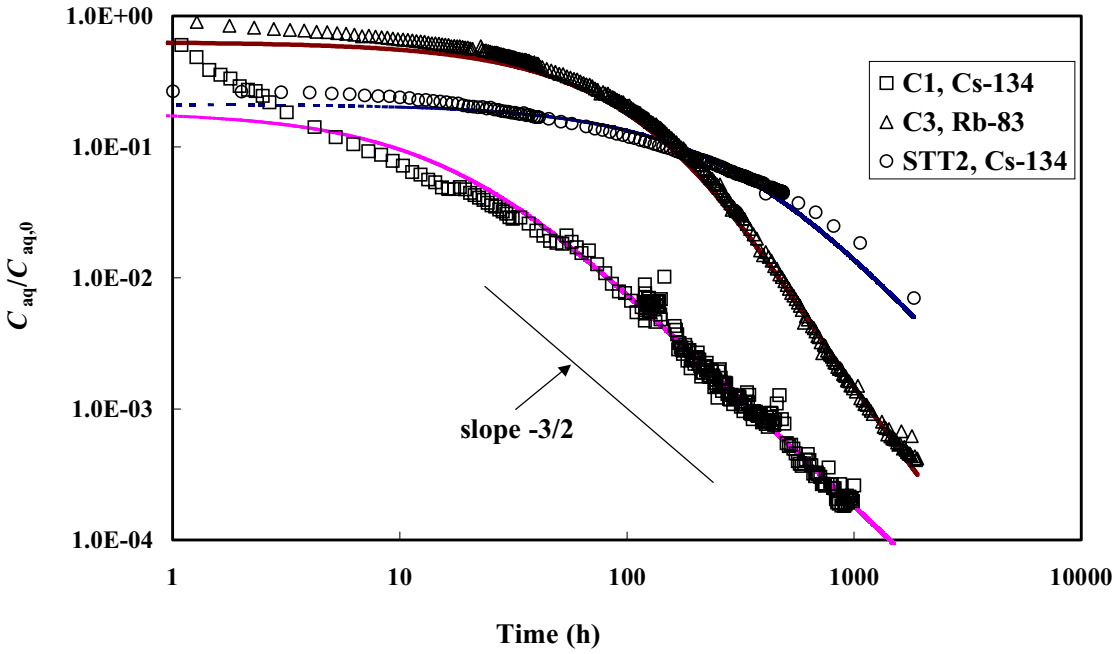

Figure 5-5. *Fit of a non-linear (Freundlich isotherm) sorption model to the injection curves for $^{134}Cs^{+}$ (injection C1 in TRUE Block Scale, injection STT2 in TRUE-1) and ^{83}Rb (injection C3 in TRUE Block Scale).*

Table 5-2. Numerical values of the parameters obtained from fitting a non-linear sorption approach to the injection curves.

Injection	Tracer	K_F (m)	n_F
TRUE Block Scale (C1)	$^{134}Cs^{+}$	$1.3 \cdot 10^{-1}$	0.38
TRUE Block Scale (C3)	$^{83}Rb^{+}$	$3.1 \cdot 10^{-2}$	0.50
TRUE-1 (STT-2)	$^{134}Cs^{+}$	$2.8 \cdot 10^{-1}$	0.45

It should also be pointed out that other possible retention processes taking place in the injection borehole (e.g., heterogeneous matrix diffusion, kinetically hindered sorption/desorption) may give rise to a behaviour of the tracers that erroneously can be interpreted by a non-linear sorption model. Additional investigations are probably necessary to obtain a clearer picture of this issue.

First order kinetics approach

A first-order kinetics approach (see Appendix 1 for details) has been used for interpretation of the injection curves of $^{134}Cs^{+}$ (Block Scale, injection C1) and $^{83}Rb^{+}$ (Block Scale, injection C3). The rate constants for the sorption and desorption reactions (k_s and k_{des}, respectively) were varied in order to fit the experimental results. The results are presented in Figure 5-6 and it is noted that systematic deviations from the model are obtained, especially for Cs^{+} in the C1 injection. On the contrary, for the TRUE-1 STT2 injection the first order kinetics approach can very well explain the shape of the injection curve. However, one should be aware of the fact that the injection curve of Cs^{+} in the TRUE Block Scale experiment has a dynamic range of >3.5 orders of magnitudes compared to the injection curve of Cs^{+} in the TRUE-1 STT2 injection (1.5 orders of magnitudes). Limitations in the applicability of the first order kinetics sorption model are therefore more likely to be obvious in the former case (TRUE Block Scale) than in the latter (TRUE-1).

An additional consideration in succeeding to fit the first order kinetics sorption model to the data of the Cs^{+} injection in the TRUE-1 STT2 injection is that only the data obtained after the exchange of the water in the injection section has been used in the interpretation. (See /Winberg et al, 2000/ for the exact injection procedure for the TRUE-1 tracer experiment). As a validation, the sorption parameters obtained were used for calculating the sorption before the exchange of the groundwater in the injection section. The results of that calculation indicated that the sorbed amount was underestimated by a factor 5 compared to the actual experimental results.

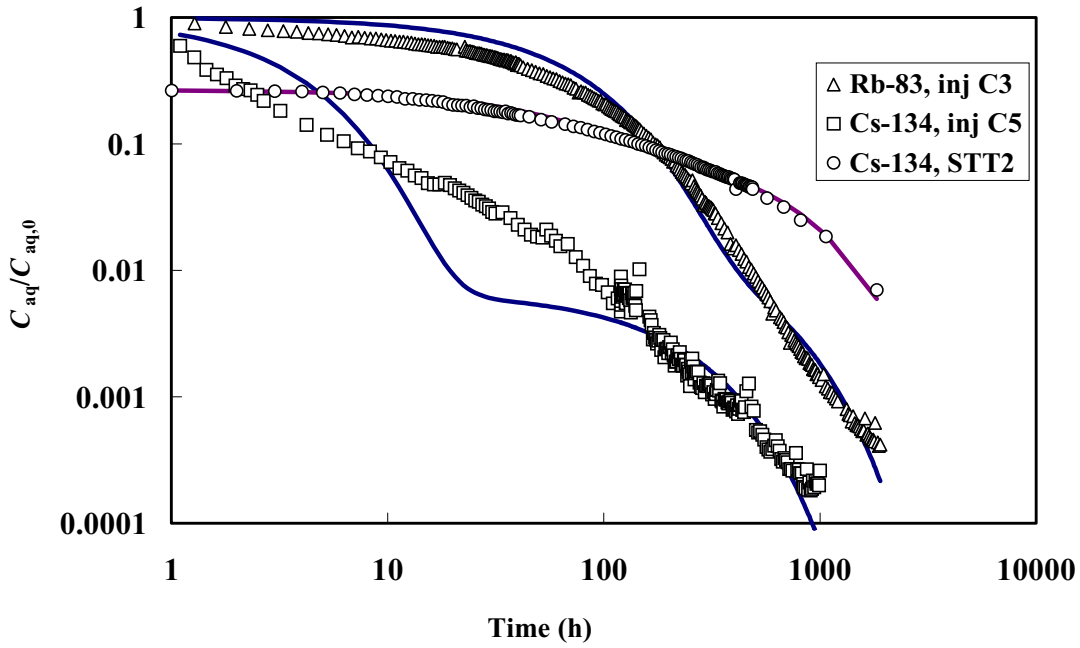

Figure 5-6. *Results of the fitting of a first order kinetics sorption model to the injection curves for $^{134}Cs^{+}$ (injection C1 in TRUE Block Scale and injection STT2 in TRUE-1) and $^{83}Rb^{+}$ (injection C3 in TRUE Block Scale).*

Table 5-3. Numerical values of the parameters obtained from the fitting of a first order kinetics sorption approach to the injection curves.

Injection	Tracer	k_s (s^{-1})	k_{des} ($m^{-1}s^{-1}$)	K_a (m) (=k_s/ k_{des})
TRUE Block Scale C1	$^{134}Cs^+$	$9.1 \cdot 10^{-8}$	$1.8 \cdot 10^{-6}$	$5.1 \cdot 10^{-2}$
TRUE Block Scale C3	$^{83}Rb^+$	$1.8 \cdot 10^{-9}$	$7.3 \cdot 10^{-7}$	$2.4 \cdot 10^{-3}$
TRUE-1 (STT-2)	$^{134}Cs^+$	$2.6 \cdot 10^{-9}$	$4.7 \cdot 10^{-7}$	$5.4 \cdot 10^{-3}$

5.2.2 Qualitative interpretation of breakthrough curves

An important step in evaluating tracer breakthrough curves is to simply study the shape of the breakthrough curves and some key parameters that can be derived from it. These parameters also facilitate comparison between different breakthrough curves. The first step in the evaluation process is to plot the data in both linear (lin-lin), cf Appendix 2, and logarithmic scales (log-log), cf Chapter 6. When doing this, data points that deviate very much from the rest are removed or re-analysed. The reason for plotting in both linear and logarithmic scales is that the logarithmic scale overemphasises the rising part of the breakthrough curve and could also, due to the scale, be somewhat misleading when comparing breakthrough curves. The data are then transformed from concentration (mg/l) to mass flux (mg/h) by multiplying concentrations with the pumping rate and finally normalising by dividing with the input mass. This procedure makes it possible to directly compare different breakthrough curves provided that the injection procedure is similar. Thus, the next step is to co-plot breakthrough curves from different tests performed in the same flow geometry, different solutes, or different flow paths, respectively.

An important step in the evaluation process is to study the log of events, i.e. a listing of pump failures, power failures or other disturbing activities. By doing this at an early stage much effort could be saved. Instead of trying to explain e.g. the occurrence of double peaks by means of a dual fracture model, the real reason might simply be a pump failure.

The parameters determined from the breakthrough curves without modelling are the travel times for 5, 50 and 95% arrival of the tracer mass (t_5, t_{50} and t_{95}) and the tracer recovery (cf Chapter 5.3). The 50% arrival time is also referred to as the "mean travel time". In addition, the "first arrival time" of the tracer is determined but this is a parameter that should be used with care. Generally, first arrival is defined as the time when the tracer concentration rises above the background level or detection limit set by the analysis equipment. Thus, first arrival is also dependent on the tracer used.

5.2.3 Modelling of advective and dispersive parameters

Evaluation of tracer tests can be done in many different ways using a variety of models and concepts. The TRUE Block Scale tracer tests have been evaluated with several different concepts and tools thoroughly described in /Poteri et al, 2002/. In addition, all tests have been evaluated using a "standard" procedure similar to the one used in TRUE-1 /Winberg et al, 2000/. The main reason for using this standard procedure has been to be able to compare different flow paths and also to enable comparison with the TRUE-1 results using a simple and robust model.

The concept used is a one-dimensional advection-dispersion model /Van Genuchten and Alves, 1982/ where dispersivity and mean travel times were determined using an automated parameter estimation program, PAREST /Nordqvist, 1994/. PAREST uses a non-linear least square regression where regression statistics (correlation, standard errors and correlation between parameters) also are obtained.

The chosen one-dimensional model assumes a constant fluid velocity and negligible transverse dispersion, cf Equation (5-20).

$$\frac{\partial C}{\partial t} = D_L \frac{\partial^2 C}{\partial x^2} - v \cdot \frac{\partial C}{\partial x} \qquad (5\text{-}20)$$

where, D_L is the dispersion coefficient, v is fluid velocity (m/s), C is concentration of solute, x is distance from the injection point (m), and t is time (s).

According to /Ogata and Banks, 1961; Zuber, 1974/, the dispersion in a radially converging flow field can be calculated with good approximation by equations valid for one-dimensional flow. Although a linear flow model (constant velocity) is used for a converging flow field, it can be demonstrated that breakthrough curves and parameter estimates are similar for Peclet numbers of about 10 and higher.

/Van Genuchten, 1982/ gives a solution for step input with dispersion over the injection boundary /cf Winberg et al, 1996/. Variable injection schemes were simulated by superposition of the solution. The fit of the breakthrough curves using a three-parameter fit included velocity v, dispersion coefficient D_L, and the so called F-factor, a proportionality factor that accounts for the dilution in the fracture system (same definition as pf in Section 5.2.4).

Based on the mean travel times, t_0, determined from the parameter estimation, the hydraulic fracture conductivity, K_{fr} (m/s), was calculated assuming radial flow and validity of Darcy's law /Gustafsson and Klockars, 1981/;

$$K_{fr} = \ln\left(\frac{r}{r_w}\right) \cdot \frac{\left(r^2 - {r_w}^2\right)}{2 \cdot t_0 \cdot \Delta h} \qquad (5\text{-}21)$$

where, r is travel distance (m), r_w is borehole radius (m), t_m is mean travel time of tracer (s), and Δh is head difference between injection and pumping section(m).

The equivalent fracture aperture (mass balance aperture), δ (m), was calculated from:

$$\delta = \frac{Q_{bh} \cdot t_0}{\pi\left(r^2 - r_w{}^2\right)} \tag{5-22}$$

where Q_{bh} (m^3/s), is the mean pumping rate.

Flow porosity, θ_k, was calculated using:

$$\theta_k = \frac{K}{K_{fr}} \tag{5-23}$$

where K is the hydraulic conductivity of the packed-off section of the borehole determined from steady state evaluation of the interference test /Moye, 1967/:

$$K = \left(\frac{Q_{bh}}{\Delta h \cdot L_{bh}}\right)^{\frac{1+\ln\left(L_{bh}/2r_w\right)}{2\pi}} \tag{5-24}$$

where L_{bh} (m) is the length of the packed-off section. It should be noted that the term flow porosity might be misleading to use in a fractured heterogeneous rock as it is defined for a porous media. However, it is often used in fractured media as a scaling factor for solute transport, but then defined over a finite thickness which, in this case, was chosen to 1.0 m.

5.2.4 Modelling of retention parameters

The evaluation of the Phase C tracer tests also included modelling using a one-dimensional advection-dispersion model with matrix diffusion and sorption. Unlike earlier modelling approaches within the TRUE-project, the evaluation this time also included sorption and diffusion parameters by fitting the so-called A-parameter which is a lumped parameter including both matrix diffusion and sorption. The governing equations may be written as /Moreno et al, 1983/:

$$R_a \frac{\partial C_f}{\partial t} - D_L \frac{\partial^2 C_f}{\partial x^2} + v \frac{\partial C_f}{\partial x} - \frac{2}{\delta} D_e \frac{\partial C_p}{\partial z}\Big|_{z=0} = 0 \tag{5-25}$$

for the fracture, and:

$$\frac{\partial C_p}{\partial t} - \frac{D_e}{\varepsilon + \rho} \frac{\partial^2 C_p}{\partial z^2} = 0 \tag{5-26}$$

for the matrix. C_f and C_p are the solute concentrations in the fracture and rock matrix, respectively, D_L is the longitudinal dispersion coefficient (m^2/s), v is the average water velocity (m/s), R_a is the linear retardation coefficient in the fracture, D_e is the effective pore diffusivity, δ is the fracture aperture (m), K_d is the linear sorption distribution coefficient for the rock matrix (m^3/kg), ε is the matrix porosity, and ρ is the bulk density of the rock matrix (kg/m^3).

For zero initial concentration and a constant concentration at the inlet during the tracer injection, a solution to the above equations is given by /Tang et al, 1981/. The parameters that were estimated using PAREST (cf Chapter 5.2.1) were the mean travel time, t_m, Peclet number, *Pe*, the so called *pf*-factor, the retardation factor, R_a, and the so called A-parameter where,

$$Pe = \frac{v \cdot x}{D_L} \tag{5-27}$$

and the proportionality factor, *pf*, introduced in order to obtain the actual concentration in the sampling borehole, C_{bh},

$$C_{bh} = pf \cdot C(t) \tag{5-28}$$

where *pf* represents the dilution in the sampling borehole and other proportional losses. In an ideal radially converging flow field, *pf* equals the (dimensionless) ratio of the injection flow rate to the pumping flow rate. However, under non-ideal conditions *pf* may also be used to account for e.g. incomplete mixing and incomplete recovery. In addition, since flow rates and tracer injection concentration (i.e. injected tracer mass) likely can not be used with absolute certainty, *pf* may be used as an estimation parameter which also account for such uncertainties.

$pf = (Q_{inj}/Q) \cdot \Pi$ (other possible proportional effects), see text above (5-29)

In the model, it is thus assumed that a non-time dependent surface retardation is occurring for the transport in the fracture and that the surface retardation is dependent on the fracture aperture, δ (m); all according to:

$$R_a = \left(1 + \frac{2K_a}{\delta}\right) \tag{5-30}$$

$$t_0' = R_a t_0 \tag{5-31}$$

where K_a is the surface sorption coefficient (m), t'_0 (h) is the residence time of a sorbing tracer and t_0 (h) is the residence time of a conservative tracer. Furthermore, a contact time dependent retardation process is occurring and can be described by the parameter A, which is defined by:

$$A = \frac{\delta R_a}{2\sqrt{D_e(\varepsilon + K_d \rho)}} = \frac{\delta + 2K_a}{2\sqrt{D_e(\varepsilon + K_d \rho)}} \tag{5-32}$$

where ρ is the density of the rock. The modelling procedure is further described and discussed in Chapters 6.3 and 7.3.

5.3 Tracer mass recovery

Tracer mass recovery R (%) is a good indicator of the level of control of a performed tracer test and has been one of the key entities in selecting suitable flow paths for tests with radioactive sorbing tracers. There may be several reasons for mass losses in a tracer test:

- background flow carrying tracer mass to another sink (e.g. the main access tunnel),
- sorption (irreversible),
- tracer degradation (biological or physical),
- exchange with stagnant zones along the flow path,
- "dilution" (parts of the mass below detection limit),
- too short sampling time (test duration),
- enhanced diffusion/sorption in fracture rim zone,
- enhanced diffusion/sorption in fine-grained fault gouge.

In the TRUE Block Scale tracer tests only a few of the 16 tested flow paths have shown full mass recovery (cf Table 2-1). The most common explanation has been too short sampling time but it is also clear that the background flow is of great importance. This is further discussed in Chapter 6.

Tracer mass recovery has been calculated in two different ways. Common for both methods is that the tracer mass recovered in the pumping borehole is determined by integration of the breakthrough curves for mass flux (mg/h) versus time (h). The injected mass is determined in the same way but also by weighing the tracer solution vessel during the injection procedure. The latter method (weighing) is considered to be more accurate than the integration method /Andersson et al, 2001c/. The reason for this is that the integration relies upon a relatively small number of samples that are integrated over some period of time. This procedure is sensitive to the early time data as the main part of the tracer mass leaves the borehole very shortly after the start of the injection. In addition, the integration method relies upon evaluation of the injection flow rate by means of the dilution of tracer with time, as described in Chapter 5.1. Therefore, the tracer mass recoveries presented in this report have generally been calculated based on weighing.

6 Experimental results and evaluation

6.1 Introduction

This chapter summarises all experimental results from tracer tests performed within the TRUE Block Scale Project and results of the basic evaluation. The term "flow path" will generally be applied to a pair of sink and source sections, although the actual (physical) flow path between them may be different depending on the boundary conditions and the spatial distribution of flow porosity. Each flow path investigated is unique and the aspects regarding transport that are addressed differ and include e.g. transport in single paths, network transport, background fractures, and fracture intersection zones (FIZ), or combinations thereof.

The uniqueness of each flow path requires that each is described individually. However, such a description would possibly be difficult to fully grasp for the reader so instead, an initial division of flow paths into single structure and network flow paths has been done. The single structure flow paths have further been divided according to the interpreted deterministic hydraulic structure where they were performed in. This division relies upon the most recent hydro-structural model presented by /Andersson et al, 2002/. There are also a few flow paths where more extensive experimental efforts have been done, in particular the work with sorbing tracers (paths I–III, see Table 6-1). Therefore, special emphasis has been put on describing these flow paths and the tests performed therein.

Table 6-1. Summary of flow paths tested in the TRUE Block Scale Project.

Flow path no.	Source	Sink	Structures	Distance (m)*	Tests	Comment
I	KI0025F03:P5	KI0023B:P6	#20,21	14 (16)	A-4, B-1, B-2, C1, C4	
II	KI0025F03:P7	KI0023B:P6	#23,21	17 (97)	A-4, B-2, C2	
III	KI0025F02:P3	KI0023B:P6	#13,21,#22	33 (33)	PT-4, B-2, C3	
IV	KI0025F03:P6	KI0023B:P6	#22,21	15 (73)	A-4, B-1, B-2	
V	KI0025F03:P3	KI0023B:P6	#21	27 (27)	B-2	
VI	KI0025F02:P5	KI0023B:P6	#20,21	21 (21)	B-1	
VII	KI0025F02:P6	KI0023B:P6	#22,21	18 (65)	PT-4, B-2	
VIII	KA2563A:S1	KI0023B:P6	#19,21	55 (130)	PT-4, B-2	
IX	KA2563A:S4	KI0023B:P6	#20,21	16 (16)	ESV-1c, PT-4	
X	KI0023B:P4	KI0023B:P6	#13,21	15 (48)	ESV-1c	No bt 220 h
XI	KI0025F:R4	KI0023B:P6	#20,21	42 (47)	ESV-1c	No bt 220 h
XII	KI0025F02:P3	KI0025F03:P5	#13,21,20	26 (37)	A-5	No bt 643 h
XIII	KI0025F02:P5	KI0025F03:P5	#20	11 (11)	A-5	
XIV	KI0025F02:P6	KI0025F03:P5	#22,20	12 (57)	A-5	
XV	KI0025F03:P6	KI0025F03:P5	#22,20	12 (65)	A-5	
XVI	KA2563A:S4	KI0025F03:P5	#20	29 (29)	A-5	

* Distance in space (Euclidean), distance within brackets = distance along interpreted deterministic structures.
bt = breakthrough

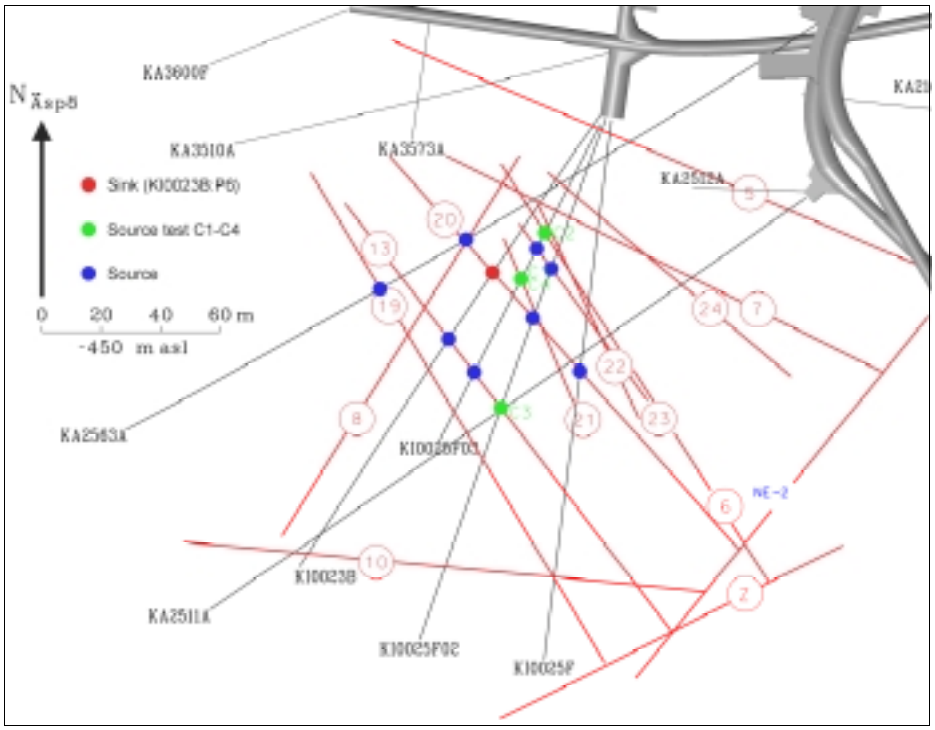

Figure 6-1. *Overview of the experimental geometry and packer locations for tracer tests using KI0023B:P6 as sink (flow paths I–XI). Position of sinks and sources are related to borehole intersections with the numbered structures and therefore represent different depths.*

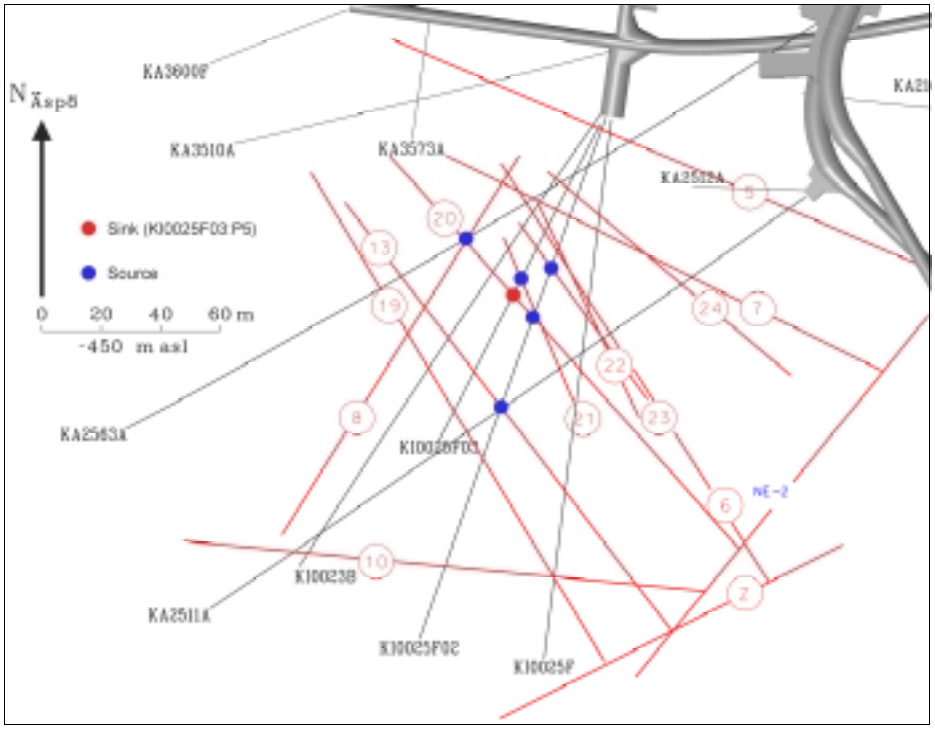

Figure 6-2. *Overview of the experimental geometry and packer locations for tracer tests using KI0025F03:P5 as sink (flow paths XII–XVI).*

In total 16 different flow paths have been tested with cross-hole tracer tests. For three of the flow paths, tracer breakthrough could not be detected (during the given experimental time period). Eight of the flow paths are interpreted as network paths and eight as single structure paths based on the hydro-structural model. Six of the latter eight are located within Structure #20 and the remaining two are located in Structure #21. Only two different sinks have been used, KI0023B:P6, the main sink, and KI0025F03:P5, which was investigated as an alternative sink during Phase A of the project /Andersson et al, 2000a/. Table 6-1 presents the pairs of sinks-sources, structures involved, type of flow path (number of structures), and a reference to the test acronym (cf. Table 2-1).

6.2 Transport of conservative tracers

6.2.1 Flow paths within Structure #20

The six flow paths tested within Structure #20 (flow paths # I, VI, IX, XI, XIII and XVI, see Table 6-1) provide a relatively large span of distances ranging between 11 and 47 metres, cf Figures 6-1, 6-2 and 6-3 and Table 6-2. The flow paths are considered to be of the type "single structure" flow paths on the basis of the hydrostructural interpretation. The figures also shows that the experimental area is intersected by two other structures, #21 and #22, and that tests have been performed across these intersections. It should also be noted that the main sink, KI0023B:P6, in fact is located within Structure #21 which means that the term "single structure" flow path is not strictly correct. However, the interpreted intercepts with Structures #20 and #21 in KI0023B are very closely located implying that more than 90% of the path length is within Structure #20 for all of the six tested paths.

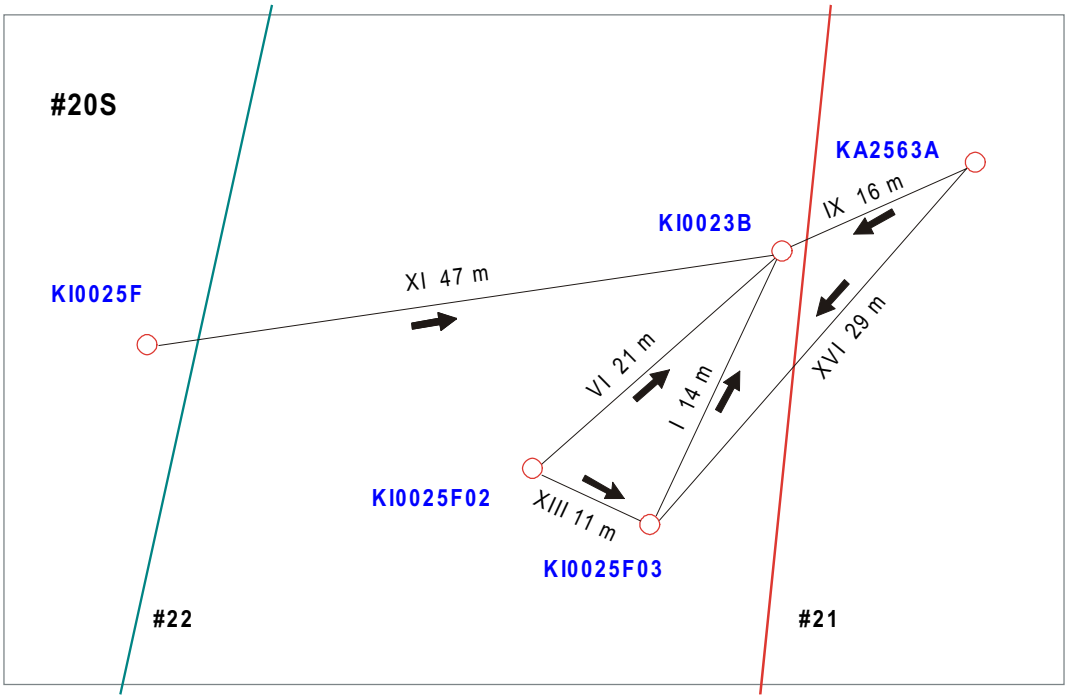

Figure 6-3. *Experimental geometry and distances for tracer tests performed in flow paths located within the plane of Structure #20 (plane view from the south).*

Flow path I, KI0025F03:P5 – KI0023B:P6

This 14 metre long flow path was found to be one the flow paths best suited for tests with radioactive sorbing tracers due to the observed high mass recovery and relatively short travel times. The flow path has been tested in five different tests of which one (B-1, cf Table 2-1) with a reduced pump rate and one (A-4) with a passive injection. The three remaining tests have all been performed with almost the same boundary conditions, a forced injection (45 ml/min) and a pumping rate of about 2 l/min. Details of the injection and pumping is given in Table 6-2.

Comparing the breakthrough of conservative tracers in the four tests performed at a similar pumping rate at the sink (2 l/min) shows some interesting characteristics (Figure 6-4). Firstly, the passive injection performed in test A-4 (Uranine) produces a significantly different breakthrough curve than the others. This is an indication that the tests reflect different, or partly different, flow paths between the injection and pumping sections depending on the difference in input signals. Secondly, the three tests performed at similar injection conditions are very consistent in terms of shape, although a slight difference can be seen during test B-2g caused by a somewhat higher pumping rate.

The test performed at a lower pumping rate, B-1a (Helium), shows a delayed and broader peak but with a similar shape of the rising and falling parts of the curve. The delay is about a factor 2, which also is the difference in pumping rate relative to the other experiments.

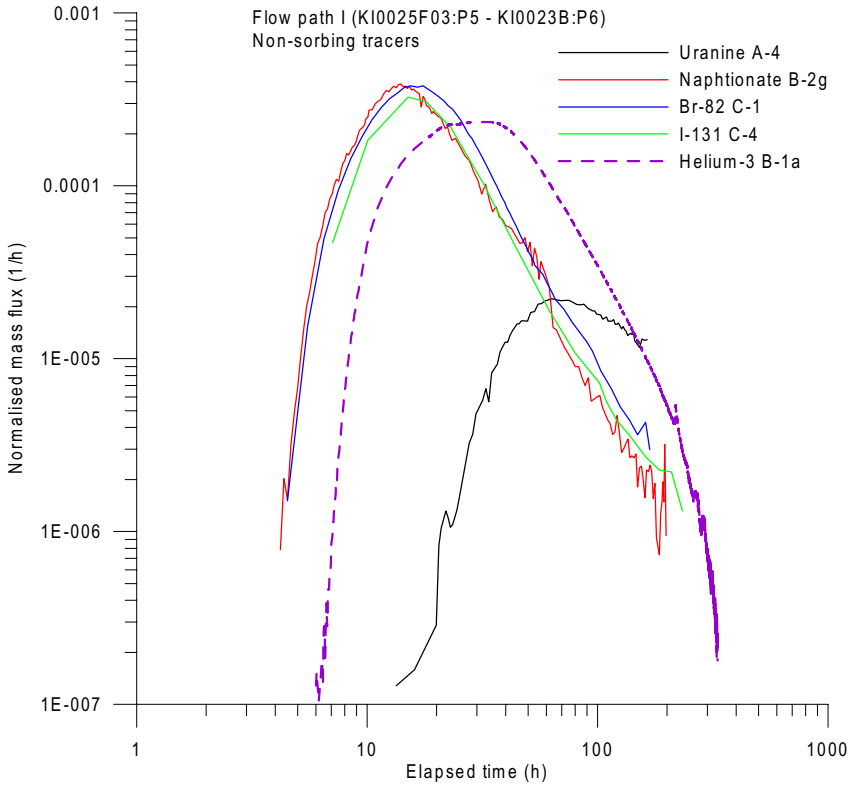

Figure 6-4. *Flow path I – Normalised tracer breakthrough curves for conservative tracers during tests A-4 (passive injection), B-1a (Helium, a tracer with higher diffusivity), B-2g, C1 and C4. Lin-lin plot is given in Appendix 2.*

The advective and dispersive transport parameters derived from the evaluation of the breakthrough curves for conservative tracers indicate a fast flow path with a dispersivity of about 2 m and an equivalent flow aperture of about 3 mm (cf Table 6-2).

- Two of the tracer injections, B-1a and B-2g, also included Helium (He-3) which has a significantly higher diffusivity than the reference tracers (dyes or metal complexes). In test B-1a the Helium breakthrough could unfortunately not be compared to the reference tracer (Uranine) due to the low input concentration in combination with a high "background" concentration, originating from a previous performed injection of Uranine. However, according to the mathematical formulation /e.g. Hadermann and Heer, 1996/ follows that the slope of the late-time part of the breakthrough curve can be used for identification of matrix diffusion processes. A slope of $t^{-3/2}$ indicates matrix diffusion in a double-porosity medium. In both test B-1a and B-2g the slope is steeper, about $t^{-5/2}$ (cf Figures 6-4 and 6-5), but still not as steep as would have been the case if only advection and dispersion were active processes. In test B-2g , the He-peak is lower and retarded compared to the reference Naphtionate and the tailing is somewhat more accentuated.

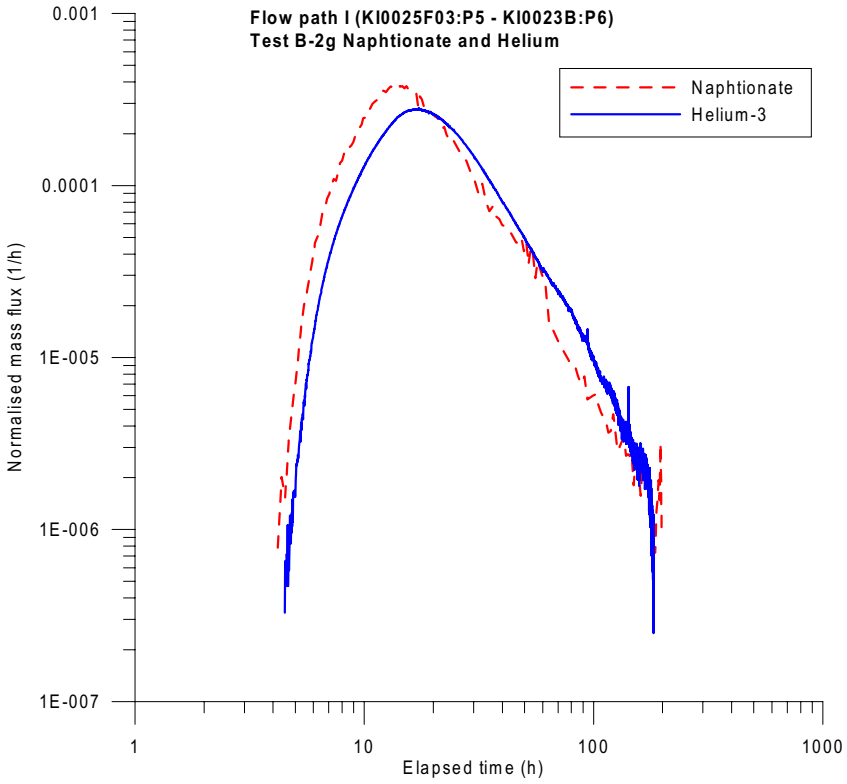

Figure 6-5. *Flow path I – Comparison between tracer breakthrough of Naphtionate and Helium-3 in test B-2g.*

The first steep part of the tracer breakthrough curve is probably governed by rapid advective transport in a relatively high transmissive flow path while the lower and retarded He peak indicates that diffusion as a transport process is accentuated for the more diffusive He. The longer tailing of the He breakthrough curve can also be explained by the more diffusive He. This effect is even more pronounced in the longer flow path IV (cf Chapter 6.2.3). The similar tracer recovery measured for He and the reference tracers indicate that no sorption processes biased the comparison related to diffusion.

Other flow paths within Structure #20

The other five flow paths tested within Structure #20 are three with KI0023B:P6 as sink and injection in KI0025F (Path XI), KA2563A (Path IX) and KI0025F02 (Path VI) and two with KI0025F03:P5 as sink with injection in KA2563A (Path XVI) and KI0025F02 (Path XIII), cf Figure 6-3, and Table 6-1.

A comparison of these five flow paths within structure #20 and also adding flow path I (Figures 6-6 and 6-7 and Table 6-2) shows:

- The mean travel times increase with increasing flow path length, with the exception of Path VI where the test was performed with reduced pumping rate.
- Dispersivity varies between 0.6 m and 6 m with the lower values for the shorter distances.
- The hydraulic fracture conductivity of the flow paths varies within one order of magnitude. The higher values are seen for the flow paths using KI0025F03:P5 as sink section.
- Tracer mass recovery vary between 40 and 100% with higher recovery noted for the shorter flow paths, indicating that background flow may influence the longer flow paths (cf Figure 6-7). Both flow paths using KA2563A:S4 as source section (Path IX and Path XVI) are passing the intersection between Structures #20 and #21 and an alternative explanation to the low recovery may be that the fracture intersection zone (FIZ) acts like a drain carrying away some of the tracer mass to an alternate sink. The zero mass recovery from injection in KI0025F (Path XI) is most probably an effect of a too short sampling period in relation to the long distance.

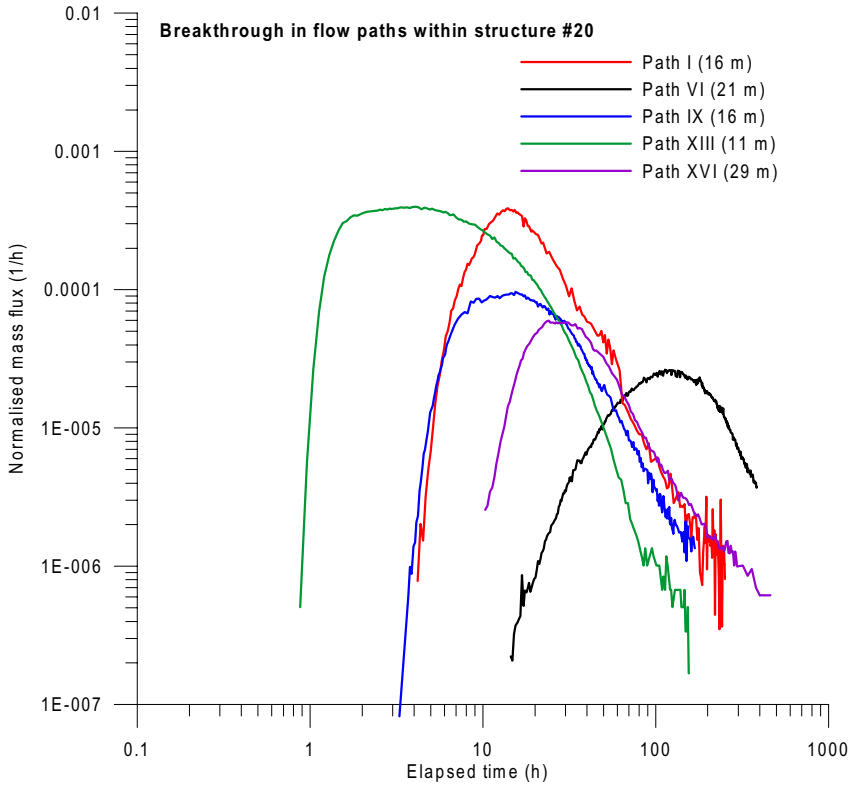

Figure 6-6. *Comparison of tracer breakthrough for conservative tracers in five flow paths within Structure #20, cf Table 6-2 and Figure 6-7. Lin-lin plot is given in Appendix 2.*

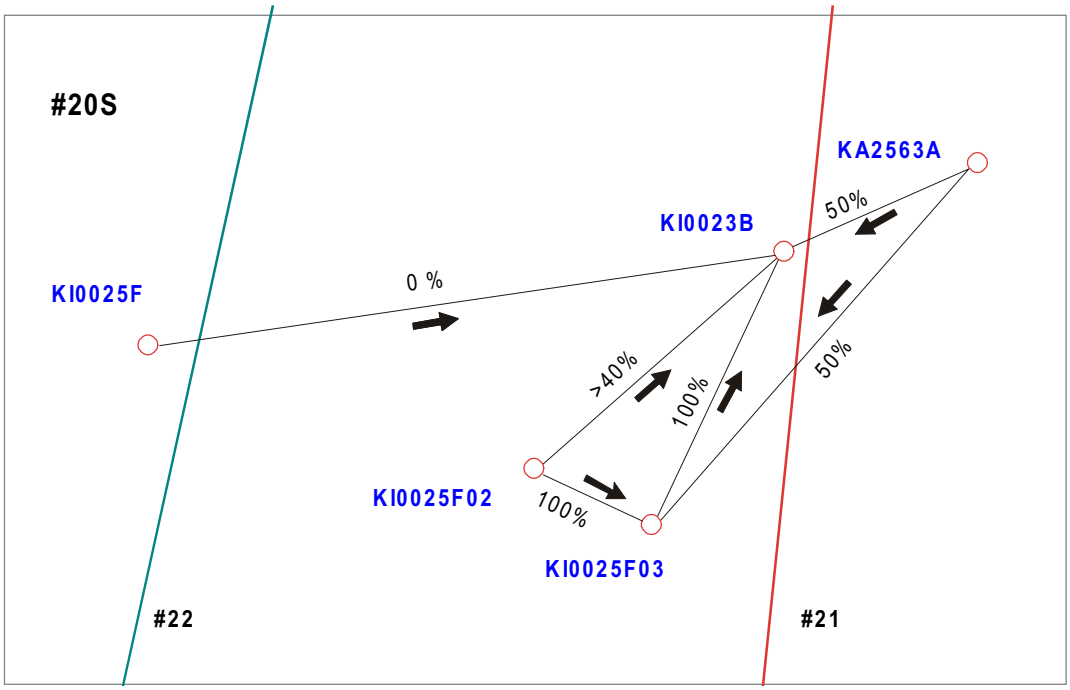

Figure 6-7. *Tracer mass recovery for flow paths located within the plane of Structure #20 (plane view from south) cf Table 6-2 and Figure 6-3.*

Table 6-2. Measured and evaluated parameters from tracer tests in flow paths within Structure #20 (cf Chapter 5 for definitions).

Path no.	Dist (m)	Test no.	Pump flow (ml/min)	Inj. Flow (ml/min)	*R* (%)	Head diff. (m)	First arrival (h)	Mean travel time (h)	Dispersivity (m)	Hydr. Fracture Cond. K_{fr} (m/s)	Equiv. Fracture aperture δ (m)	Flow porosity θ_k
I	14	C1	1960	45*	100	159	4.5	18	2.3	5.6E-05	3.4E-03	1.8E-03
I	14	C4	1960	45*	90	163	7	16.1	2.1	6.1E-05	3.1E-03	1.7E-03
I	14	B-2g	2060	45*	100	164	4.5	13.5	1.9	7.2E-05	2.7E-03	1.5E-03
VI	21	B-1c	1200	10	>37	77	15.5	153	6.2	3.3E-05	8.0E-03	3.9E-03
IX	16	PT-4	250 0	11.3	47	190	4	11.5	5.3	9.8E-05	2.2E-03	1.1E-03
XI	42	ESV-1c	1040	<0.02	0	55	>250	–	–	–	–	–
XIII	11	A-5	2600	8.9	97	214	1	1.4	0.6	3.1E-04	5.9E-04	6.9E-05
XVI	29	A-5	2600	9.5	47	217	10	24	3.7	1.5E-04	1.4E-03	1.5E-04

* Forced injection

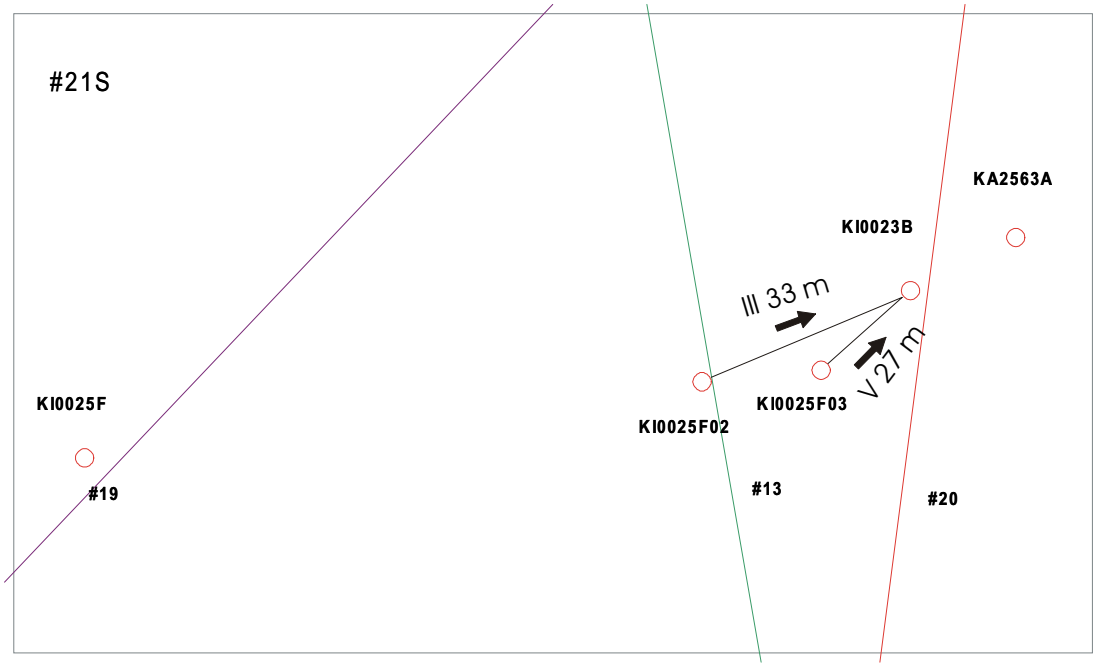

***Figure 6-8**. Experimental geometry and distances for tracer tests performed in flow paths located within Structure #21 (view from south), cf Table 6-3.*

6.2.2 Flow paths within Structure #21

The two flow paths tested within Structure #21, having path lengths of 33 and 27 m, are oriented in a similar direction along the structure using the same sink (KI0023B:P6). Flow path III is of particular interest due to the relatively long distance and noted high tracer mass recovery and was therefore selected as a candidate for the tests with sorbing tracers (Phase C). Flow path III has been tested at three different occasions over a

period of one year with similar pumping and injection flow rates, but the results are somewhat different depending on differences in the boundary conditions (pumping rates). The following characteristics can be identified from Figure 6-9 and Table 6-3:

- The mean travel time for flow path III is very sensitive to the pumping rate at the sink. A 20% reduction of the pumping rate increases the mean travel time with a factor 4. Similar observations can be made for dispersivity, which increases with decreasing pumping rate. A possible explanation could be that the transport is spread over a larger surface induced by the changed boundary condition.

- Path V is slower than path III despite the fact that the distance is shorter. The mass recovery is also much lower for path V than for path III. One possible explanation for this may be that the forced injection has injected the tracer into stagnant portions of the structure, or in parts connected to another "global" sink.

- Both paths have less steep tails ($\sim t^{-3/2}$) than the single structure paths within Structure #20. This indicates effects of diffusion.

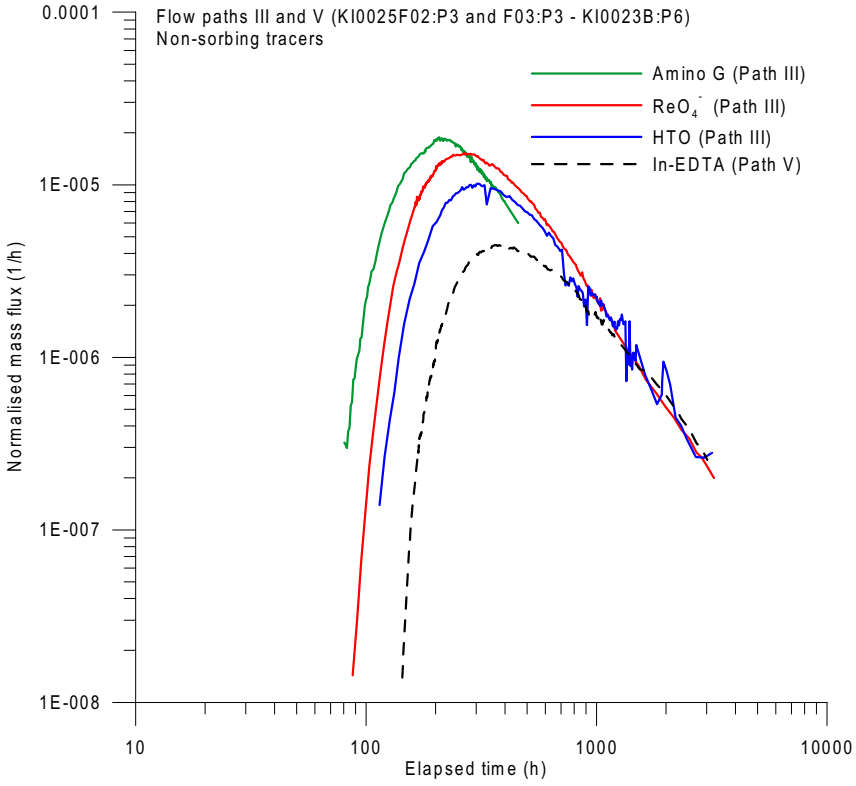

Figure 6-9. *Comparison of breakthrough curves in flow path III and V within Structure #21, cf Table 6-3 and Figure 6-8. Lin-lin plot is given in Appendix 2.*

Table 6-3. Measured and evaluated parameters from tracer tests in flow paths within Structure #21 (cf Chapter 5 for definitions), cf Figure 6-8 and 6-9.

Path no.	Dist (m)	Test no.	Pump flow (ml/min)	Inj. Flow (ml/min)	*R* (%)	Head diff. (m)	First arrival (h)	Mean travel time (h)	Dispersivity (m)	Hydr. Fracture Cond. K_{fr} (m/s)	Equiv. Fracture aperture δ (m)	Flow porosity θ_k
III	33	C3	1960	1.8	>73	181	114	514	9.6	1.2E–05	1.6E–02	8.1E–03
III	33	PT-4	2500	1.9	>63	215	85	140	2.9	4.1E–05	5.2E–03	2.7E–03
III	33	B-2b	2060	1.6	98	186	83	286	7.0	1.9E–05	1.0E–02	5.5E–03
V	27	B-2e	2060	9.6*	49	187	150	561	4.5	6.3E–06	3.0E–02	1.7E–02

* Forced injection

6.2.3 Network flow paths

In total eight flow paths have been interpreted as "network" flow paths implying that there are more than one interpreted deterministic structure involved along the flow path (cf Table 6-1). Two of the flow paths (X and XII) did not produce any measurable tracer breakthrough within the relatively short sampling period (~220–640 hours) assigned for the tests. Four of the remaining flow paths used KI0023B:P6 as a sink (paths II, IV, VII and VIII) and the two remaining used KI0025F02:P5 as sink (paths XIV and XV).

When analysing and interpreting these data it was at first not obvious how to present the different flow paths in order to obtain a basis for a meaningful comparison. The route that was chosen here was to plot the breakthrough of all paths in one plot, and list the evaluated and measured parameters in a similar fashion as for the single structure flow paths (Figure 6-10 and Table 6-4). The graphs and the evaluated parameters show:

- The mean travel times and dispersivities are generally low in relation to the projected distance along the structures, with the exception of flow path VIII. This may be an indication that the actual in situ flow paths in general are shorter than the projected ones due to the presence of unidentified structures (or single fractures) making up "short-cuts" between the sink and source along the projected flow path.
- Tracer mass recovery is generally rather low (<60%) except for path II.
- All paths have less steep tails ($t^{-4/2}$–$t^{-3/2}$) than the single structure paths within Structure #20, with the exception of path XV, which also has a low dispersivity and seems to be dominated by advection.
- Flow path IV, tested at two different pumping rates at the sink, exhibits a lower dispersivity for the higher pumping rate, which could be an effect of the injection procedure where forced injection was used at the lower pumping rate which possibly could create larger dispersion.

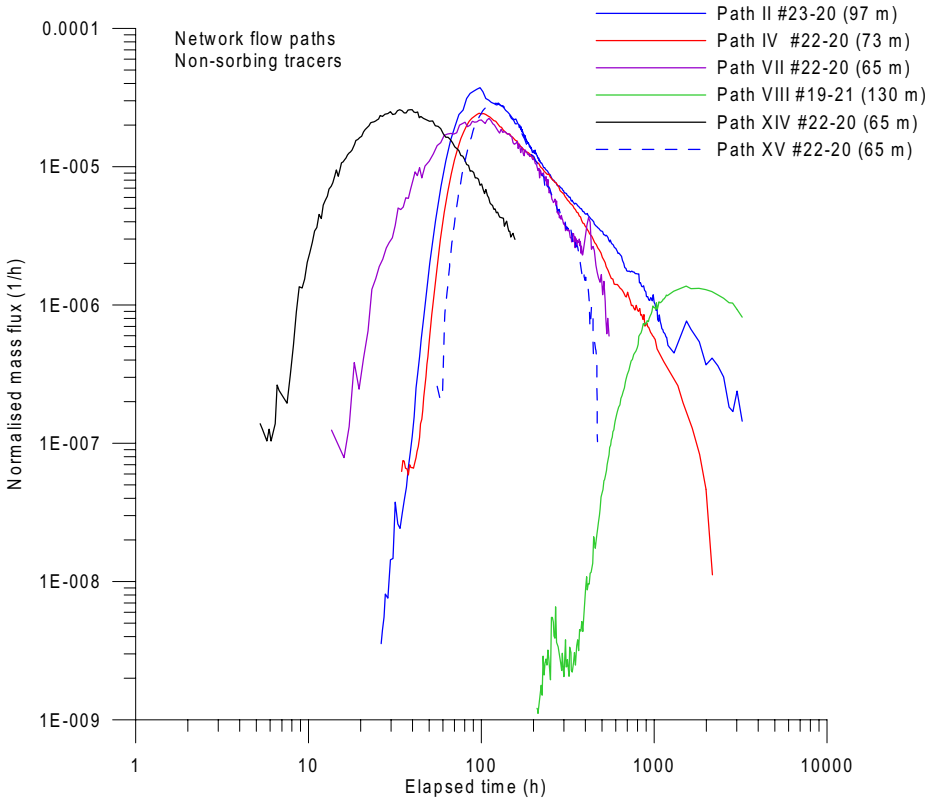

Figure 6-10. *Comparison of tracer breakthrough in six "network" flow paths, cf Table 6-1 and Figures 6-1 and 6-2. Lin-lin plot is given in Appendix 2.*

Table 6-4. Measured and evaluated parameters from tracer tests in "network" flow paths (cf Chapter 5 for definitions), cf Table 6-1 and Figures 6-1 and 6-2.

Path no.	Dist (m)*	Test #	Pump flow (ml/min)	Inj. Flow (ml/min)	*R* (%)	Head diff. (m)	First arrival (h)	Mean travel time (h)	Dispersivity (m)**	Dispersivity (m)***	Hydr. Fracture Cond. K_{fr} (m/s)	Equiv. Fracture aperture δ (m)	Flow porosity θ_k
II	97	C2	1960	9.0****	80	171	38	282	4.2	24	5.1E–06	3.6E–02	2.0E–02
II	97	B-2d	2060	8.4****	88	178	43	119	2.4	14	1.2E–05	1.6E–02	9.1E–03
IV	73	A-4	2300	5.7	>34	194	48	109	1.2	5.8	8.9E–06	2.1E–02	1.2E–02
IV	73	B-1b	1200	11.2****	>46	89	46	160	2.4	12	1.3E–05	1.6E–02	9.9E–03
IV	73	B-2a	2060	11.8****	60	182	44	147	2.7	13	7.0E–06	2.6E–02	1.5E–02
VII	65	PT-4	2500	5.8	>39	204	19	98	5.0	18	1.4E–05	1.4E–02	8.0E–03
VII	65	B-2h	2060	12.7	49	178	21	123	5.4	19	1.3E–05	1.5E–02	8.2E–03
VIII	130	B-2c	2060	0.5	>35	187	450	2182	12.8	30	7.8E–06	2.8E–02	1.5E–02
XIV	57	A-5	2600	18.2	>27	228	8	42	4.4	21	1.2E–05	1.5E–02	1.8E–03
XV	65	A-5	2600	5.5	57	237	60	126	0.9	4.9	3.8E–06	4.4E–02	5.5E–03

* Distance along structures
** Calculated using shortest distance in space
*** Calculated using distance along structures
**** Forced injection, flow calculated from tracer dilution.

6.3 Retention

The last phase of the TRUE Block Scale Tracer Test Stage, Phase C, was devoted to tests with radioactive sorbing tracers for studies of the retention properties of different flow paths. Three flow paths (I–III), showing high tracer mass recovery, were selected for these tests. The three selected flow paths have different characteristics, path I being a fast single structure flow path within Structure #20, path II being a "network" flow path with transport within Structures #23, #22 and #20, and path III being a long single structure flow path within structure #21. Thus, this selection would make it possible to study differences in retention properties between single structure paths and a network path.

Some general observations and conjectures can be made regarding the TRUE Block Scale tests with sorbing tracer tests, and in relation to the TRUE-1 results, without any type of modelling. These are presented in Section 6.3.1.

6.3.1 Preliminary conclusions regarding retention

The sorbing tracers used in the Phase C experiment were radioactive isotopes, mainly from the alkali metal and the alkaline earth metals. Within the C1/C4 experiment (transport length of ~14m with an average transport time of ~18h), the tracer behaviour was similar to the observations made in the TRUE-1 experiments. Only a very slight retardation of Na^{+} and Ca^{2+} could be observed, while the retardation of some stronger sorbing tracers (e.g., Ba^{2+}, Rb^{+}, and Cs^{+}) was more pronounced; however, still giving a measurable breakthrough curve.

For the longer flow-paths studied, experiment C2 and C3, no breakthrough of the moderately and strongly sorbing tracers used (i.e., Ba^{2+}, Rb^{+}, and Cs^{+}) could be detected over the analysed time span. It is indicated that for studies of longer flow-paths, only slightly sorbing tracers (i.e., Na^{+}, Ca^{2+} and Sr^{2+}) can be used.

The use in experiment C4 of tracers influenced by hydrolysis (i.e., Mn^{2+}, Co^{2+} and Zn^{2+}) verified the hypothesis that the small differences in hydrolysis constants for these cations can cause very different retardation for the tracers. In fact, a very large loss of Co^{2+} and Zn^{2+} was observed already in the injection borehole /cf Andersson et al, 2001c/. A part of this sorption can be explained by adsorption on the borehole equipment. This observation together with the absence of breakthrough for Zn^{2+} together with the very large retardation of Co^{2+}, indicated that Co^{2+} and Zn^{2+} represent a limit when the hydrolysis give such strong sorption that the use of the tracer in this type of a dynamic in situ experiment is futile.

6.3.2 Evaluation modelling procedure

The evaluation and interpretation of the breakthrough curves has included a number of different modelling concepts /Poteri et al, 2002/. This report describes only the "standard" basic approach employed to the evaluation of all tests performed within the TRUE Block Scale project (cf Chapter 5) and previously also to the evaluation of the TRUE-1 tests /Winberg et al, 2000/. In the modelling performed, each sorbing tracer breakthrough curve has been fitted together with the results of a simultaneously injected conservative tracer, two by two but also up to four tracers simultaneously. Additionally, calibration calculations have also been performed using only the data for the conservative tracers. Examples of model fits are shown in Figures 6-12 and 6-13 for the runs in flow path I (tests C1 and C4).

The simulations included two basic cases. In the first case the A-parameter was fixed to the laboratory data for the conservative tracer, i.e., the diffusivity and the porosity was fixed. A value on the A-parameter of 82400 was chosen based on laboratory experiments using Äspö diorite /Byegård et al, 1998/, giving a formation factor, F_D, equal to $6 \cdot 10^{-5}$ ($D_e = D_w \cdot F_D$, where D_e is the effective diffusivity and D_w is the diffusivity in water), ε=0.004, and an equivalent fracture aperture, δ, arbitrarily set to 4 mm. In accordance with the definition of a conservative tracer, the retardation coefficient, R_a, was set to 1. In the fittings, the following parameters were thus used for the calibration procedure, cf definitions in Section 5.2.4:

- the A-parameter for the sorbing tracer,
- the retardation coefficient, R_a for the sorbing tracer,
- the mean transport time (t_0), same value for all included tracers,
- the dispersivity, Peclet number (Pe), same value for all included tracers,
- the proportionality factor (pf), same value for all included tracers.

A special case was also run where pf was estimated to study the variation of this parameter.

A total number of 5 to 13 fitting parameters were used for the fitting of two to four data sets. When the data for the conservative tracer was used, only the three latter parameters were varied in order to fit the data, i.e., three free parameters for one data set.

The second basic case was performed as described above, with the exception that the A-parameter for the conservative tracer was also used as a fitting parameter. This implied that the diffusivity and the porosity were not fixed by the laboratory data as was done in the first case. Estimation of the A-parameter was only done for a selection (1–3) of the sorbing tracers in each test.

A comparison between the two different modelling procedures shows that when all A-parameters are estimated, significant matrix diffusion can be applied to the conservative tracer, quite contrary to what is assumed when the modelling is performed with a fixed and very high A-parameter for the conservative tracer. The fits are also generally better in the former case. This suggests the influence of diffusion-like process which is further discussed in Chapter 7.

6.3.3 Flow path I

The main focus for this 14 m long single structure flow path has been to study retention by injecting a mixture of different radioactive sorbing tracers. The short travel time made it possible to perform two injections (C1 and C4) three months apart using partly different tracers. Figure 6-11 shows the tracer breakthrough from both injections in log-log (shown in lin-lin in Appendix 2), and Table 6-5 illustrates the large span of travel times (t_{50}) for the different species, ranging from about 20 hours for the conservative tracers to more than 1000 hours for the most sorbing ones ($^{58}Co^{2+}$). A comparison between injections C1 and C4 ($^{47}Ca^{2+}$) reveals that there is a slight difference between the two tests. A small reduction (<5%) of the injection flow rate in test C4 has resulted in a somewhat longer travel time. However, there is no significant change in the shape of the breakthrough curve and further the parameters derived from the modelling of the tests are consistent.

The results for flow path I are presented in Table 6-6. The results of the simulations show:

- It is not possible to get a good fit to the experimental data by invoking only advection and dispersion, especially for the tail of the breakthrough. Addition of diffusion to the model significantly improves the model fits (cf. Figure 6-13).

- The order of retardation between the species, $Na^{+}<Ca^{2+}<Ba^{2+}\approx Rb^{+}<Cs^{+}$ is consistent with earlier tracer tests in TRUE-1 /Winberg et al, 2000/ and laboratory data /Byegård et al, 1998/.

- Simultaneous fit of four tracers generally improves the fits by reducing standard errors and weighted sum of square differences between measured points and simulation.

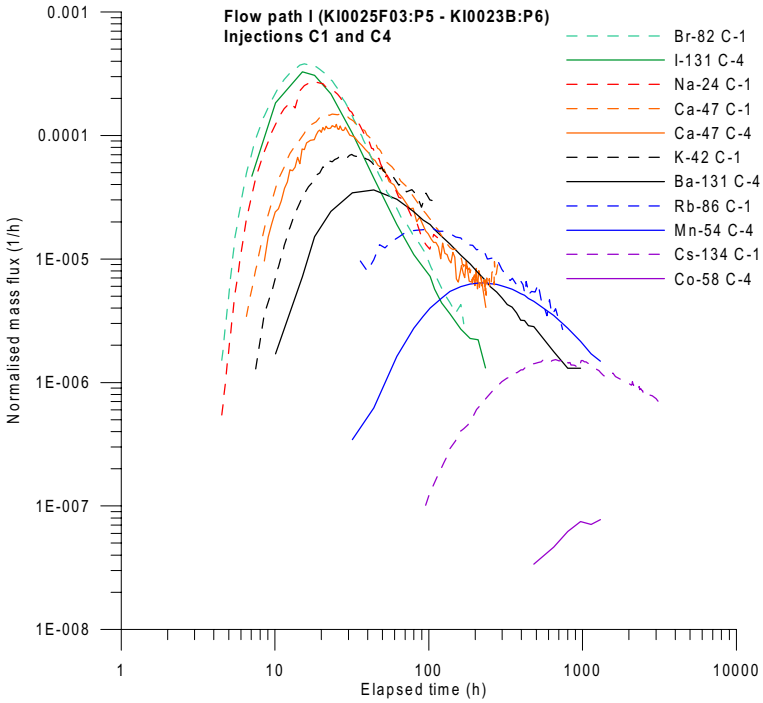

Figure 6-11. *Normalised tracer breakthrough for all tracers injected in tests C1 and C4, cf Figure 6-7. Lin-lin plot is given in Appendix 2.*

Table 6-5. TRUE Block Scale Tests C1 and C4, flow path I (KI0025F03:P5 – KI0023B:P6). Tracer travel times, t_5, t_{50} and t_{95} and tracer mass recovery based on total injected amount (t_t is the time for the last sample taken).

Tracer	t_5 (h)	t_{50} (h)	t_{95} (h)	t_t (h)	Mass recovery *R* (%)
C1					
$^{82}Br^-$	9	20	49	160	100
$^{24}Na^+$	10	27	110	110	96
$^{47}Ca^{2+}$	14	46	260	300	98
$^{42}K^+$	21	100	A	110	53
$^{86}Rb^+$	66	400	A	730	67
$^{134}Cs^+$	530	5000	–	5800	53
C4					
$^{82}Br^-$	9	23	A	38	69
$^{131}I^-$	9	22	A	220	90
$^{47}Ca^{2+}$	16	A	–	69	49
$^{131}Ba^{2+}$	28	290	A	890	67
$^{54}Mn^{2+}$	150	1110	–	3700	71
$^{58}Co^{2+}$	–	–	–	3500	3
$^{65}Zn^{2+}$	–	–	–		0

A = Short-lived isotope that had decayed before the specified mass recovery could be reached.

Table 6-6. Evaluated parameters for the tracers in flow path I during tests C1 and C4 using PARETT (advection-dispersion-sorption-matrix diffusion model). Simultaneous fits of one conservative and one to three sorbing tracers. Values within brackets are standard errors in percent. Definitions of parameters are found in Chapter 5.

Run no.	Tracers	t_0 (h)	*Pe*	D_L/v^* (m)	D_L/v^{**} (m)	*pf* (10^{-3})	R_a	*A* ($s^{1/2}$)
C1								
1:1	$^{82}Br^-$	18.0 (1)	6.0 (3)	2.3	2.7	14.5	1 (fixed)	82400 (fixed)
1:2	$^{82}Br^-$	18.0 (1)	6.0 (2)	2.3	2.7	14.5	1 (fixed)	82400 (fixed)
	$^{24}Na^+$						1.1 (5)	820 (38)
1:3	$^{82}Br^-$	18.0 (1)	6.0 (2)	2.3	2.7	14.5	1 (fixed)	82400 (fixed)
	$^{86}Rb^+$						5.3 (48)	280 (61)
1:4	$^{82}Br^-$	18.0 (1)	6.0 (2)	2.3	2.7	14.5	1 (fixed)	82400 (fixed)
	$^{134}Cs^+$						15.6 (22)	200 (25)
1:5	$^{82}Br^-$	14.6 (1)	8.5 (2)	1.6	1.9	16.2	1 (fixed)	760 (4)
	$^{134}Cs^+$						6.4 (27)	65 (28)
1:6	^{82}Br	14.6 (1)	8.5 (2)	1.6	1.9	16	1 (fixed)	744 (3)
	$^{24}Na^+$						1.08 (2)	349 (7)
	$^{86}Rb^+$						3.8 (22)	144 (25)
	$^{134}Cs^+$						6.4 (22)	65 (22)
1:7	^{82}Br	14.6 (1)	8.6 (1)	1.6	1.9	16 (0.4)	1 (fixed)	735 (3)
	$^{24}Na^+$					17 (3)	1.05 (2)	292 (10)
	$^{86}Rb^+$					17 (13)	3.3 (45)	118 (57)
	$^{134}Cs^+$					14 (5)	10 (18)	115 (21)
C4								
4:1	$^{131}I^-$	20.4 (5)	4.1 (12)	3.4	3.9	18.9	1(fixed)	82400 (fixed)
4:2	$^{131}I^-$	20.4 (2)	4.1 (5)	3.4	3.9	18.8	1(fixed)	82400 (fixed)
	$^{47}Ca^{2+}$						1.4 (12)	380 (28)
4:3	$^{131}I^-$	20.4 (3)	4.1 (8)	3.4	3.9	18.4	1(fixed)	82400 (fixed)
	$^{131}Ba^{2+}$						2.1 (9)	210 (13)
4:4	$^{131}I^-$	18.7 (4)	5.1 (10)	2.7	3.1	20.6	1(fixed)	82400 (fixed)
	$^{54}Mn^{2+}$						10.2 (10)	300 (13)
4:5	$^{131}I^-$	13.9 (7)	8.2 (13)	1.7	2.0	19.8	1(fixed)	500 (20)
	$^{131}Ba^{2+}$						1.4 (12)	85 (18)
4:6	$^{131}I^-$	16.5 (5)	7.5 (11)	1.9	2.1	20	1 (fixed)	905 (26)
	$^{47}Ca^{2+}$						1.2 (19)	205 (33)
	$^{131}Ba^{2+}$						1.8 (9)	139 (13)
	$^{54}Mn^{2+}$						7.1 (9)	187 (13)
4:7	$^{131}I^-$	16.6 (4)	7.5 (9)	1.9	2.1	21 (3)	1 (fixed)	870 (22)
	$^{47}Ca^{2+}$					19 (12)	1.2 (18)	236 (39)
	$^{131}Ba^{2+}$					16 (3)	2.1 (7)	205 (13)
	$^{54}Mn^{2+}$					21 (2)	7.1 (7)	187 (10)

* D_L/v calculated using the Euclidean distance, 14 m.

** D_L/v calculated using the distance along interpreted deterministic structures, 16 m, cf Figure 6-1.

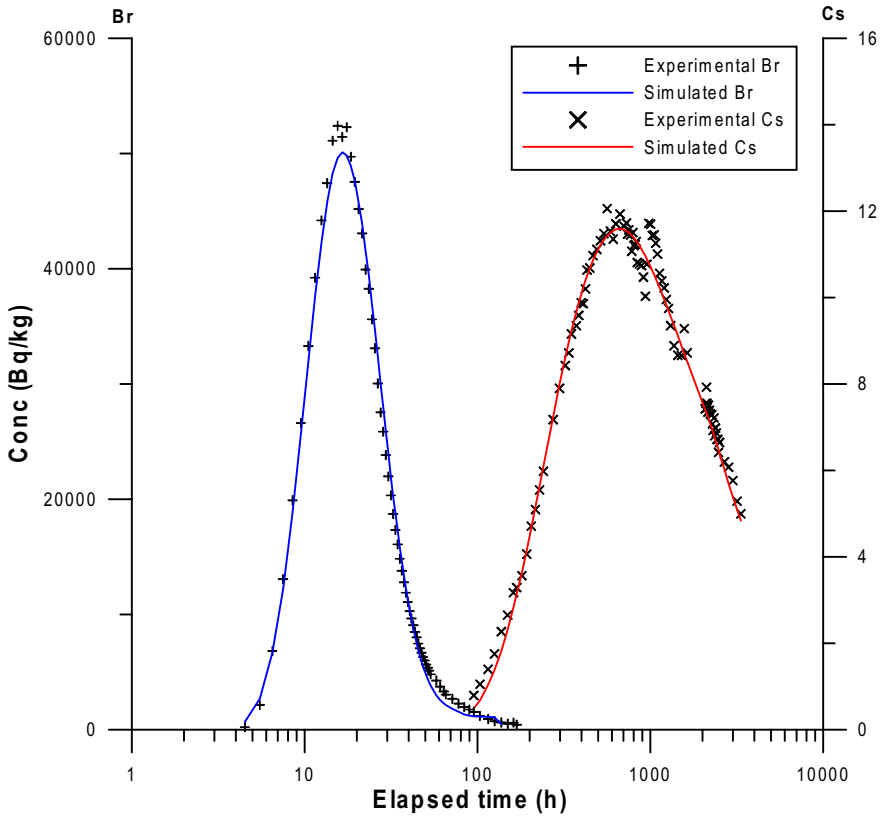

Figure 6-12. *Simulaneous model fit of Br^- and Cs^+ in test C1 (flow path I).*

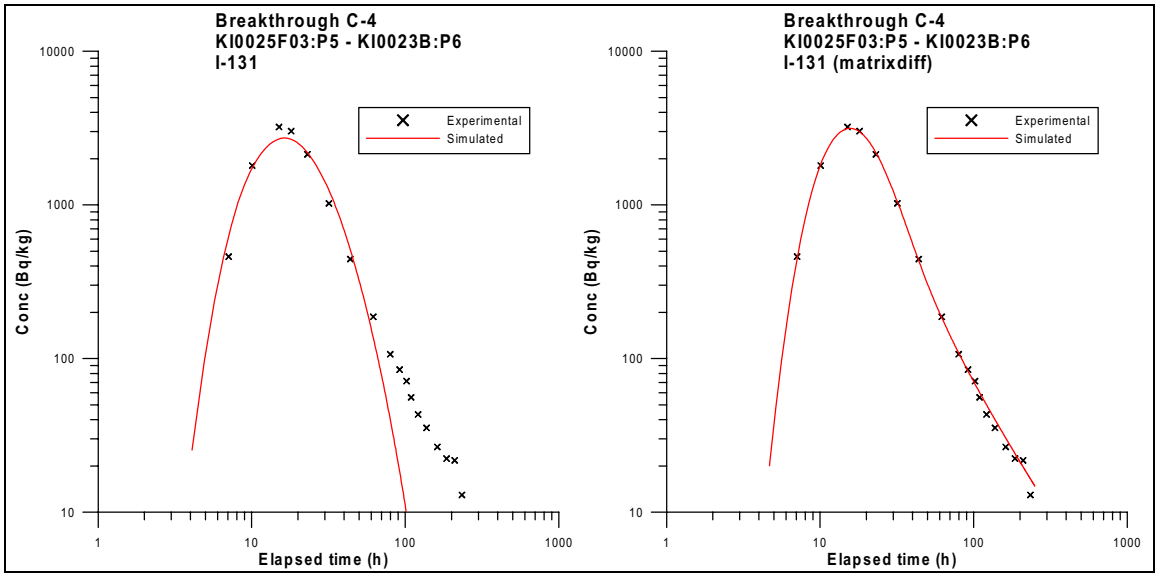

Figure 6-13. *Model simulations of tracer breakthrough of $^{131}I^-$ in test C4 without matrix diffusion (left) and including matrix diffusion (right).*

6.3.4 Flow path II

The retention properties of this network flow path were investigated by injecting a solution of ^{186}Re (ReO_4^-), $^{47}Ca^{2+}$, $^{131}Ba^{2+}$ and $^{137}Cs^+$ as part of injection C2. The idea was to use species that could be directly compared between flow paths I and II without interference between the two injections that were performed only six days apart. The result after about 7.5 months of sampling (Ba^{2+} could only be followed up to 3 months due to the short half-life) was that no Ba^{2+} and Cs^+ had been recovered whereas 80% of ReO_4^- and 30% Ca^{2+} had been recovered (Table 6-7 and Figure 6-14) (breakthrough curves shown in lin-lin in Appendix 2). The results of the basic evaluation modelling presented in Table 6-8 and Figure 6-15 show that:

- The mean travel time and dispersivity is significantly higher than for path I.
- The model fit to the experimental data is not that good and the uncertainties in the parameter estimates are much larger than for the corresponding results from path I.
- The A-parameter for the conservative tracer and for the sorbing tracer Ca^{2+} is somewhat higher than for path I, indicating less retention than for path I.

Table 6-7. TRUE Block Scale Test C2, flow path II (KI0025F03:P7 – KI0023B:P6). Tracer travel times, t_5, t_{50} and t_{95} and tracer mass recovery at t_t based on total injected amount (t_t is the time for the last sample taken).

Tracer	t_5 (h)	t_{50} (h)	t_{95} (h)	t_t (h)	Mass recovery R (%)
$^{186}ReO_4^-$	94	260	A	500	80
$^{47}Ca^{2+}$	300	A	–	800	29
$^{131}Ba^{2+}$	–	–	–	1900	no breakthrough
$^{137}Cs^+$	–	–	–	5300	no breakthrough

A = Short-lived isotope that had decayed before the specified mass recovery could be reached.

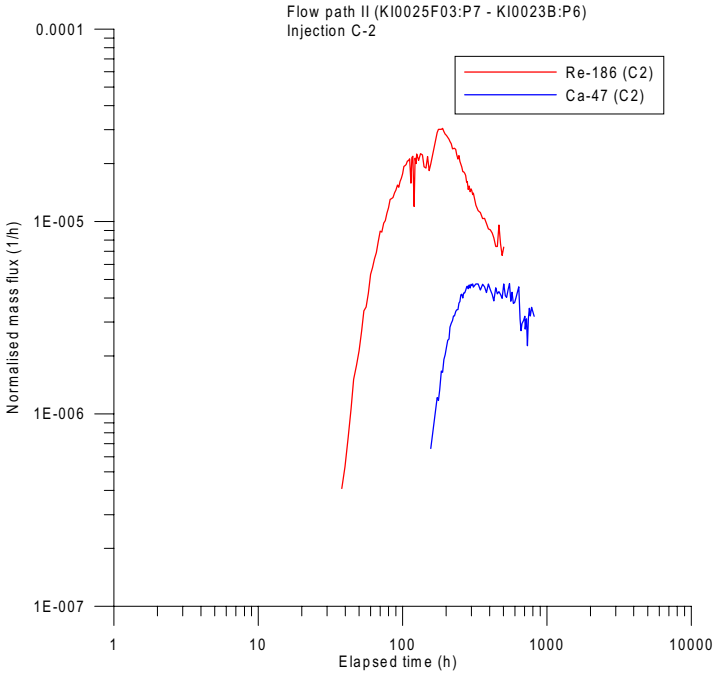

Figure 6-14. *Normalised tracer breakthrough for $^{186}ReO_4^-$ and $^{47}Ca^{2+}$ injected in test C2. Lin-lin plot is given in Appendix 2.*

Table 6-8. Evaluated parameters for the tracers in flow path II during test C2 using PAREST (advection-dispersion-sorption-matrix diffusion model). Simultaneous fit of Re and Ca, with and without a fixed A-parameter. Values within brackets are standard errors in percent. Definitions of parameters are found in Chapter 5.

Run no.	Tracers	t_0 (h)	*Pe*	D_L/v* (m)	D_L/v** (m)	*pf* (10^{-3})	R_a	*A* ($s^{1/2}$)
C2 2:1	$^{186}ReO_4^-$	282 (4)	4.1 (6)	4.2	24	3.8	1 (fixed)	82400 (fixed)
2:2	$^{186}ReO_4^-$ $^{47}Ca^{2+}$	280 (3)	4.1 (5)	4.1	23	3.8	1 (fixed) 2.4 (4)	82400 (fixed) 1200 (9)
2:3	$^{186}ReO_4^-$ $^{47}Ca^{2+}$	274 (49)	3.9 (52)	4.3	25	6.4	1 (fixed) 1.7 (25)	1320 (146) 390 (84)

* D_L/v calculated using the Euclidean distance, 17 m.
** D_L/v calculated using the distance along interpreted deterministic structures, 97 m, cf Figure 6-1.

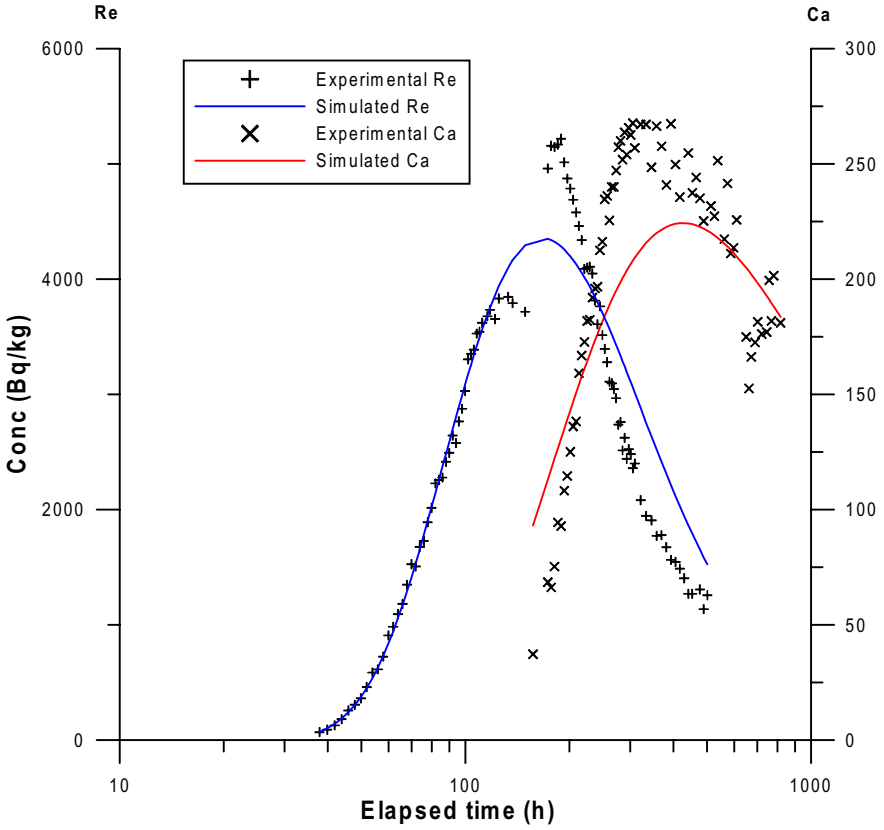

Figure 6-15. *Comparison of measured and simulated breakthrough of $^{186}ReO_4^-$ and $^{47}Ca^{2+}$ from test C2, flow path II. Simultaneous run of Re and Ca, A-parameters estimated for both tracers.*

6.3.5 Flow path III

The retention properties of this 33m long more complex fracture flow path were investigated by injecting a solution of tritiated water (HTO), $^{22}Na^+$, $^{85}Sr^{2+}$, $^{83}Rb^+$ and $^{133}Ba^{2+}$. The idea was to use species that could be compared to the ones used in flow path I (Na, Rb and Ba). The result, after about 8 months of sampling, was that no breakthrough of Ba and Rb had been monitored, whereas 73% of HTO, 79% of Na and 52% Sr had been recovered at the sink (Table 6-9 and Figure 6-16) (breakthrough curves shown in lin-lin in Appendix 2). The results of the basic evaluation modelling presented in Table 6-10 and Figure 6-17 show:

- High dispersivity and long travel times.
- A significantly higher *A*-parameter than for flow paths I and II, indicating less influence of diffusion.
- It was possible to simultaneously fit *A*-parameters for HTO, Na and Sr. The uncertainty in the parameter estimates is somewhat higher but retention parameters are in the same range as those obtained with runs using a fixed A-parameter for the conservative tracer.

Table 6-9. TRUE Block Scale Test C3, flow path III (KI0025F02:P3 – KI0023B:P6). Tracer travel times, t_5, t_{50} and t_{95} and tracer mass recovery at t_t based on total injected amount (t_t is the time for the last sample taken).

Tracer	t_5 (h)	t_{50} (h)	t_{95} (h)	t_t (h)	Mass recovery *R* (%)
HTO	230	820	–	3050	73
$^{22}Na^{+}$	340	1500	–	5600	79
$^{85}Sr^{2+}$	640	3000	A	3100	52
$^{83}Rb^{+}$	–	–	–	5300	no breakthrough
$^{133}Ba^{2+}$	–	–	–	5700	no breakthrough

A = Short-lived isotope that had decayed before the specified mass recovery could be reached.

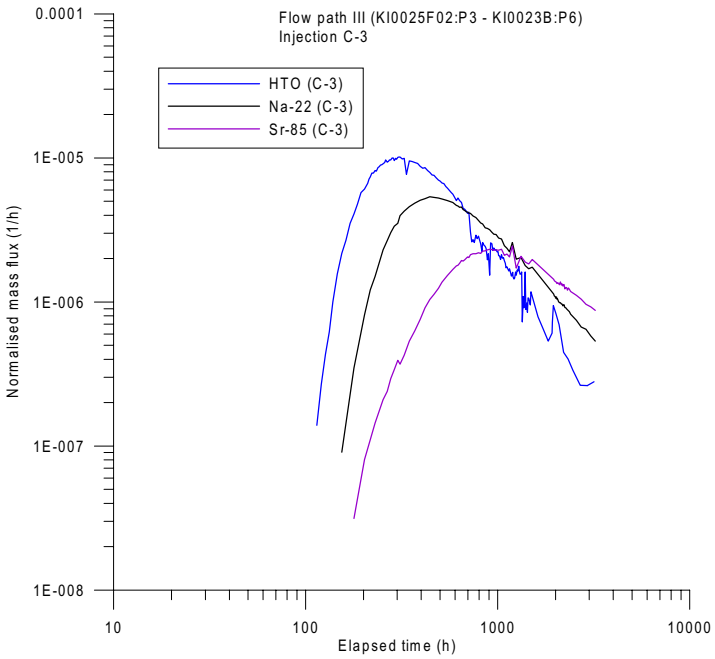

Figure 6-16. *Normalised tracer breakthrough for HTO, $^{22}Na^{+}$-.and $^{85}Sr^{2+}$ injected in test C3. Lin-lin plot is given in Appendix 2.*

Table 6-10. Evaluated parameters for the tracers in flow path III during test C3 using PAREST (advection-dispersion-sorption-matrix diffusion model). Simultaneous fit HTO and one to two sorbing tracers. Values within brackets are standard errors in percent. Definitions of parameters are found in Chapter 5.

Run no.	Tracers	t_0 (h)	*Pe*	D_L/v (m)	*pf* (10^{-3})	R_a	*A* ($s^{1/2}$)
C3 3:1	HTO	514 (2)	3.7 (5)	9.0	0.85	1 (fixed)	82400 (fixed)
3:2	HTO $^{22}Na^{+}$	562 (2)	3.1 (4)	10.6	0.90	1 (fixed) 1.7 (2)	82400 (fixed) 7510 (18)
3:3	HTO $^{85}Sr^{2+}$	521 (2)	3.6 (4)	9.2	0.85	1 (fixed) 3.2 (3)	82400 (fixed 3530 (11)
3:4	HTO $^{22}Na^{+}$ $^{85}Sr^{2+}$	432 (11)	4.1 (15)	8.0	1.11	1 (fixed) 1.8 (2) 3.5 (4)	2413 (36) 2320 (31) 2051 (25)

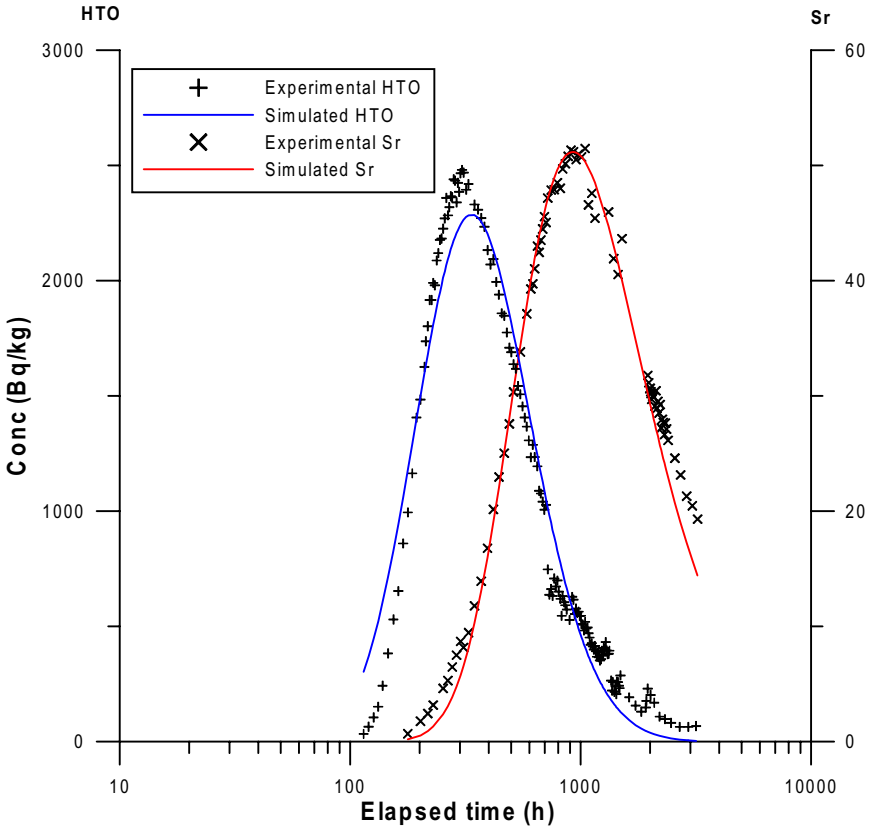

Figure 6-17. *Comparison of measured and simulated breakthrough of HTO (Tritiated water) and $^{85}Sr^{2+}$ from test C3, flow path III. Simultaneous run of HTO and Sr, A-parameter fixed for HTO.*

7 Discussion and conclusions

7.1 Experimental methodology

The experimental methodology applied in the TRUE Block Scale Project relies strongly on the experiences from the previously performed First TRUE Stage /Winberg et al, 2000/. The strategy for selecting test geometry suitable for tracer tests has been focused very much on satisfactory high mass recovery and the selection of a suitable sink. This is somewhat different compared to the strategy in TRUE-1 where the sink was selected early on and the main work was focused on selecting injection points. A high mass recovery, meaning a good control of the flow field, has been the main factor for selecting sinks and injection points.

The selection of the sink has been governed by the existing short-circuit between Structures #6 and #20 in borehole KI0023B. The sink finally selected, KI0023B:P6, is in fact located adjacent to the short-circuit, providing flow from Structure #6 towards Structure #20 rather than the opposite, which is in the direction of the ambient flow direction (towards the main tunnel). Two alternative sinks were also explored but none of them could provide as many different, and high-recovery, flow paths as the one selected. However, it should be noted that successful, high-recovery, tracer tests are possible to perform also using the alternative sinks (KI0025F03:P4 and KI0025F03:P5).

The methodology for selecting suitable injection points based on cross-hole tracer dilution responses in combination with cross-hole pressure responses was found to be very useful and discriminating. Although the method is not entirely unambiguous due to the directional aspect of flow, it is clear that the method has enabled location of suitable injection points that not had been discovered based on pressure responses alone.

The equipment and methodology for performance of the tracer tests are based on experiences from TRUE-1. Most parts of the equipment were exactly the same but some adjustments were found necessary due to the increasing length scale and complexities experienced in the TRUE Block Scale tracer tests. The main differences in the TRUE Block Scale array compared to the situation at the TRUE-1 array are:

- Higher ambient pressures (about 500 kPa).
- Larger distances from the tunnel to test sections involved in tests (up to 250 m).
- Longer section intervals (up to 10 m).
- More dilution in the system due to longer distances between boreholes and larger volumes in the borehole sections involved in the tests.

The distance from the tunnel and longer section lengths resulted in increased volumes and residence times in the equipment, which entailed a need of some minor adjustments of the injection technique, and equipment compared to TRUE-1. The main difference was that the use of Helium made it necessary to use stainless steel tubing and to introduce the Helium into the fracture within a relatively short period of time.

Therefore, a forced injection method was introduced creating an unequal dipole flow field (ratio of about 1:100).

The most difficult factor to consider was the dilution in combination with the need for many different conservative tracers in order to avoid interference between the different tests and flow paths due to recovery in progress of earlier injected tracers. This problem was also encountered when Uranine, injected in a slow flow path during Phase A arrived and seriously hampered measurements during Phase B. A separate project aiming at identifying new possible conservative tracers was initiated. The metal-complexes identified and later used during Phase B were found to work very well, see Sections 4.1 and 4.4.

The strategy for selecting sorbing tracers is also similar to the one employed in TRUE-1. Thus, a selection of radioactive, γ-emitting cations from the alkali metal and alkaline earth metal groups was used. The selection and distribution between different injections and flow paths was made such that comparisons could be made between different flow paths and that no interference between the isotopes should occur. The most short-lived isotopes were used in the fast flow paths and different isotopes of the same cation were used in different flow paths (e.g. $^{22}Na^{+}$ – $^{24}Na^{+}$). This strategy worked very well and enabled direct comparisons between different flow paths for the same cation in three cases. A list of suitable cationic tracers which have been used in the Phase C tests are indicated in Table 7-1.

7.2 Transport of conservatve tracers

The tracer tests performed in the TRUE Block Scale borehole array have covered a very large span of distances (11–130 m) and travel times (1.5 – >2000 hours) providing a unique data set for transport in fractured rock. The tracer tests with non-sorbing (conservative) tracers have mainly been focused on identifying flow paths with sufficiently high mass recovery (>80%), but have also provided the possibility to obtain transport parameters for 13 different flow paths within a rock volume of about 50×50×50 m.The evaluation and interpretation of the tracer breakthrough curves indicates the response of a heterogeneous system both within single structures and in the network of fractures. The two single structures investigated with tracer tests, #20 and #21, both show a variation of about one order of magnitude in hydraulic fracture conductivity, equivalent fracture aperture and flow porosity. However, the two structures are different in character where #20 seems to be a more narrow and high conductive single structure whereas #21 probably is more complex. The latter has a lower hydraulic fracture conductivity but higher flow porosity and a characteristic of the breakthrough curves more resembling that of the network flow paths. Thus, Structure #21 more likely consists of several sub-parallel structures than a single fracture.

The six network flow paths investigated over distances between 12–55 m in space and 57–130 m along the structures, according to the hydro-structural model, show a large variation in mean travel times (42–2200 hours) but at the same time exhibit a relatively narrow range of hydraulic fracture conductivity and equivalent fracture aperture (within a factor 3). Notable is also that the transport parameters obtained are within the same

Table 7-1. Examples of tracers used in the TRUE Block Scale experiment that can be used for simultaneous comparison of several flow-paths using different radioactive isotopes of the same cation.

Element	Short-lived tracer	Half-life	Long-lived tracer	Half-life
Na^+	$^{24}Na^+$	15 h	$^{22}Na^+$	2.6 y
Ca^{2+}/Sr^{2+}	$^{47}Ca^{2+}$	4.5 d	$^{85}Sr^{2+}$	65 d
Rb^+	$^{86}Rb^+$	18.7d	$^{83}Rb^+$	86.2 d
Cs^+	$^{134}Cs^+$	2.06 y	$^{137}Cs^+$	30.2 y
Ba^{2+}	$^{131}Ba^{2+}$	11.5 d	$^{133}Ba^{2+}$	10.5 y

span as for Structure #21. This again may indicate that Structure #21 is made up of a network of structures, rather than one single structure. The similarity in evaluated equivalent apertures stems from the t/r^2 dependence embedded in the definition of this entity, cf Equation 5-22. This implies that the slower flow path may either be made up of several minor flow paths (giving a larger aperture when integrated) or one single flow path with a large aperture.

The flow paths (I, II and III) tested with radioactive sorbing tracers in injections were interpreted to involve 1–3 structures with flow paths varying in length between 16–97 m, where I<III<II. The results from the tracer tests, cf values of t_{50ref} in Table 7-2, indicates a different relative flow path length distribution, with I<<II<III. The noted disparity in residence time compared to what could be expected from the hydro-structural model can partly be explained by effects of yet unknown background/splay fractures. Alternatively the difference can be attributed to effects of the internal constitution of participating structures (heterogeneity).

7.3 Retention

7.3.1 Retention evaluated from injection data

Previously in the TRUE Programme, values of the surface distribution coefficient K_a have been evaluated from performed laboratory experiments /Byegård et al, 1998/. As part of the TRUE Block Scale Project, attempts were made to evaluate surface distribution coefficients from the retardation in the injection sections observed in the injection curves from TRUE-1 /Winberg et al, 2000/ and TRUE Block Scale. The K_a values evaluated were found to be of a magnitude equitable to the laboratory K_a values from TRUE-1. Evaluation of data from TRUE Block Scale and TRUE-1 using a matrix diffusion approach shows typical –3/2 slopes in log-log, indicative of diffusion effects. However, it is noted that sorption/desorption kinetics may give similar effects. Analysis of the TRUE Block Scale C1 injection data using a sorption kinetics model showed clear deviations from the model. This was contrary to what was seen for the TRUE-1 STT-2 injection. The noted difference was attributed to smaller dynamic range of

relative concentration for STT-2 (1.5 orders of magnitude) compared to TRUE Block Scale C1 (> 3.5 orders of magnitude), which is expected to make the latter data set more discriminating than the former. In the TRUE in situ experiments, effects of non-linear sorption effects introduced by chemical concentration gradients have been avoided by using radioactive isotopes in element concentration below what is found in nature. Despite these precautions, the non-linear approach was tested. It was noted for Cs, in the case of TRUE Block Scale C1 that the initial loss could not be satisfactory explained. In the case of Rb in TRUE Block Scale C3, the whole injection curve could be explained well. In both cases the slope of the experimental curves is less than what the non-linear sorption model gives. It is difficult to identify a mechanistic explanation for the Freundlich isotherm fitting the injection curves so well. One possible explanation could be that background concentration of the elements in question is present in another chemical form (colloidal or fixed on microscopic fault breccia fragments) compared to the ionic form in which the tracers were injected.

Table 7-2. Retardation factors based on recovery, $R_{50\%}$, (unless specified otherwise) for the different TRUE-1 tests /Winberg et al, 2000/ and the TRUE Block Scale tests C1–C4. The notation t_{50ref} refers to the elapsed time when 50% recovery was obtained for the conservative tracers. In cases where the recovery of the sorbing tracer was less than 5%, a minimum mass recovery is estimated from the last sampling time. The notation n.b. means no breakthrough.

	TRUE-1 Detailed scale			**TRUE Block Scale**		
	STT1	**STT1b**	**STT2**	**C1/C4**	**C2**	**C3**
Tracer	r=4.7m t_{50ref}=36h	r=5,1m t_{50ref}=11h	r=4.7m t_{50ref}=79h	r=14 (16)m t_{50ref}=20h	r=17 (97)m t_{50ref}=260h	r=33 (>33)m t_{50ref}=820h
Uranine	Ref [1]	Ref [1]	Ref [1]			
Br^-		1.03 [2]	1.1	Ref [1]		
I^-		1.03 [2]				
ReO_4^-					Ref [1]	
HTO	1.1	1.04 [2]	1.2			Ref [1]
Na^+	1.4	1.5	1.5	1.4		1.8
K^+		1.9 [2]		5.1		
Ca^{2+}	1.2 [2]		1.9	2.3	4.1 [3]	
Sr^{2+}	1.8	3.2	2.4			3.6
Rb^+	9	20	15	20		>23 [4] n.b.
Ba^{2+}	5		12	13	>20 [4] n.b.	>25 [4] n.b.
Cs^+	230 [3]		130 [4]	250	>56 [4] n.b.	
Mn^{2+}				50		
Co^{2+}		300 [3]		>390 [4]		
Zn^{2+}				>390 [4] n.b.		

[1] Used as reference tracer, i.e., the tracer in relation to which the retardation factors have been calculated.
[2] R_{peak}
[3] $R_{25\%}$
[4] $R_{5\%}$

7.3.2 Retention evaluated from in situ breakthrough data

Three flow paths (I–III) were investigated with a set of radioactive sorbing tracers, mainly monovalent and divalent cations from the alkali metal and alkaline earth metal groups. The results show both similarities and differences when compared to the TRUE-1 tracer tests. Firstly, the order of retention between the different species is the same as in TRUE-1 and in the laboratory tests, i.e. $Na^{+}<Ca^{2+}\approx Sr^{2+}<<Ba^{2+}\approx Rb^{+}<Cs^{+}$. Another similarity is that the retardation, expressed as $R_{50\%}$, i.e.;

$$R_{50\%} = \frac{t_{50\%}(sorbing)}{t_{50\%}(conservative)} \tag{7-1}$$

is about the same for most species when comparing TRUE-1 to the results of injection C1 and C4 in Structure #20 (flow path I), cf Table 7-2. However, for the breakthroughs of sorbing tracers in C2 and C3 (Na^{+} in flow path III and Ca^{2+} in flow path II) a 30–80% stronger retardation (expressed as $R_{50\%}$) is obtained compared to that seen in C1. It is noted that after some 3300 hours, no breakthrough has been observed for the more sorbing tracers, ^{137}Cs (C2) and ^{83}Rb (C3).

7.3.3 Comparison of in situ retention with laboratory data

In the approach used for the basic modelling the experiments (cf Eq. 5-26), the retention obtained is described by the surface retardation coefficient (R_a) and the A-parameter which is lumped parameter including the fracture aperture (δ), the surface sorption coefficient (K_a), the matrix porosity (ε_p), the effective diffusion coefficient (D_e), and the linear sorption bulk distribution coefficient for the rock matrix (K_d) (cf Eq. 5-32). For the comparison of the retention in the in situ experiments to retention parameters determined in laboratory experiments, the following procedure has been applied:

Under the somewhat rough assumption that the transport takes place in a single parallel plate fracture, the fracture aperture can be calculated directly from the residence time of the conservative tracer; according to Eq. (5-22). By inserting Eq. (5-22) into the general expression of the surface retardation coefficient, Eq. (5-30) and rearranging, the surface sorption distribution coefficient (K_a) can be calculated according to:

$$K_a = \frac{(R_a - 1)\left(r^2 - r_w{}^2\right)\pi}{2Qt_0} \tag{7-2}$$

Furthermore, by inserting Eq. (5-22) in Eq. (5-32), a lumped sorption/matrix diffusion parameter can be identified according to

$$D_e(\varepsilon + K_d \rho_b) = \left(\frac{Qt_0 R_a}{2A\pi\left(r^2 - r_w{}^2\right)} \right)^2 \tag{7-3}$$

Using these calculations, the surface retardation coefficients K_a and a product of the parameters determining matrix diffusion , $D_e(\varepsilon+K_d\rho_b)$ were calculated directly from the results of the parameters estimated from the modeling (i.e., R_a and A). A direct comparison and laboratory data can thus be obtained and the results of these calculations are presented in Table 7-3.

Table 7-3. Retention parameters calculated using the parameters, R_a and A obtained from the modelling (cf Chapter 5). The calculated retention parameters are compared to the corresponding values determined in laboratory experiments using Äspö diorite /Byegård et al, 1998/. Values estimated based on the analysis of the mineralogy of the clay fraction of the fault gouge material /Andersson et al, 2002/ are also presented for comparison.

	Surface retention parameter,		Matrix diffusion retention parameter				
	In situ [1]	ÄD, lab	In situ [2]	ÄD, lab		Fault gouge material (<125μm)	
Tracer	K_a (m)	K_a (m)	$D_e(\varepsilon+K_d\rho)$ (m^2/s)	K_d (m^3/kg)	$D_e(\varepsilon+K_d\rho)$ (m^2/s)	K_d (m^3/kg)	$D_e(\varepsilon+K_d\rho)$ (m^2/s)
C1	run# 1:6						
$^{82}Br^-$	–	–	$(3.5\pm0.2)\cdot10^{-12}$	–	$4\cdot10^{-16}$	–	$2\cdot10^{-11}$
$^{24}Na^+$	$(1.1\pm0.1)\cdot10^{-4}$	$7\cdot10^{-7}$	$(1.8\pm0.2)\cdot10^{-11}$	$1.4\cdot10^{-6}$	$5\cdot10^{-16}$	$7\cdot10^{-5}$	$3\cdot10^{-11}$
$^{86}Rb^+$	$(4\pm1)\cdot10^{-3}$	$5\cdot10^{-4}$	$(1.4\pm0.6)\cdot10^{-9}$	$4\cdot10^{-4}$	$1\cdot10^{-13}$	$1\cdot10^{-2}$	$3\cdot10^{-9}$
$^{134}Cs^+$	$(7\pm2)\cdot10^{-3}$	$8\cdot10^{-3}$	$(1.9\pm0.8)\cdot10^{-8}$	$8\cdot10^{-4}$	$2\cdot10^{-13}$	$1\cdot10^{-1}$	$3\cdot10^{-8}$
C2	run# 2:3, r = 17m						
$^{186}ReO_4^-$	–	–	$(1.9\pm0.7)\cdot10^{-10}$	–	$4\cdot10^{-16}$	–	$2\cdot10^{-11}$
$^{47}Ca^{2+}$	$(1.3\pm0.4)\cdot10^{-2}$	$4\cdot10^{-6}$	$(6\pm3)\cdot10^{-9}$	$5.2\cdot10^{-6}$	$7\cdot10^{-16}$	$4\cdot10^{-4}$	$5\cdot10^{-11}$
C2	run# 2:3, r = 97m						
$^{186}ReO_4^-$	–	–	$(1.8\pm0.7)\cdot10^{-13}$	–	$4\cdot10^{-16}$	–	$2\cdot10^{-11}$
$^{47}Ca^{2+}$	$(4\pm1)\cdot10^{-4}$	$4\cdot10^{-6}$	$(6\pm3)\cdot10^{-12}$	$5.2\cdot10^{-6}$	$7\cdot10^{-16}$	$4\cdot10^{-4}$	$5\cdot10^{-11}$
C3	run# 3:4						
HTO	–	–	$(9\pm5)\cdot10^{-12}$	–	$4\cdot10^{-16}$	–	$3\cdot10^{-11}$
$^{22}Na^+$	$(6\pm2)\cdot10^{-3}$	$7\cdot10^{-7}$	$(3.2\pm1.5)\cdot10^{-11}$	$1.4\cdot10^{-6}$	$5\cdot10^{-16}$	$7\cdot10^{-5}$	$3\cdot10^{-11}$
$^{85}Sr^{2+}$	$(1.8\pm0.5)\cdot10^{-3}$	$8\cdot10^{-5}$	$(1.6\pm0.6)\cdot10^{-11}$	$4.7\cdot10^{-6}$	$7\cdot10^{-16}$	$4\cdot10^{-4}$	$6\cdot10^{-11}$
C4	run# 4:6						
$^{131}I^-$	–	–	$(3\pm1)\cdot10^{-12}$	–	$4\cdot10^{-16}$	–	$2\cdot10^{-11}$
$^{47}Ca^{2+}$	$(2.5\pm0.8)\cdot10^{-4}$	$4\cdot10^{-6}$	$(8\pm4)\cdot10^{-11}$	$5.2\cdot10^{-6}$	$7\cdot10^{-16}$	$4\cdot10^{-4}$	$5\cdot10^{-11}$
$^{131}Ba^{2+}$	$(1.3\pm0.2)\cdot10^{-3}$	$2\cdot10^{-4}$	$(4\pm1)\cdot10^{-10}$	$2\cdot10^{-4}$	$2\cdot10^{-14}$	$9\cdot10^{-3}$	$1\cdot10^{-9}$
$^{54}Mn^{2+}$	$(9\pm1)\cdot10^{-3}$	–	$(3.6\pm0.8)\cdot10^{-9}$	No data available			

1) From Equation (7-2)

2) From Equation (7-3)

It is obvious that evaluation of the K_a and $D_e(\varepsilon+K_d\rho)$ from the in situ data is strongly dependent of the travel distance, r, (cf Eq. 7-1 and 7-2). As discussed earlier there are two distances determined for each flow path, the Euclidean distance and the distance along connected structures. The distance used in the calculations of the parameters presented in Table 7-3 is the Euclidean distance. For flow path II (C2), evaluations has been performed using both the Euclidean distance (17 m) and the distance from the interpretation calculated from the structural model (97 m). A large difference can be observed in the evaluated values of the K_a and $D_e(\varepsilon+K_d\rho)$ in test C2 depending on which distance used (cf Table 7-3). Using the shorter distance implies increased numerical values of the retention parameters and vice versa. The difference in the K_a (determined only for Ca^{2+}) is a factor 32 while the difference in $D_e(\varepsilon+K_d\rho)$ (determined for both ReO_4^- and Ca^{2+}) is a factor 1000.

In Table 7-3, comparisons are also made with the corresponding retention parameters obtained in laboratory experiments (surface sorption experiments and matrix diffusion experiments) for the Äspö diorite material. The comparisons show that the mass transfer processes are much more pronounced in the in situ experiments than what can be explained by applying the laboratory data for diffusion and surface sorption obtained for intact Äspö diorite rock. The only exception is the K_a for Cs^+ where the laboratory and in situ data are quite similar. A possible explanation for the observed discrepancies is that the in situ transport actually takes place in fractures where the dominant rock material in contact with the groundwater is the fine-grained fault gouge material. It was therefore decided to investigate the possibility if the high mass transfer seen in the results of the in situ experiment could be explained by interaction with fine-grained fault gouge material. An attempt was therefore made to investigate the highest possible retention parameters that could be explained by an interaction with a fault gouge material. The following assumptions were used in the calculations:

- K_d values were estimated using the mineralogical data for the clay fraction (<125 μm) of the fault breccia material sampled in the KI0023B intercept with Structure #20, the in situ groundwater composition data and the literature values of the cation-exchange capacities and selectivity coefficients for the different identified mineral fractions /cf Andersson et al, 2002/.
- A porosity (ε) of 20% was assumed for the fine-grained fault gouge, based on the projections made by /Mazurek et al, 1997/.
- The effective diffusivities (D_e) was estimated from the Archie´s law /Parkhomenko, 1967/, i.e.;

  $$D_e = D_w \cdot 0.71 \cdot \varepsilon^{1.58} \qquad (7\text{-}4)$$

  here D_w is diffusivities for the different tracers in pure water, tabulated by /Mills and Lobo, 1989/.

The calculated sorption/matrix diffusion parameters for fault gouge material using this concept are presented for comparison in Table 7-3. As can be seen, the results are similar to the values calculated from the estimated in situ retention parameters. This is an indication that the retention characteristics obtained within the time frames (days-months) of this type of in situ experiments may be dominated by the influence of the small amount

of fracture filling materials. However, for the non-sorbing tracers (HTO and Br^-) the $D_e(\varepsilon + K_d\rho)$ calculated for fault gouge is somewhat higher than what could be interpreted for the in situ experiment. A possible explanation to this is that these tracers have penetrated the thin layers of fault gouge material and that these tracers are also influenced by diffusion in rock materials with lower porosity combined with lower diffusivity.

8 Acknowledgement

The careful reviews of early versions of this report by Ingvar Rhén (Sweco), Les Knight (Nirex), Jan-Olof Selroos (SKB) are gratefully acknowledged.

9 List of abreviations and symbols

A	parameter used to account for matrix diffusion	(–)
A_s	geometrical rock surface area of a borehole section	(m^2)
C	tracer concentration	(mole/m^3)
C_0	initial concentration of tracer	(mole/m^3)
C_{ads}	concentration of tracer in attached to the surface of a borehole section	(mole/m^3)
C_{aq}	concentration of tracer in a borehole section	(mole/m^3)
$C_{aq,0}$	initial concentration of tracer in a borehole section	(mole/m^3)
C_f	concentration of the tracer in the fracture	(mole/m^3)
C_{in}	concentration of tracer in a groundwater flowing in to a borehole section	
C_{out}	concentration of tracer in a groundwater flowing out of a borehole section	
C_p	concentration of the tracer in the rock matrix	(mole/m^3)
D_L	dispersion coefficient (longitudinal)	(m^2/s)
D_e	effective pore diffusivity	(m^2/s)
D_w	diffusivity in pure water	(m^2/s)
F	proportional factor used in modeling of breakthrough curves	(–)
F_D	formation factor	(–)
Δh	head difference between the injection and pumping section	(m)
I	hydraulic gradient	(–)
K	hydraulic conductivity	(m/s)
K_a	surface sorption coefficient	(m^3/kg)
K_d	matrix sorption coefficient	(m^3/kg)
K_F	empirical constant used in the Freundlich equation	(mole^{nF-1} $m^{(3nF-2)}$)
K_{fr}	hydraulic fracture conductivity	(m/s)
k_s	rate constant for a surface sorption reaction	(s^{-1})
k_{des}	rate constant for a surface desorption reaction	($m^{-1}s^{-1}$)
L_{bh}	length of a packed-off borehole section	(m)
M_{tot}	total amount of injected tracer	(mole)
n_F	empirical exponential factor used in the Freundlich isotherm	(–)
Pe	Peclet number (dispersion parameter)	(–)
pf	proportional factor used in modeling of breakthrough curves	(–)
Q	withdrawal flow rate	(m^3/s)
Q_{bh}	groundwater flow through a borehole section	(m^3/s)
Q_{in}	groundwater flow through in to a borehole section	(m^3/s)
Q_{inj}	injection flow	(m^3/s)
Q_{out}	groundwater flow through out of a borehole section	(m^3/s)
q_w	Darcy velocity	(m/s)
r	distance between injection and withdrawal borehole sections	(m)
r_w	borehole radius	(m)
R	recovery of a tracer	(%)
R_a	surface retardation coefficient	(–)
$R_{50\%}$	Recovery based retardation coefficient, cf Chapter 7	(–)
t	time	(s)
t_0	mean travel time of a conservative tracer	(s)
t'_0	residence time of a sorbing tracer	(s)
t_5	travel time for 5% recovery	(h)

t_{50}	travel time for 50% recovery	(h)
t_{95}	travel time for 95% recovery	(h)
t_t	travel time for last sample taken	(h)
T	transmissivity	(m^2/s)
V	volume of a borehole section	(m^3)
v	fluid velocity	(m/s)
x	distance from the injection point	(m)
α	factor accounting for distortion of flow caused by a borehole	(–)
δ	fracture aperture	(m)
ε	matrix rock porosity	(–)
θ_k	flow porosity	(–)
Π	Multiplicator (accounting for proportional effects)	(–)
ρ	density of the rock	(kg/m^3)

10 References

Abelin H, Birgersson L, 1987. 3-D migration experiment – report 1: site praparation and documentation. Stripa Project TR 87-19, SKB, Stockholm, Sweden.

Abelin H, Birgersson L, Gidlund J, 1987a. 3-D migration experiment – Report 2: instrumentation and tracers. Stripa Project TR 87-20, SKB, Stockholm, Sweden.

Abelin H, Birgersson L, Gidlund J, Moreno L, Neretnieks I, Widén H, Ågren T, 1987b. Part I: 3-D migration experiment – Report 3: performed experiments, results and evaluation. Stripa Project TR 87-21(a), SKB, Stockholm, Sweden.

Abelin H, Birgersson L, Gidlund J, Moreno L, Neretnieks I, Widen H, Ågren T, 1987c. Part II: 3-D migration experiment – Report 3: performed experiments, results and evaluation. Appendices 15, 16 and 17. Stripa Project TR 87-21(b), SKB, Stockholm, Sweden.

Ahlbom K, Smellie J A T, 1991. Overview of the Fracture Zone Project at Finnsjön, Sweden. J. of Hydrology, 126 (1991), pp. 1–15.

Andersson K, 1983. Transport of radionuclides in water/mineral systems. Diss. Chalmers University of Technology, Göteborg, Sweden.

Andersson P, Nordqvist R, Persson T, Eriksson C-O, Gustafsson E, Ittner T, 1993. Dipole tracer experiment in a low-angle fracture zone at Finnsjön – results and interpretation. The Fracture Zone Project – Phase 3. Swedish Nuclear Fuel and Waste Management Company. SKB Technical Report 93-26.

Andersson P, Winberg A, 1994. INTRAVAL Working Group 2 summary report on Phase 2 analysis of the Finnsjön test case. Swedish Nuclear Fuel and Waste Management Company. SKB Technical Report TR-94-07.

Andersson P, 1995. Compilation of tracer tests in fractured rock. Swedish Nuclear Fuel and Waste Management Company, SKB Äspö Hard Rock Laboratory, Progress Report 25-95-05.

Andersson P, Ludvigson J-E, Wass E, Holmqvist M, 2000a. TRUE Block Scale Project Tracer Tests Stage. Interference tests, dilution tests and tracer tests, Phase A. Swedish Nuclear Fuel and Waste Management Company. Äspö Hard Rock Laboratory. International Progress Report IPR-00-28.

Andersson P, Wass E, Holmqvist M, **Fierz T, 2000b.** TRUE Block Scale Project Tracer Tests Stage. Tracer tests, Phase B. Swedish Nuclear Fuel and Waste Management Company. Äspö Hard Rock Laboratory. International Progress Report IPR-00-29.

Andersson P, Ludvigsson J-E, Wass E, 2001a. Preliminary Characterisation Stage – Combined interference tests and tracer tests – Performance and preliminary evaluation. Swedish Nuclear Fuel and Waste Management Company, Äspö Hard Rock Laboratory, International Progress Report IPR-01-44.

Andersson P, Ludvigsson J-E, Wass E, Holmqvist M, 2001b. Detailed Characterisation Stage – Interference tests and tracer tests PT-1 – PT-4. Swedish Nuclear Fuel and Waste Management Company, Äspö Hard Rock Laboratory. International Progress Report IPR-01-52.

Andersson P, Byegård J, Holmqvist M, Skålberg M, Wass E, Widestrand H, 2001c. TRUE Block Scale Tracer Test Stage. Tracer test, Phase C. Swedish Nuclear Fuel and Waste Management Company. Äspö Hard Rock Laboratory. International Progress Report IPR-01-33.

Andersson P, Byegård J, Dershowitz W, Doe T, Hermanson J, Meier P, Tullborg E-L, Winberg A, 2002. TRUE Block Scale Project. Final report. 1. Characterisation and model development. Swedish Nuclear Fuel and Waste Management Company. SKB Technical Report TR-02-13 (in prep).

Birgersson L, Ågren T, 1992. Site characterization and validation – tracer migration experiment in the Validation Drift, Report 1: Instrumentation, site preparation and tracers. Stripa Project TR 92-02, SKB, Stockholm, Sweden.

Birgersson L, Widén H, Ågren T, Neretnieks I, Moreno L, 1992a. Tracer migration experiments in the Stripa mine: 1980–1991. Stripa Project TR 92-25, SKB, Stockholm, Sweden.

Birgersson L, Widén H, Ågren T, Neretnieks I, Moreno L, 1992b. Site characterization and validation – tracer migration experiment in the Validation Drift, Report 2, Part 1: performed experiments, results and evaluation. Stripa Project TR 92-03, SKB, Stockholm, Sweden.

Birgersson L, Widén H, Ågren T, Neretnieks I, Moreno L, 1992c. Site characterization and validation – tracer migration experiment in the Validation Drift, Report 2, Part 2: breakthrough curves in the Validation Drift. Appendices 5–9. Stripa Project TR 92-03, SKB, Stockholm, Sweden.

Byegård J, Skarnemark G, Skålberg M, 1991. Radioactive tracer study performed in a dipole geometry in a highly conductive fracture zone. Mat. Res. Soc. Symp. Proc. Vol 212. Material Research Society 1991.

Byegård J, Albinsson Y, Skarnemark G, Skålberg M, 1992. Field and laboratory studies of the reduction and sorption of Technetium(VII). Radiochimica Acta 58/59, 239–244.

Byegård J, 1993. The possibility of using slightly sorbing cations in the tracer experiments in the Äspö Hard Rock Laboratory. A literature survey and some basic considerations. Swedish Nuclear Fuel and Waste Management Company. Äspö Hard Rock Laboratory. Progress Report 25-93-14.

Byegård J, Johansson H, Skålberg M, Tullborg E-L, 1998. The interaction of sorbing and non-sorbing tracers with different Äspö rock types. Swedish Nuclear Fuel and Waste Management Company. SKB Technical Report TR-98-18. ISSN 0284-3757.

Byegård J, Skarnemark G, Skålberg M, 1999. The stability of some metal EDTA, DTPA and DOTA complexes; Application as tracers in groundwater studies, J. Radioanal. Nucl. Chem. 241, 281–290.

Byegård J, Skarnemark G, Skålberg M, 2000. Transport modelling of tracers influenced by kinetic hindered sorption – applied to laboratory and in siu studies of lanthanide EDTA Complexes, Journal of Contaminant Hydrology 42 (2000), 165–186.

Cvetkovic V, Cheng H, Selroos J-O, 2000. Evaluation of Tracer Retention Understanding Experiments (first stage) at Äspö. Swedish Nuclear Fuel and Waste Management Company. Äspö Hard Rock Laboratory. International Cooperation Report ICR-00-01.

Dershowitz B, Klise K, 2002. TRUE Block Scale Project. Process discrimination studies using the Channel Network model. Swedish Nuclear Fuel and Waste Management Company. Äspö Hard Rock Laboratory. International Progress Report IPR-02-XX (in prep).

Doe T, 2001. TRUE Block Scale Project – Reconciliation of the March'99 structural model and hydraulic data. Swedish Nuclear Fuel and Waste Management Company. Äspö Hard Rock Laboratory. International Progress Report IPR-01-53.

Eikenberg J, Frick U, Fierz T, Bühler Ch, 1992. On-line detection of stable helium isotopes in migration experiments, Tracer Hydrogeology, Hötzl and Werner (eds), Balkema, Rotterdam, ISBN 9054100842.

Elert M, 1999. Evaluation of modelling of the TRUE-1 radially converging tests with conservative tracers, The Äspö Task Force on Modelling of Groundwater Flow and Transport of Solutes., Tasks 4C and 4D. Swedish Nuclear Fuel and Waste Management Company (SKB), Technical Report TR-99-04.

Elert M, Svensson H, 2001. Evaluation of modelling of the TRUE-1 radially converging tests with conservative tracers, The Äspö Task Force on Modelling of Groundwater Flow and Transport of Solutes, Tasks 4E and 4F. Swedish Nuclear Fuel and Waste Management Company (SKB), Technical Report TR-01-12.

Frick U, Alexander W R, Baeyens B, Bossart P, Bradbury M H, Bühler, Eikenberg J, Fierz Th, Heer W, Hoehn E, McKinley I G, Smith P A, 1992. Grimsel Test Site – The Radionuclide Migration Experiment – Overview of Investigations 1985–1990. NAGRA Technical Report NTB 91-04.

Frost L H, Kozak E T, Everitt R A, Serzu M H, Lodha G S, Gascoyne M, Davison C C, 1998. Transport properties in moderately fractured rock experiment, Stage 1 Groundwater flow domain characterization report. Ontario Hydro, Nuclear Waste Management Report No: 06819-REP-01200-0021 R00.

Gnirk P, 1993. OECD/NEA International Stripa Project 1980–1992 – Overview Volume II – Natural Barriers, January 1993. ISBN 91-971906-3-2.

Guimerà J, Vives L, Carrera J, Martinez L, Gómez P, Turrero M J, Alonso J, Hernán P, 1996. Hydrogeochemical implications in the flow analysis of El Berrocal site. In: Use of hydrogeochemical information in testing groundwater flow models. Proceedings of an International OECD/NEA Workshop, Borgholm Sweden, 1–3 September 1997, pp. 175–194. OECD/NEA ISBN 92-64-16153-8.

Guimerà J, García-Gutiérrez M, Yllera A, Carrera J, Hernández-Benítez A, Saaltink P, 1997. "Design, performance and interpretation of tracer tests at El Berrocal site (Spain). In: Field tracer experiments: Role in the prediction of radionuclide migration. Synthesis and Proceedings of an international NEA/EC GEOTRAP workshop, pp. 171–187. NEA/OECD. ISBN 92-64-16013-2.

Gustafson G, Ström A, 1995. The Äspö Task Force on Modelling of groundwater Flow and Transport of Solutes. Evaluation report on Task No 1, the LPT2 large scale field experiment. Swedish Nuclear Fuel and Waste Management Company. Äspö Hard Rock Laboratory, International Cooperation Report ICR-95-05.

Gustafsson E, Klockars C-E, 1981. Studies of groundwater transport in fractured crystalline rock under controlled conditions using non-radioactive tracers. Swedish Nuclear Fuel and Waste Management Company. SKBF/KBS Technical Report TR 81-07.

Hadermann J, Heer W, 1996. The Grimsel (Switzerland) migration experiment: integrating field experiments, laboratory investigations and modelling. Journal of Contaminant Hydrology 21 (1996), 87–100.

Hautojärvi A, Taivassalo V, 1994. The INTRAVAL Project – Analysis of the Tracer Experiments at Finnsjön by the VTT/TVO Project Team, Report YJT-94-24, Nuclear Waste Commission of Finnish Power Companies, December 1994, Helsinki.

Heer W, Hadermann J, 1996. Grimsel test site: Modelling radionuclide migration field experiments. NAGRA Technical Report 94-18, National Cooperative for the Disposal of Radioactive Waste, Wettingen, Switzerland.

Hermanson J, Doe T, 2000. TRUE Block Scale Project Tracer test stage. March'00 structural and hydraulic model based on borehole data from KI0025F03. Swedish Nuclear Fuel and Waste Management Company. Äspö Hard Rock Laboratory. International Progress Report IPR-00-34.

Hermanson J, Follin S, Nilsson P, Nyberg G, Winberg A, 2002. TRUE Block Scale – Updating of the structural-hydraulic model and compilation of scoping data set. Swedish Nuclear Fuel and Waste Management Company. Äspö Hard Rock Laboratory. International Progress Report IPR-02-13.

Holmqvist M, Andersson P, Byegård J, Fierz T, in prep. Tests of new possible non-reactive tracers – experimental description and evaluation. Swedish Nuclear Fuel and Waste Management Company. Äspö Hard Rock Laboratory. International Progress Report IPR in prep.

Ittner T, Byegård J, 1997. Test of tracer sorptrion on equipment. Swedish Nuclear Fuel and Waste Management Company. Äspö Hard Rock Laboratory. International Progress Report HRL-97-28.

Jacob A, Mazurek M, Heer W, 2002. Solute transport in crystalline rocks at Äspö – II: Blind predictions, inverse modelling and lessons learnt from test STT1. Accepted for publication in Journal of Contaminant Hydrology.

James R O, Healy T W, 1972. Adsorption of hydrolyzable metal ions in the oxide-water interface, J. Colloid Interface Sci. 40, 42–52.

Jensen M R, 2001. The moderately fractured rock experiment: Background and overview. In: First TRUE Stage – Transport of solutes in an interpreted single fracture – Proceedings from the 4th International Äspö Seminar, September 9–11, 2000. Swedish Nuclear Fuel and Waste Management Company. Technical Report TR-01-24.

Liedke L, Zuidema P, 1988. The fracture system flow test. In: Grimsel Test Site from 1983 to 1990. Nagra Bullentin, Special Edition 1988, pp. 41–45.

Liedke L, Götchenberg A, Jobman M, Siemering W, 1994. Grimsel Test Site – Fracture system flow test – Experimental and numerical investigations of mass transport in fractured rock. NAGRA Technical Report 94-02E.

Marschall P, Vomvoris S (eds), 1995. Grimsel test Site – Devleopments in hydrotesting, fluid logging and combined salt/heat tracer experiments in the BK site (Phase III). NAGRA Technical Report 94-02E.

Mazurek M, Bossart P, Eliasson T, 1997. Classification and characterization of water-conducting features at Äspö: Results of investigations on the outcrop scale, Swedish Nuclear Fuel and Waste Management Company. SKB ICR-97-01

Mazurek M, Jakob A, Bossart P, 2002. Solute transport in crystalline rocks at Äspö – I: Geological basis and model calibration. Accepted for publication in Journal of Contaminant Hydrology.

Mills R, Lobo V M M, 1989. Self-diffusion in electrolyte solutions – a critical examination of data compiled from the literature, Elsevier, Amsterdam.

Moreno L, Neretnieks I, Klockars C-E, 1983. Evaluation of some tracer tests in the granitic rock at Finnsjön. SKBF/KBS Teknisk Rapport TR 83-38.

Moye D G, 1967. Diamond drilling for foundation exploration. Civil Eng. Trans., Inst. Eng. Australia (Apr. 1967), 95–100.

Neretnieks I, 2002. A stochastic multi-channel model for solute transport – analysis of tracer tests in fractured rock. Journal of Contaminant Hydrology 55(3–4): 175–211, 2002.

Nordqvist R, 1994. Documentation of some analytical flow and transport models implemented for use with PAREST – Users manual. GEOSIGMA Internal Report GRAP 94 006, Uppsala.

NRS, 1996. Rock Fractures and fluid flow – Contemporary understanding and applications. National Research Council. National Academy Press, Washington D.C. ISBN 0-309-04996-2.

Ogata A, Banks R, 1961. A solution to the differential equation of longitudinal dispersion in porous media. U.S. Geol. Surv. Prof. Paper 411-A, Washington.

Parkhomenko E I, 1967. Electrical properties of rock, Plenum Press, New York, p. 268.

Poteri A, Billaux D, Cvetkovic V, Dershowitz B, Gómez-Hernández J-J, Hautojärvi A, Holton D, Medina A, Winberg A, 2002. TRUE Block Scale Project. Final Report – 3. Modelling of flow and transport. Swedish Nuclear Fuel and Waste Management Company. Technical Report TR 02-15 (in prep).

Rhén I, Svensson U, Andersson J-E, Andersson P, Eriksson C-O, Gustafsson E, Ittner T, Nordqvist, 1992. Äspö Hard Rock Laboratory: Evaluation of the combined long term pumping and tracer tests (LPT2) in borehole KAS06. Swedish Nuclear Fuel and Waste Management Company, SKB Technical Report TR-92-32.

Rivas P et al, 1998. El Berrocal project – Summary Report. European Commission. EUR 17830 EN. ISBN 92-828-2147-1.

Sawada A, Uchida M, Shimo M, Yamamoto H, Takahara H, Doe T W, 2000. Non-sorbing tracer migration experiments in fractured rock at the Kamaishi mine, northeast Japan. Eng. Geology 56 (2000), pp. 75–96.

Shimo M, Yamamoto H, Uchida M, Sawada A, Doe T W, Takahara Y, 1999. In situ test on flow and mass transport properties of fractured rocks. In: Proc. of 9th International Congress on Rock Mechanics, Paris, 1999 (Vouille, G and Beretst, P. eds), pp. 1401–1404. Balkema Publishers.

Skagius K, Svedberg G, Neretnieks I, 1982. A study of strontium and cesium sorption on granite. Nucl. Techn. 59, 302–313.

SKB, 2001. First TRUE Stage – Transport of solutes in an interpreted single fracture. Proceedings from the 4th International Seminar, Äspö, September 9–11, 2000. Swedish Nuclear Fuel and Waste Management Company, SKB Technical report TR-01-24.

Smart P L, Laidlaw I M S, 1977. An evaluation of some fluorescent dyes forwater tracing. Water Resour. Res. 13(1), 15–33.

Smith R M, Martell A E, 1989. "Critical Stability Constants", (latest update 1989), Plenum Press, New York.

Stetzenbach K, Farnham I, 1994. Organic anionic tracers: Chemistry and toxicity. Proceedings from the second tracer workshop. Univ. of Texas at Austin, Nov. 14–15, pp. 23–32

Säfvestad A, Nilsson A-C, 1999. Compilation of groundwater chemistry data January 1995 to April 1998. Swedish Nuclear Fuel and Waste Management Company. Äspö Hard Rock Laboratory. International Progress Report IPR-99-13.

Tang G H, Frind E O, Sudicky E A, 1981. Contaminant transport in fractured porous media. An analytical solution for a single fracture. Water Resources Research, Vol 17, p. 555.

Van Genuchten M Th, 1982. One-dimensional analytical transport modeling, in Proceedings: Symposium on unsaturated flow and transport modeling. Rep. PNL-SA-10325, Pacific Northwest Lab., Richland, Washington.

Van Genuchten M Th, Alves W J, 1982. Analytical solutions of the one-dimensional convective-dispersive solute transport equation. U.S. Dep. Agric. Tech. Bull.1661.

Winberg A (ed), 1996. First TRUE Stage – Tracer Retention Understanding Experiments: Descriptive structural-hydraulic models on block and detailed scales on the TRUE-1 site. Swedish Nuclear Fuel and Waste Management Company. Äspö Hard Rock Laboratory. International Cooperation Report ICR 96-04.

Winberg A, Andersson P, Hermanson J, Stenberg L, 1996. Results of the SELECT Project – Investigation Programme for Selection of Experimental Sites for the Operational Phase. Swedish Nuclear Fuel and Waste Management Company. Äspö Hard Rock Laboratory. Progress Report PR HRL-96-01.

Winberg A, 1997. Test plan for the TRUE Block Scale Experiment. Swedish Nuclear Fuel and Waste Management Company. Äspö Hard Rock Laboratory. International Cooperation Report ICR 97-02.

Winberg A (ed), 1999. Scientific and technical ststus. Position report prepared for the 2nd TRUE Block Scale review meeting, Stockholm, Nov 17 1998. Swedish Nuclear Fuel and Waste Management Company. Äspö Hard Rock Laboratory. International Progress Report IPR-99-07.

Winberg A (ed), 2000. Final report of the detailed characterisation stage – Compilation of premises and outline of programme for tracer tests in the block scale. ICR-00-02 – Report on Detailed characterisation stage. Swedish Nuclear Fuel and Waste Management Co, Äspö Hard Rock Laboratory. International Cooperation report ICR 00-02.

Winberg A, Andersson P, Hermanson J, Byegård J, Cvetkovic V, Birgersson L, 2000. Äspö Hard Rock Laboratory, Final report of the first stage of the tracer retention understanding experiments, Swedish Nuclear Fuel and Waste Management Company, SKB Technical report TR-00-07.

Winberg and Hermanson, 2002. TRUE Block Scale Experiment – Allocation of experimental volume. Swedish Nuclear Fuel and Waste Management Company. Äspö Hard Rock Laboratory. International Progress Report IPR-02-14.

Winberg A, Andersson P, Byegård J, Poteri A, Cvetkovic V, Dershowitz B, Doe T, Hermanson J, Gómez-Hernández J-J, Hautojärvi A, Billaux D, Tullborg E-L, Meier P, Medina A, 2002. TRUE Block Scale Project. Final Report – 4. Synthesis of flow, transport and retention in the block scale. Swedish Nuclear Fuel and Waste Management Company. Technical Report TR-02-16 (in prep).

Zuber A, 1974. Theoretical possibilities of the two-well pulse method. Isotope Techniques in Groundwater Hydrology 1974, Proc. Symp., Vienna 1974, IAEA,Vienna.

Appendix 1

First order kinetics approach

One possibility is that the shape of the injection curves is influenced by kinetically hindered sorption and desorption. Attempts have therefore been made in order to interpret the sorption from a first order kinetics perspective, i.e.;

$$C_{\text{aq}} \underset{k_{\text{des}}}{\overset{k_{\text{s}}}{\rightleftharpoons}} C_{\text{ads}} \tag{A-1}$$

where k_{s} (s^{-1}) is the rate constant for the sorption reaction and k_{des} ($\text{m}^{-1}\text{s}^{-1}$) is the rate constant for the desorption reaction. A system consisting of an isolated borehole section where the tracer injected sorbs and desorbs with a kinetically hindered mechanism, can thus be described by the following equations:

$$\frac{dC_{\text{aq}}}{dt} = -\frac{Q}{V}C_{\text{aq}} - \frac{A}{V}\frac{dC_{\text{ads}}}{dt} \tag{A-2}$$

and

$$\frac{dC_{\text{ads}}}{dt} = k_{\text{s}}C_{\text{aq}} - k_{\text{des}}C_{\text{ads}} \tag{A-3}$$

where the following boundary conditions are applicable:

$$t = 0, \quad C_{\text{aq}} = C_{\text{aq,0}} \quad C_{\text{ads}} = C_{\text{ads,i}} \tag{A-4}$$

$$t = \infty, \quad C_{\text{aq}} = 0 \qquad C_{\text{ads}} = 0 \tag{A-5}$$

An analytical solution this system has been obtained by Laplace-transformation, giving the following equation:

$$C_{\text{aq}} = \frac{\left(C_{\text{aq,0}}s_0 + k_{\text{des}}C_{\text{aq,0}} + k_{\text{des}}k_2C_{\text{ads,0}}\right)\cdot e^{(s_0 t)} - \left(C_{\text{aq,0}}s_1 + k_{\text{des}}C_{\text{aq,0}} + k_{\text{des}}k_2C_{\text{ads,0}}\right)\cdot e^{(s_1 t)}}{s_0 - s_1} \tag{A-6}$$

where:

$$s_0 = \frac{Q/V + k_{\text{des}} + k_{\text{s}}A/V}{2} + \sqrt{\left(\frac{Q/V + k_{\text{des}} + k_{\text{s}}A/V}{2}\right)^2 - \frac{Ak_{\text{des}}}{V}} \tag{A-7}$$

and

$$s_1 = \frac{Q/V + k_{\text{des}} + k_{\text{s}}A/V}{2} - \sqrt{\left(\frac{Q/V + k_{\text{des}} + k_{\text{s}}A/V}{2}\right)^2 - \frac{Ak_{\text{des}}}{V}} \tag{A-8}$$

Appendix 2

Plots of breakthrough curves in lin-lin space

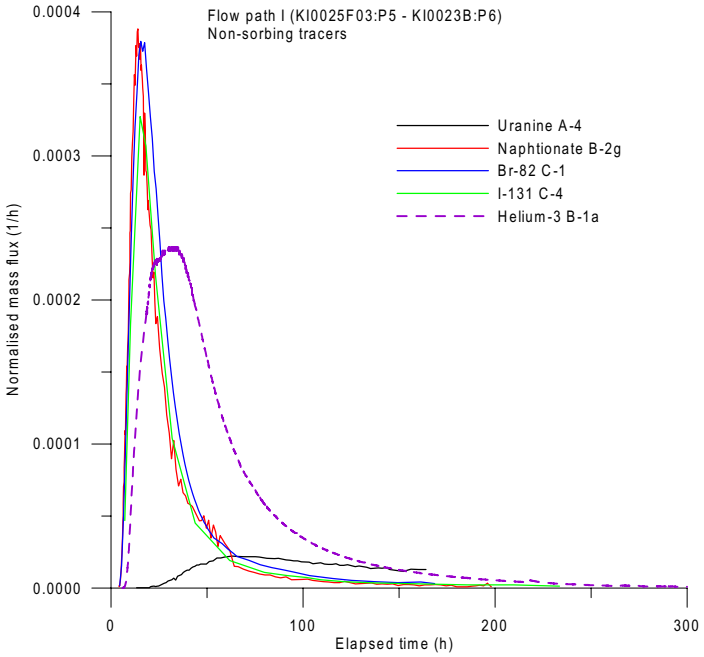

Figure A2-1. *Flow path I – Normalised tracer breakthrough curves for conservative tracers during tests A-4 (passive injection), B-1a (Helium, a tracer with higher diffusivity), B-2g, C1 and C4. See also Figure 6-4.*

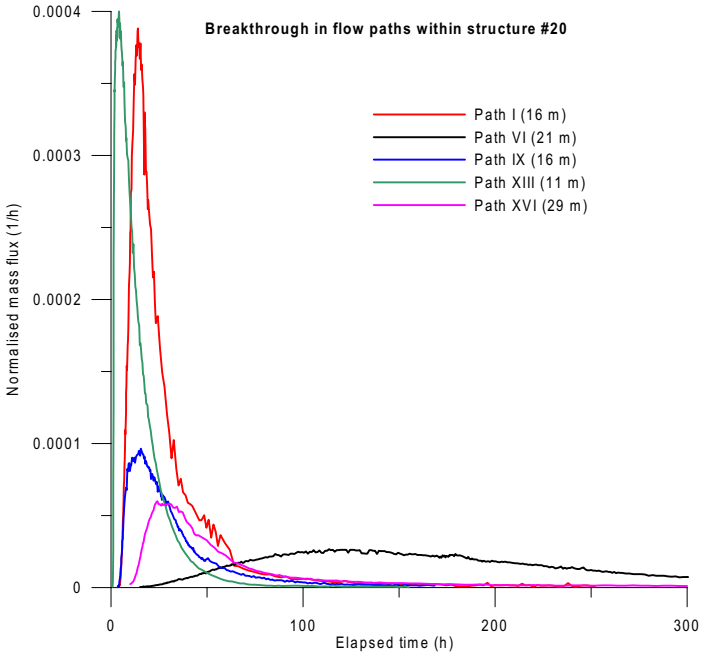

Figure A2-2. *Comparison of tracer breakthrough for conservative tracers in five flow paths within Structure #20. See also Figure 6-6.*

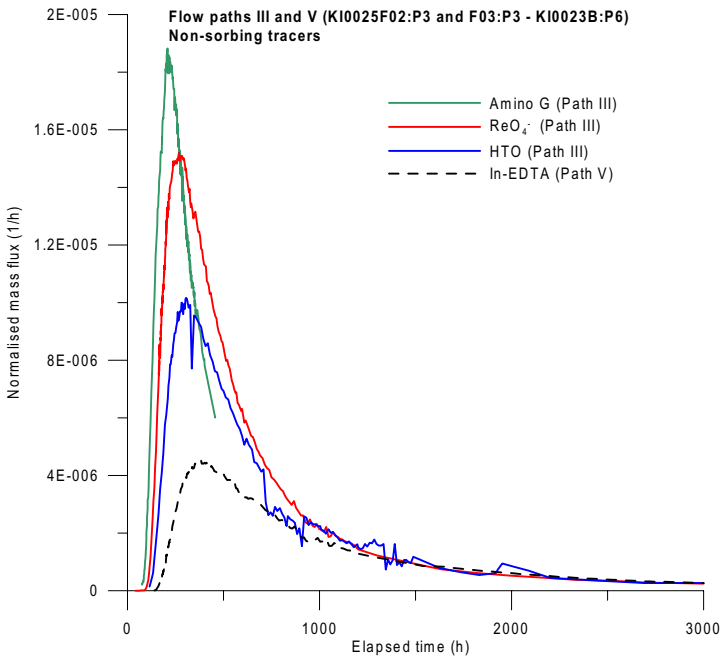

Figure A2-3. *Comparison of breakthrough curves in flow path III and V within Structure #21, cf Table 6-3 and Figure 6-8. See also Figure 6-9.*

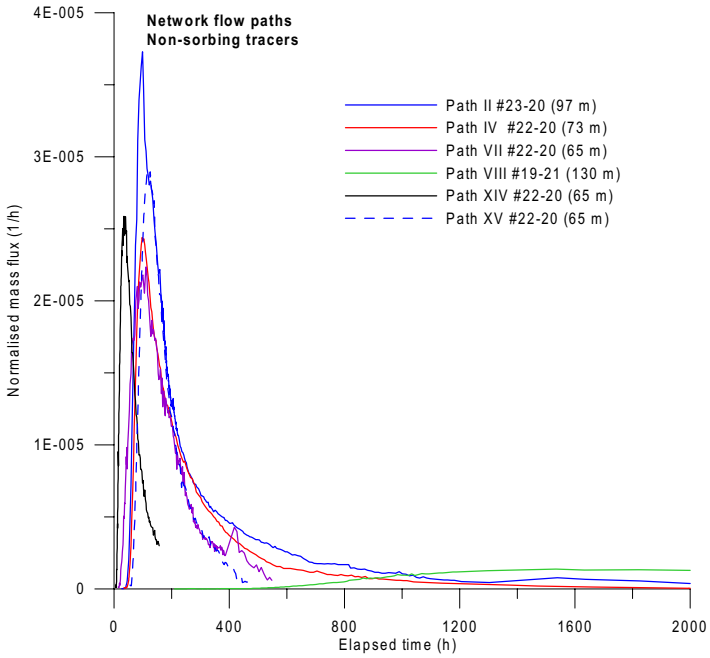

Figure A2-4. *Comparison of tracer breakthrough in six "network" flow paths, cf Table 6-1 and Figures 6-1 and 6-2. See also Figure 6-10.*

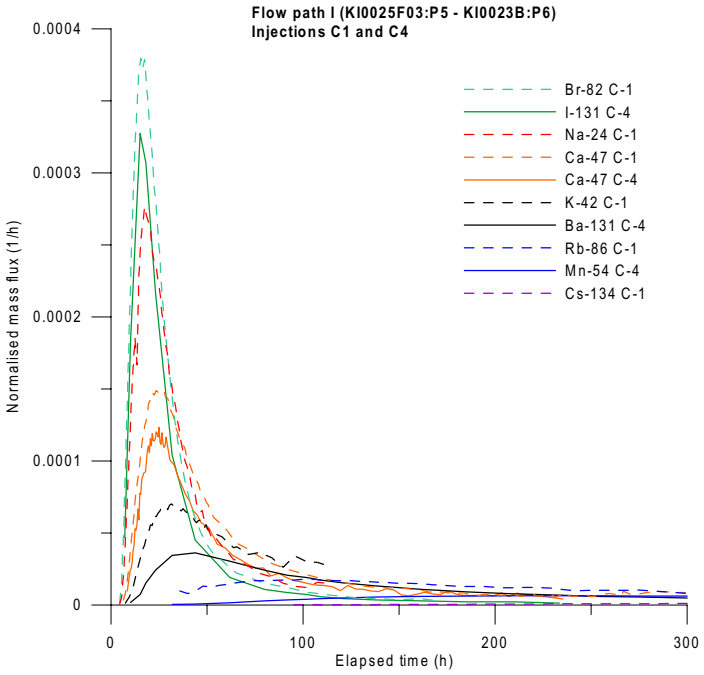

Figure A2-5. *Normalised tracer breakthrough for all tracers injected in tests C1 and C4. See also Figure 6-11.*

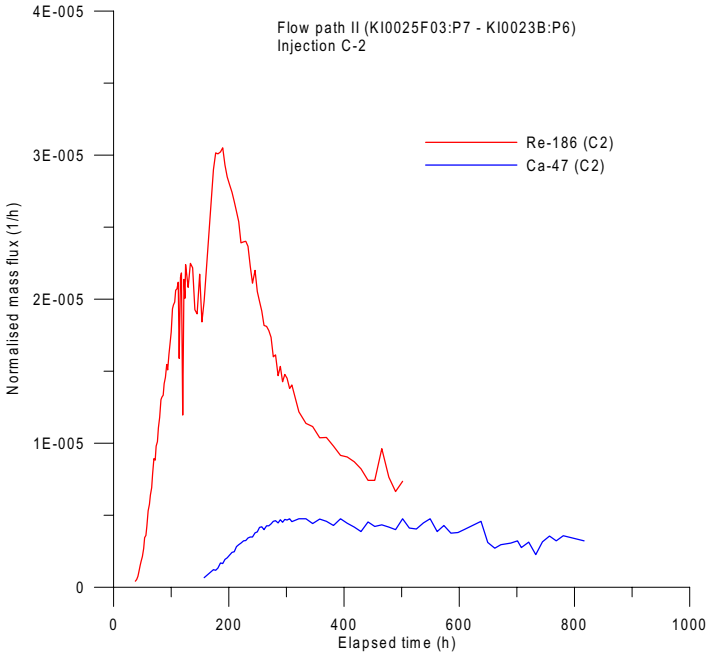

Figure A2-6. *Normalised tracer breakthrough for $^{186}ReO4^-$ and $^{47}Ca^{2+}$ injected in test C2. See also Figure 6-14.*

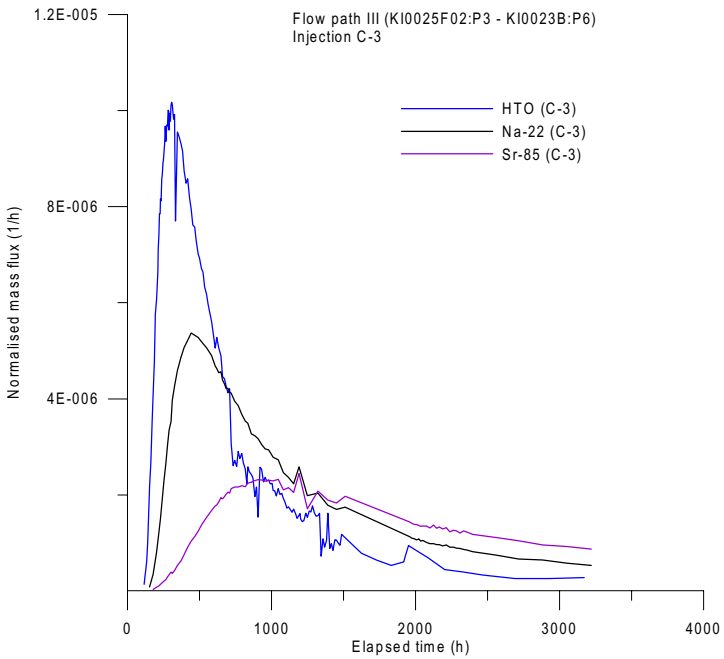

Figure A2-7. *Normalised tracer breakthrough for HTO, $^{22}Na^{+}$- and $^{85}Sr^{2+}$ injected in test C3. See also Figure 6-16.*

ISSN 1404-0344

CM Digitaltryck AB, Bromma, 2002